THE JOURNAL
OF
CHEMICAL PHYSICS

VOLUME 1 NOVEMBER, 1933 NUMBER 11

An X-Ray Study of the Binary Alloys of Silicon with Ag, Au, Pb, Sn, Zn, Cd, Sb and Bi

ERIC R. JETTE AND EMERY B. GEBERT, *School of Mines, Columbia University*

(Received September 8, 1933)

The lattice constants of the binary alloys of silicon with silver, gold, lead, tin, zinc, cadmium, antimony and bismuth have been measured. It is shown that the lattice constants of the elements in these alloys are practically identical with those of the pure elements. This fact leads to the interpretation that mutual solubility of the elements in these alloys occurs to only a very slight extent. It is further observed that silicon forms no compounds with any of these elements.

FOR each of the eight binary silicon alloy systems included in the present report, analogy with silicon alloys of closely related elements and, in at least one case, the earlier results of thermal and microscopic analysis would lead us to expect compound formation or appreciable ranges of solid solution or both. It was, therefore, surprising that not a single case of compound formation was observed in these alloys, and, further that in none of these systems was there a range of solid solution of sufficient magnitude to be detected by the method applied.

The method used in the present investigation was the determination of the lattice constants by means of the x-ray crystal structure analysis. The usual procedure for determining the limit of a solid solution range is to measure the lattice constants at several different compositions within the homogeneous solid solution range and then for the same phase when in equilibrium with the neighboring solid phase. By projecting this last value to the curve for the homogeneous range, the equilibrium composition can be established, frequently with a high degree of accuracy. Aside from the precision attainable in the measurement of the lattice constants, the accuracy of the method depends upon the difference in radii of the atoms concerned and the actual extent of the solid solution range. These two factors, however, are not entirely independent; general experience shows that if the atomic radii differ by more than about 10 percent, the solid solution range will be limited. The limit seems to be set by the amount of distortion caused by the foreign atoms which the lattice can withstand. This qualitative rule is subject to further restrictions due to influences which would cause positive deviations from Raoult's law or give rise to compound formation.

In the present cases, the usual procedure could not be applied because of the entirely insignificant changes in the lattice constants observed even when the neighboring solid phases were in equilibrium. The cameras used were of the Bohlin type as modified by Phragmén.[1] They were calibrated empirically with NaCl as the standard. Only the most deviated reflections of radiation from an iron target were used for calculating the lattice constants. The error for substances having cubic symmetry is certainly

[1] Westgren, Trans. Inst. Min. Met. Eng.; Inst. of Metals Div. 1931, p. 13.

not greater than ± 0.001A; in the tetragonal and hexagonal systems, $\pm 0.001-0.002$A for the smaller constant and possibly $\pm 0.003-0.004$ for the length of the c axis when this is more than 10A.

As a first approximation, which is certainly sufficient for the present cases, we may assume that the change of the lattice constant is a linear function of the atomic composition and further that it may be calculated from the difference in the radii of the atoms concerned. The differences between the radius of the silicon atoms and the radii of the other atoms varies about 15 to 50 percent. Calculation shows that with the accuracy attainable in determining the lattice constants, solid solubility of one element in another in these alloys, amounting to 0.2 atom percent, should have been indicated with certainty, while for Si in Pb, Zn or Cd, as well as for Pb or Bi in Si the detectable limit is about 0.1 atom percent. As already noted, no solubility of this order was observed.

Materials

Silicon of exceptional purity was supplied by the Electro Metallurgical Company through the courtesy of Dr. F. M. Becket. It had the following analysis: Si, 99.79 percent; Fe, 0.027; Al, 0.008; Ca, 0.014; C, 0.004; O_2, 0.002; N_2, 0.1; H_2, trace.

Bismuth: Merck's C.P. with total maximum impurities of approximately 0.04 percent.

Antimony and cadmium: Kahlbaum "Zur Analyse."

Gold and silver: Specially refined material from the U. S. Metals Refining Company, in each case 99.99+ pure.

Lead: Merck's C.P. with total maximum impurities amounting to 0.1 percent.

Tin: Baker's "Analyzed" with total metallic impurities of approximately 0.03 percent.

Zinc: Eimer and Amend, "Tested Purity" with total metallic impurities amounting to approximately 0.2 percent chiefly Pb and Cd.

Preparation of Alloys

For each of the systems, alloys were made by at least two different methods. It was early realized that the miscibility of the two elements and the formation of sound and uniform ingots might be seriously interfered with by the presence of thin oxide films, especially on the silicon. Accordingly it was attempted in each system to make at least one alloy at temperatures above the melting point of silicon, i.e., above 1420°C. This was successful except in the cases of zinc and cadmium. These elements when added to liquid silicon in a hydrogen atmosphere, boiled off completely; the alloys were, therefore, prepared by heating mixtures of the two elements just below the boiling point of zinc and cadmium respectively for several days.

In most cases, weighed amounts of the two elements were sealed off in an evacuated quartz tube, heated to the desired temperature and quenched; in the remaining cases melting was conducted in a hydrogen atmosphere. Microscopic examination of the ingots showed a relatively uniform distribution of the phases in each case. Filings of these ingots were then made and annealed in vacuo for several days or, in some cases, weeks to allow equilibrium to be reached. These final annealing temperatures are recorded in Table I. It is to be emphasized that every care was exercised, (1) to maintain the original purity of the materials, (2) to provide adequate opportunity for any reaction or solution phenomena to take place, and (3) to permit final equilibrium relations to be established.

Results and Discussion

The experimental results are summarized in Table I. All results are included except those from photographs on which the lines did not permit accurate measurement or of alloys which had separated into two distinct layers before solidification. The main result has already been mentioned, namely, that no clear-cut evidence of solid solution was found and for none of the systems examined did the films contain lines other than these corresponding to the two elements of the system.

Arrivant[2] found silver to dissolve in solid silicon to the extent of 10 percent.[3] The maxi-

[2] Arrivant, Comptes Rendus **147**, 859 (1908). Cf. L. Loskiewicz, Congr. Intern. Mines (Liege 22–28 June, 1930).

[3] According to J. L. Haughton (personal communication) the original thermal diagram by Arrivant has been incorrectly reproduced in Int. Crit. Tab. **2**, 422.

TABLE I.

Alloying element	% Si	Final anneal Temp. °C	*Lattice Constants* Alloying element	Silicon
	Pure Si	—	—	*5.4170*
Ag	Pure Ag	—	*4.0765*	—
	5.0	825	4.0769	5.4174
	40.0	635	4.0765	5.4176
	40.0	635	4.0768	5.4186*
	40.0	635	4.0771	5.4173
	40.0	825	4.0769	5.4181*
	50.0	770	4.0764	5.4167
	70.0	635	4.0773	5.4175
	80.0	825	†	5.4176
	85.0	750	4.0761*	5.4174
Pb	Pure Pb	—	*4.9385*	—
	50.0	130°	4.9375	5.4156
	50.0	150°	4.9382	5.4160
Au	Pure Au	—	*4.0693*	—
	50.0	240°	4.0682	5.4176
			a *c*	
Sn	Pure Sn	—	*5.8167* *3.1728*	—
	12.0	595°	5.8156* 3.1744*	5.4165
	50.0	150°	5.8178 3.1728	5.4184
	80.0	595°	5.8151* 3.1748*	5.4174
Zn	Pure Zn	—	*2.6581* *4.9341*	—
	50.0	275°	2.6578 4.9353	5.4164
Cd	Pure Cd	—	*2.9713* *5.6046*	—
	50.0	257°	2.9709 5.6058	5.4181
Sb[1]	Pure Sb	—	*4.295* *11.247*	—
	40.0	595°	4.296* 11.247*	†
	50.0	580°	4.297 11.243	5.4176
	80.0	595°	4.296 11.250	5.4182
Bi[1]	Pure Bi	—	*4.535* *11.836*	—
	50.0	240°	4.534 11.830	5.4161

* Value uncertain due to poor lines.

† Lines present but too poor to measure.

[1] Reported in terms of hexagonal axes instead of usual rhombohedral axes.

mum solubility from the results of Table I would be of the order of 0.2 percent by weight.

For the antimony alloys, R. S. Williams[4] found a solid solution of antimony in silicon up to 1 percent by weight and of silicon in antimony up to 0.3 percent. He also found that bismuth dissolved up to 0.8 percent of silicon. The present results indicate that the solubility of antimony in silicon is under 0.5 percent by weight. Rough calculation shows that the presence of 0.3 percent Si in antimony or 0.8 percent in bismuth would change the lattice constants of these two elements by approximately 0.25 percent and 1.5 percent respectively and it is evident from Table I that no such change has occurred. A probable reason for the difference between the older results and the present is the greater purity of the silicon used in this investigation. The silicon used by Williams, for example, contained 0.95 percent Fe and 0.4 percent Al.

The failure to find any solubility in the Au-Si system agrees with the work of Di Capua.[5] Tamaru's[6] similarly negative results in Pb-Si and Sn-Si are also confirmed.

Note added in proof: In view of the facts (1) that the preparation of silicon of a high degree of purity has been developed only during the last few years and (2) that many of the binary alloy systems of metallic elements with silicon have not yet been systematically investigated, it is of some interest to inquire what metallic elements may be expected to form compounds or extensive solid solution with silicon. In this connection it is interesting to note that silicon has been observed to form compounds with all of the first twenty elements of the periodic system except its immediate neighbors Al and P, the rare gases, and the two alkali metals Na and K. In the case of Al a small range of solid solution of silicon in aluminum is observed at high temperatures. The alloys of the alkali and alkaline earth metals with silicon, excepting Li and Ca, appear not to have been studied. Of the metallic elements remaining in the periodic system, compound formation or extensive solid solution may be expected only in the alloys with transition elements, i.e., elements having incomplete inner electron shells (atomic numbers 21–28, 39–46, 57–78). The only thoroughly established exception to this statement known to the writers is copper and it has been observed by other workers that this element in alloys sometimes exhibits the behavior of a transition element. The basis for these generalizations was found chiefly in the results of x-ray structure analysis.

[4] R. S. Williams, Zeits. f. anorg. Chemie **55**, 1 (1907).

[5] Di Capua; Atti della reale accademia nazionale dei Lincei **291**, 111 (1920). Cf. L. Loskiewicz, reference 2, who finds that Si dissolves to a limited extent in Au.

[6] S. Tamaru, Zeits. f. anorg. Chemie **61**, 40 (1909).

Oil Lenses on Water and the Nature of Monomolecular Expanded Films

IRVING LANGMUIR, *General Electric Company, Schenectady, New York*

(Received September 8, 1933)

A higher hydrocarbon, such as tetradecane, on the surface of water forms a circular lens. The condition for the formation of such stable lenses is that the spreading coefficient $F_S=\gamma_1-\gamma_2-\gamma_{12}$ shall be negative. As the volume of the oil lens is increased, the thickness t at the center slowly approaches a limiting value given by $t_\infty^2=-2F_s\rho_1/g\rho_2(\rho_1-\rho_2)$. Equations are given by which F_S can be accurately determined from measurements of the radii of large lenses of known volume. The magnitude of the linear tension at the lens boundary is also calculated. Experiments with tetradecane on water at 25°C give $F_S=-6.2$ dynes cm^{-1} and $\gamma=26.9$. When hydrophilic molecules are introduced into the interface between the lens and the water, they give a spreading force F_{12} which causes a decrease in $-F_S$ and in t. When $t<0.1$ mm gravitational effects are negligible and the lens degenerates into a *duplex film*. If such a film is confined by a movable barrier (piston), the force per unit length F exerted on the barrier is equal to F_S. If the adsorbed molecules at the interface give a force F_{12} in accord with the gas laws, then $(F-F_0)(a-a_0)=kT$ gives the equation of state of the duplex film, where F_0 is the value of F_S in the absence of hydrophilic substances. It is shown that this equation applies to expanded oil films on water and that these are properly regarded as duplex films although they are monomolecular. The presence of a kink in the observed $F-a$ curves is attributed to the sudden appearance of micelles, each containing β-molecules when F_{12} rises to a critical value. For the fatty acids on dilute HCl, $\beta=13$. This small value is due to the crowding apart of the heads because of hydration. The esters show little or no hydration and $\beta=60$. The heat of formation of the micelles in the fatty acids is found to be $5.5+0.24n$ kg cal. per mole where n is the number of carbon atoms. The values of F_0 and a_0 for various substances are determined from data given by Adam.

FATTY acids and similar organic substances spread over the surface of water to form monomolecular films in which the active groups or heads are in contact with the water while the hydrocarbon chains or tails form a layer above the plane containing the heads. When such films are compressed by a force F (dynes per cm), they form condensed films having an area $20.5A^2$ for each molecule. This area is identical with the cross-sectional area of the molecules in stearic acid crystals in a plane parallel to that occupied by the heads of the molecules.[1] Since this plane makes an angle of 63° 38′ with the axis of the hydrocarbon chains, there is strong evidence that the hydrocarbon chains in these condensed films of normal fatty acids on water are inclined about 27° from the vertical.

With the lower fatty acids, such as lauric and myristic acids, when the films are only slightly compressed, they occupy much larger areas than $20.5A^2$. There are many different substances which give, under these conditions, a rather definite area of about $50A^2$ per molecule. Adam has called these films liquid expanded films. The tendency to form these expanded films increases as the hydrocarbon chain is shortened, or as the temperature is raised, the effect of each additional CH_2 group in the chain being equivalent to a lowering of temperature of about 8°C.

In two papers[2, 3] in 1925 I offered an explanation of the existence of these expanded films. I pointed out that in these films there are really two surfaces which form the upper and lower boundaries of the hydrocarbon part of the film. Since the thicknesses of these films are several times that of the hydrocarbon chain, the region between these boundaries must be regarded as essentially a typical hydrocarbon liquid in which the molecules possess all the natural freedom of motion of such liquids with the single restriction

[1] Alex. Müller, Proc. Roy. Soc. (London) **A114**, 542 (1927).

[2] I. Langmuir, Colloid Symposium Monograph **3**, 48 (1925).

[3] I. Langmuir, an article, *The Effects of Molecular Dissymmetry on the Properties of Matter*, in a book entitled *Colloid Chemistry*, Jerome Alexander, **1**, 525 (1926).

that the molecules are constrained to keep one end in contact with the lower surface. A higher normal hydrocarbon liquid on a water surface does not spread; it must therefore require a definite spreading force F to pull a hydrocarbon liquid out over a water surface to form an expanded film. Such a force must have its origin in some property imparted by the heads. At the interface between the hydrocarbon liquid and the underlying water there are, in the case of a fatty acid film, carboxyl groups. Even if these do not exert repulsive forces on one another, they should at least tend to spread within the available surface as a two-dimensional gas, and thus exert a two-dimensional gas pressure F which will counteract the normal tendency of the hydrocarbon layer to draw together.

It was shown that this theory leads to an equation of state of the form

$$(F-F_0)(a-a_0)=kT.$$

By taking the values $F_0=-13$ and $a_0=18$, this gave very satisfactory agreement with Adam's early data[3a] for myristic acid at 32.5°. This theory as given in the papers referred to was presented briefly in about four pages and there was no detailed analysis of the experimental curves.

Adam has definitely rejected this theory.[4] For example, in his book he says:

> Langmuir suggested that the molecules adhere by their chains, and that the heads are in a state of constant agitation, the chains tending to make a condensed, and the heads a gaseous film. But since it is not the length of the chains, but the nature of the heads, which determine whether the films are liquid or vapor expanded, and since those heads which probably have the greatest attraction for one another laterally form liquid expanded films, a better suggestion seems to be the reverse of Langmuir's, *that the heads tend to hold the molecules together, while the chains try to disrupt the film.*

Adam considers, however, that "the detailed structure of the liquid expanded films is difficult to decide."

Rideal[5] offers no explanation of expanded films and does not accept those previously proposed by the writer.

The evidence in support of the theory proposed is, however, so striking that it needs to be presented in more detail than has been done previously. It is clear that Adam has misunderstood the theory and does not see its widespread application to his own experimental data. A recent more thorough examination of Adam's published results has led me to extend the theory that I proposed in 1925 so that it now seems to offer a nearly complete theory of all observed characteristics of expanded films.

Characteristics of Typical Monomolecular Films

The complete curve giving F as a function of a, the area per molecule, such as that represented by Fig. 1, represents essentially an equation of state for a 2-dimensional system which may

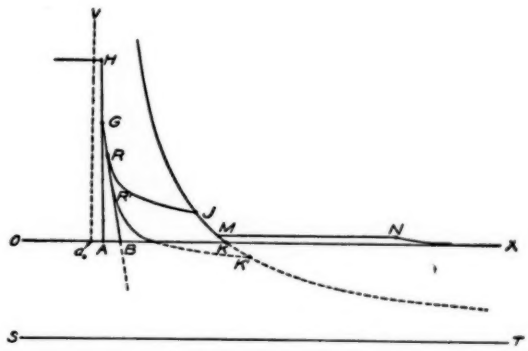

FIG. 1. Diagram of F–a curves for typical monomolecular films.

contain gas, liquid and solid phases. The lines shown in Fig. 1 may not all be observable with any single substance for reasons that will be discussed later. Since only positive values of F are directly observable, all those portions of the curves which correspond to negative values in Fig. 1 can be inferred only from theoretical considerations.

The line AGH corresponds to a typical condensed film such as that of stearic acid on pure water at room temperature. When such fatty acids are placed on water containing dilute hydrochloric acid, a break occurs at G so that the curve below G is given by BG. Adam believes

---

[3a] N. K. Adam, Proc. Roy. Soc. **A101**, 516 (1922).

[4] N. K. Adam, *Physics and Chemistry of Surfaces*, Clarendon Press (1930), page 75.

[5] E. K. Rideal, *Introduction to Surface Chemistry*, Cambridge University Press, pp. 101–104.

that the area corresponding to B is that of the heads of the molecules.

With a liquid expanded film such as myristic acid on dilute hydrochloric acid, the observed $F-a$ curve leaves the line GB near R and gradually flattens out as it approaches J where there is a sharp kink, and it then falls more rapidly along a line JK to a definite point M. It then extends horizontally along the line MN until at some point N it begins to fall again approaching the horizontal axis asymptotically as a continues to increase. The theory proposed in 1925 indicated that the line JK is part of a rectangular hyperbola in which the horizontal asymptote ST lies at a distance F_0 below the horizontal axis OX, and the vertical asymptote is represented by the dotted line at V corresponding to an abscissa a_0.

It is the plan of the present paper to develop a theory which gives the mechanism underlying each part of the broken line shown in Fig. 1, and by which quantitative information regarding the fundamental properties of molecules may be obtained.

Large Free Lenses of Oil on Water

Let us consider the conditions for equilibrium between a pure water surface (I) and a thin layer of an oil (II) placed upon the water. We assume provisionally that the film, although of a thickness large compared to that of the oil molecules, is yet so thin that gravity plays no appreciable part in causing it to flow out over the surface. We are then surely justified in assuming that the oil film has an upper surface (surface tension γ_2) and a lower surface (interfacial tension γ_{12}) which do not influence one another.

For equilibrium between this thin oil film and the water it is necessary that the surface tension γ_1 of the water shall balance the sum of γ_2 and γ_{12} for the film. Let us put

$$F_S=\gamma_1-\gamma_2-\gamma_{12}. \tag{1}$$

If $F_S>0$, that is, if γ_1 is greater than $\gamma_2+\gamma_{12}$, the oil spreads over the water until it covers the whole surface or until the film becomes so nearly monomolecular that $\gamma_2+\gamma_{12}$ increases to the value γ_1.

If $F_S<0$, the oil film contracts and gathers into one or more lenses of such thickness that gravity can prevent any further contraction. Harkins has called F_S the spreading coefficient.

Harkins' data[6] for normal chain hydrocarbons on water show that F_S is $+3.3$ for hexane, 1.7 for heptane, and 0.3 (dynes cm^{-1}) for octane. No data seem to be available for γ_{12} or F_S for the higher liquid hydrocarbons. If, however, the rate of decrease of F_S per CH_2 observed by Harkins continues beyond octane, the value of hexadecane should be $F_S=-11.7$. For paraffin oil (Squibbs' petrolatum) which probably consists mostly of saturated cyclic hydrocarbons, Harkins[6] has found $F_S=-13.69$ at 20°C.

A simple direct method for determining F_S for nonspreading substances consists in measuring the diameters D of very large lenses formed when known volumes V of oil are placed on surfaces of water. Except when the density of the oil is very close to that of water, the curvature of the interface between the oil and the water becomes negligible at a distance of 2 or 3 cm from the edge of the lens. For lenses of a diameter greater than about 6 cm, the central part of the lens is thus of a uniform thickness. For a series of lenses of increasing radius R, the central thickness t slowly approaches a limiting value t_∞ which may be readily calculated by the following method.

Let z be a coordinate which measures vertical distances upward from the plane of the water surface (far from the boundary of the lens). Then since the oil is lighter than water (and only such oils can form large lenses), Z_2, the level of the upper surface of the lens, will have a positive value. The pressure at the lower surface (the interface) at Z_{12} must be the same as in the water phase at the same level. This condition gives

$$Z_2=t(\rho_1-\rho_2)/\rho_1 \tag{2}$$

and

$$Z_{12}=-t\rho_2/\rho_1, \tag{3}$$

where ρ_1 is the density of the water and ρ_2 that of the oil.

Consider now a lens so large that the curvature of the boundary is negligible. The *total* force per unit length acting across a portion of a vertical plane cutting the lens far from the boundary consists of the surface tension forces $\gamma_1+\gamma_{12}$ and

[6] W. D. Harkins, Colloid Symposium Monograph 6, 26 (1928).

the hydrostatic liquid pressures. From the free surface down to the depth y in any liquid this latter force is the pressure integral $\int p\,dy$ and is thus equal to $(1/2)g\rho y^2$. Thus down to the interface at Z_{12} the total spreading force per unit length in the central part of the large lens is

$$F_2=(1/2)g\rho_2 t^2-\gamma_2-\gamma_{12}. \tag{4}$$

For equilibrium, this must equal the spreading force F_1 in the water, remote from the lens boundary, down to the same depth Z_{12}. This force is

$$F_1=(1/2)g\rho_1 Z_{12}^2-\gamma_1. \tag{5}$$

Equating F_2 and F_1, eliminating Z_{12} by Eq. (3), and combining with Eq. (1) we have

$$t_\infty^2=-2F_S\rho_1/g\rho_2(\rho_1-\rho_2). \tag{6}$$

From a knowledge of t_∞ we can thus calculate the spreading coefficient F_S. The actual thickness t at the center of a lens, however, often differs from t_∞ by as much as one percent even for lenses as large as 60 cm in diameter. This is due to the fact that there is a linear tension f (a one-dimensional analogue of pressure) along the perimeter of the lens acting to keep the lens in a circular form. This force, which is of considerable magnitude (6.5 dynes for paraffin oil on water) must be balanced by an increase in the spreading force F_2-F_1 by means of an increase in t, just as the surface tension in a soap bubble is balanced by the increased air pressure within the bubble. This effect can be taken into account by subtracting a term f/R from the 2nd member of Eq. (4) before equating to F_1. In this way we obtain

$$t^2=t_\infty^2(1-f/F_SR). \tag{7}$$

Calculation of the Linear Tension of a Cylindrical Lens Boundary

A plane through the vertical axis of symmetry of a large lens cuts the free surfaces and the interface in the manner illustrated in Fig. 2. As R is made to increase indefinitely, the surfaces represented by the meridian curves in this figure become noncircular cylinders with horizontal elements.

Consider now the horizontal forces acting across a vertical plane which is perpendicular to the meridian plane, but near the lens boundary. Let α be the angle which the tangent to any meridian makes with a horizontal plane and let y be the vertical distance of any point from the horizontal plane at which $\alpha=0$.

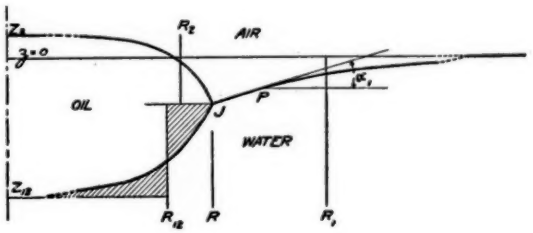

Fig. 2. Profile of a lens on water.

If we take the spreading force F (associated with any surface) to be zero when the surface is horizontal ($\alpha=0$), then we have for the spreading force F_r in a radial direction

$$F_r=\gamma(1-\cos\alpha)-\tfrac{1}{2}g\rho y^2. \tag{8}$$

For equilibrium, with a truly cylindrical lens boundary, F_r must be constant and hence equal to zero. Thus putting $F_r=0$ we obtain

$$y^2=a^2(1-\cos\alpha), \tag{9}$$

where a is the Laplace capillary constant defined by

$$a^2=2\gamma/g\Delta\rho \tag{10}$$

and $\Delta\rho$ is the difference of density on the two sides of a phase boundary. Eq. (9) may also be written

$$y=2^{\frac{1}{2}}a\sin(\alpha/2). \tag{11}$$

An equation of this form holds for each of the three surfaces.

Now consider the horizontal forces acting across the meridian plane near a lens boundary. Here the surface tension force per unit of horizontal distance is $\gamma/\cos\alpha$ (instead of $\gamma\cos\alpha$ in the former case) and thus we have

$$F_T=\gamma(1-1/\cos\alpha)-\tfrac{1}{2}g\rho y^2. \tag{12}$$

Eliminating y by using Eq. (8) after putting $F_r=0$ we have

$$F_T=\gamma(\cos\alpha-1/\cos\alpha)=-\gamma\sin^2\alpha/\cos\alpha. \tag{13}$$

There is thus a negative spreading force (tension) in a horizontal direction which is perpendicular to that of the slope of the surface. The tension f corresponding to any one of the three surfaces that meet at the lens boundary at J

is obtained as an integral $\int F_T dx$. We may put

$$dx=(dx/dy)\cdot(dy/d\alpha)d\alpha,$$

in which $dx/dy=\cos\alpha/\sin\alpha$ and

$$dy/da=a\sin\alpha/a(1-\cos\alpha)^{\frac{1}{2}}.$$

With the value of F_T from Eq. (13) we thus find

$$f=(\gamma a/2)\int \sin^2\alpha(1-\cos\alpha)^{-\frac{1}{2}}d\alpha$$

or

$$f=(2(2)^{\frac{1}{2}}/3)\gamma a[1-\cos^3(A/2)]. \quad (14)$$

Here the integration has been carried from $\alpha=0$ to A, the angle α at the junction J where the three surfaces meet. The total linear tension acting along the perimeter of the lens is the sum of three terms

$$f=f_1+f_2+f_{12} \quad (15)$$

found from Eq. (14) by inserting the appropriate values of a and A. Since A is a rather small angle in most cases, it is useful to expand Eq. (14) in powers of A obtaining

$$f=(2^{\frac{1}{2}}/4)\gamma a A^2[1-(7/48)A^2+\cdots]. \quad (16)$$

The Meridian Curves at a Lens Boundary

The effect of the linear tension in modifying the profile curves shown in Fig. 2 for lenses of moderate size may now be determined. A horizontal plane through the junction J allows us to apply our equations separately to the three phase boundaries. Consider, for example, the free water surface. For a lens of moderate size the spreading force F_R given by Eq. (8) is not everywhere zero as in the cylindrical case but at any point P where α differs appreciably from zero, it must have a value which balances the effect of the linear tension of the parts of the surface outside of P. We may thus put

$$F_R=f_1/R_1 \quad (17)$$

where R_1 is an effective radius at which the tension may be regarded as being concentrated. In Fig. 2 the positions of R_1, R_2, and R_{12} have been chosen so that the two shaded areas (shown only for R_{12}) are equal. This assumption gives for moderate values of A

$$R_1=R+a_1/2^{\frac{1}{2}}. \quad (18)$$

Combining Eqs. (8), (17) and (10) we thus obtain[7]

$$z_1^2/a_1^2=1-\cos\alpha_1-f_1/\gamma_1 R_1 \quad (19)$$

in place of Eq. (9). It should be noted that the value of f_1 in this equation is to be obtained from Eq. (14) by replacing A by α_1. Similarly for the other two surfaces we have

$$(z_2-z_0)^2/a_2^2=1-\cos\alpha_2+f_2/\gamma_2 R_2 \quad (20)$$

and

$$(z_0-z_{12})^2/a_{12}^2=1-\cos\alpha_{12}+f_{12}/\gamma_{12}R_{12}, \quad (21)$$

where R_2 and R_{12} are obtained from equations like (18) except that the sign of the last term is reversed.

If we apply Eqs. (19), (20) and (21) to the junction J in Fig. 2, we obtain

$$z_0^2/a_1^2=1-\cos A_1-f_1/\gamma_1 R_1, \quad (22)$$

$$(Z_2-z_0)^2/a_2^2=1-\cos A_2+f_2/\gamma_2 R_2, \quad (23)$$

$$(z_0-Z_{12})^2/a_{12}^2=1-\cos A_{12}+f_{12}/\gamma_{12}R_{12}. \quad (24)$$

Expanding the first members of the last two equations, combining with the first equation so as to eliminate z_0, and eliminating Z_2 and Z_{12} by Eqs. (2) and (3) we obtain

$$\tfrac{1}{2}gt^2(\rho_1-\rho_2)\rho_2/\rho_1=-(\gamma_1-\gamma_2-\gamma_{12})+(\gamma_1\cos A_1-\gamma_2\cos A_2-\gamma_{12}\cos A_{12})+(f_1/R_1+f_2/R_2+f_{12}/R_{12}). \quad (25)$$

For equilibrium between the horizontal components of the surface tensions at the junction J we must have

$$\gamma_1\cos A_1=\gamma_2\cos A_2+\gamma_{12}\cos A_{12}. \quad (26)$$

Using this relation and introducing F_0 by Eq. (1) into Eq. (25) we find

$$t^2=[2\rho_1/g\rho_2(\rho_1-\rho_2)][-F_S+(f_1/R_1+f_2/R_2+f_{12}/R_{12})], \quad (27)$$

which agrees with Eqs. (6) and (7) except that the effective radii R_1, R_2 and R_{12} are now no longer identified with R.

---

[7] If the values of f_1 and R_1 by Eqs. (14) and (18) are inserted in these equations they may readily be shown to be identical with a rather complicated equation given by Poisson in his book *Nouvelle Theorie de l'Action Capillaire* as quoted in the Handb. der Exp. Physik **VI**, 98 (1928).

Volume of Lens

If the lens is of sufficient size to give a uniform thickness t in the central part then the volume V is

$$V=\pi R^2 t-\pi R(a_{12}^2 \sin A_{12}-a_2^2 \sin A_2). \quad (28)$$

This may be understood readily from the fact that the vertical component $\gamma \sin A$ of the surface tension at the junction multiplied by the perimeter $2\pi R$ must be the buoyant force $\rho g \Delta V$ of the displaced volume ΔV resulting from the deviations of the surface from the horizontal.

Contact Angles and the Values of A

The relation of the angles A_1, A_2 and A_{12} at the junction J to the contact angles is given in Fig. 3. The angles subtended by the three phases at the

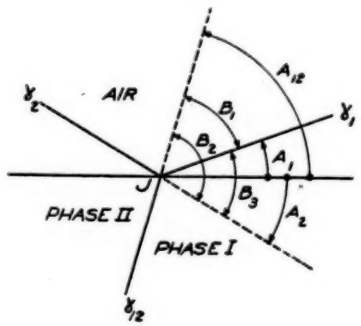

Fig. 3. Contact angles at a lens boundary.

junction J are $\pi-B_1$, B_2 and $\pi-B_3$. These angles are related to the three surface tensions by

$$\cos B_1=(\gamma_1^2-\gamma_2^2+\gamma_{12}^2)/2\gamma_1\gamma_{12}, \quad (29)$$

$$\cos B_3=(\gamma_1^2+\gamma_2^2-\gamma_{12}^2)/2\gamma_1\gamma_2, \quad (30)$$

$$B_2=B_1+B_3. \quad (31)$$

Combining these equations with Eq. (1) we have

$$\sin^2 (B_1/2)=-F_S(2\gamma_2+F_S)/4\gamma_1\gamma_{12}, \quad (32)$$

$$\sin^2 (B_3/2)=-F_S(2\gamma_{12}+F_S)/4\gamma_1\gamma_2. \quad (33)$$

Thus the angles approach zero as $-F_S$ decreases to zero. From Fig. 3 we see that

$$A_2=A_1-B_3, \quad (34)$$

$$A_{12}=A_1+B_1. \quad (35)$$

The value of A_1 may be obtained from Eqs. (22) to (24). Taking A to be a sufficiently small angle so that $(1/24)A^2$ can be neglected in comparison with unity, we may expand $1-\cos A$ in Eqs. (22) and (23). Introducing the values of f from Eq. (16) after inserting the value of R_1, etc., from Eq. (18) and eliminating Z_2 and Z_{12} by Eqs. (2) and (3), we may obtain from Eqs. (22) and (23) the following

$$b_1A_1=-2^{\frac{1}{2}}z_0, \quad (36)$$

$$b_2A_2=-2^{\frac{1}{2}}[(\rho_1-\rho_2/\rho_1)t-z_0], \quad (37)$$

where

$$b_1=a_1[1-(2^{\frac{1}{2}}/4)a_1/R+(3/16)a_1^2/R^2] \quad (38)$$

and

$$b_2=a_2[1+(2^{\frac{1}{2}}/4)a_2/R+(3/16)a_2^2/R^2]. \quad (39)$$

Eliminating z_0 we obtain a single equation in A_1 and A_2. By Eq. (34) we may then eliminate A_2 and obtain

$$A_1=\frac{b_2B_3-(\rho_1-\rho_2)2^{\frac{1}{2}}t/\rho_1}{b_1+b_2}. \quad (40)$$

Measurements of the Diameters of Lenses

By placing measured volumes (or weights) of oil on a water surface and measuring the diameters of the circular lenses that are formed, a series of values of V and R in Eq. (28) are obtained. By inserting the values of t from Eq. (7) or (27) and dividing by πR^2, this equation may be put in the form

$$V/\pi R^2=t_\infty-C_1/R+C_2/R^2, \quad (41)$$

where C_1 and C_2 can be expressed in terms of the angles $A_{1\infty}$ and $A_{2\infty}$, the values of A_1 and A_2 for a lens of very large diameter. Experimentally we may thus obtain t_∞ by plotting the average lens thickness $V/\pi R^2$ against $1/R$ and extrapolating back to the intercept t_∞ at $1/R=0$. This extrapolation may be greatly facilitated by knowledge of the theoretical values of C_1 and C_2 that can be obtained by the foregoing methods, from even approximate values of γ_1, γ_2 and γ_{12}. From the values of t_∞ thus obtained, F_S may be calculated from Eq. (6). If γ_1 and γ_2 are known, γ_{12} can then be determined from Eq. (1), and in this way new values of A_1, C_1 and C_2 can be obtained for more accurate calculations of t_∞.

The measurements of the diameters of lenses thus provide a method of determining the interfacial surface tension γ_{12}. The method becomes increasingly accurate as F_S approaches zero. Instead of calculating A_1 by Eq. (40) from surface tension data, it is very easy to make direct accurate measurements of A_1 and A_2 by an optical goniometer sighted at the junction J of large lenses. Of course such measurements by themselves give B_3 by Eq. (34) and thus by Eq. (30) give γ_{12} when γ_1 and γ_2 are known, but when F_S is small, still greater accuracy can be obtained by combining these measurements with determinations of the lens diameters.

It is also a simple matter to measure directly the linear tension f_∞ for a boundary of zero curvature and thus determine the relation of t and t_∞. This may be done by inserting two parallel vertically placed metal strips into a lens on water. One of these strips is attached to the vertical pointer of a balance (a balance to measure horizontal forces). The second strip may then be moved away from the first one so that the lens becomes so distorted as to become approximately rectangular with parallel sides. The force exerted on the other strip as indicated by the balance, is thus $2f_\infty$.

If such measurements of f_∞ are combined with direct measurements of t, t_∞ and thus F_S may be determined by Eqs. (7) and (6) without needing to know the angles A. By using two sharp points attached to micrometers arranged so that one point can be brought in contact with the upper and the other with the lower surface, accurate measurements of t can be made.

These various methods thus provide us with accurate determinations of γ_{12}. They have the advantage over the drop weight method usually used, that they are purely static methods and that they permit us to study the effects of known amounts of adsorbed substances at the interface by the methods which will be described in a later section.

Experimental Data on the Diameters of Lenses

Weighed amounts of Squibb's Petrolatum were placed on a large tray (45×75 cm) full of distilled water at 24°C, which was then covered by a sheet of glass to eliminate air currents. The diameters of the lenses were measured to 0.1 mm. The values of $V/\pi R^2$, plotted as a function of $1/R$, are indicated in Fig. 4 by small circles.

The family of curves in this figure represent the calculated relation of $V/\pi R^2$ to $1/R$ according to Eq. (28) based upon the various assumed values of γ_{12} which are given on the curves. It is seen that the experimental points, except for lenses of small diameter, agree with the curve for $\gamma_{12}=53.0$ dynes cm^{-1}. The value of $t_\infty=0.4806$ cm, given by the intercept of this curve on the $V/\pi R^2$ axis, corresponds to $F_S=-11.37$.

Harkins[6] found for this oil at 20°C, by the drop weight method, $\gamma_2=31.12$; $\gamma_{12}=55.32$, $F_S=-13.69$. This high value of γ_{12} is incompatible with our measurements on lenses. To find whether impurities were present in the oil which could lower γ_{12}, a portion was shaken with Fuller's earth and centrifuged, but the lens diameter remained unchanged. We have checked Harkins' value of γ_2 by Wilhelmy's method obtaining $\gamma_2=30.8$ at 23.5°C, which should correspond to 31.1 at 20°C.

The method of calculating the curves in Fig. 4 may be illustrated by the curve for $\gamma_{12}=53.0$. Taking $\rho_2=0.8849$ (measured at 20°C), $\rho_1=0.9982$, $\gamma_1=72.75$ we find by Eq. (1), $F_S=-11.37$ and by Eq. (6) $t_\infty=0.4806$. By Eq. (10) we get $a_1=0.3949$; $a_2=0.2681$; $a_{12}=0.9768$. Eqs. (32) and (33) give $B_1=0.3894$; $B_3=0.7039$ radians. By Eq. (40) for $R=\infty$ we find $A_1=0.1682$ and Eqs. (34) and (35) give $A_2=-0.5337$; $A_{12}=0.5576$. By Eq. (16) we obtain $f_1=0.29$; $f_2=0.81$; $f_{12}=5.44$, and by Eq. (15) $f=6.54$. Substituting these values into Eq. (27), taking the square root and expanding as a series in powers of $1/R$ we have

$$t=0.4806(1+0.288/R+0.127/R^2).$$

From this, by Eqs. (40), (38) and (39) we find

$$A_1=0.1676(1+0.0063/R)$$

and similar expressions for A_2 and A_{12} by Eqs. (34) and (35). Finally Eq. (28) gives

$$V/\pi R^2=0.4806-0.4029/R+0.0602/R^2,$$

which is the equation of the uppermost curve in Fig. 4.

Some measurements were also made of lenses of purified tetradecane on water at 25°C. The

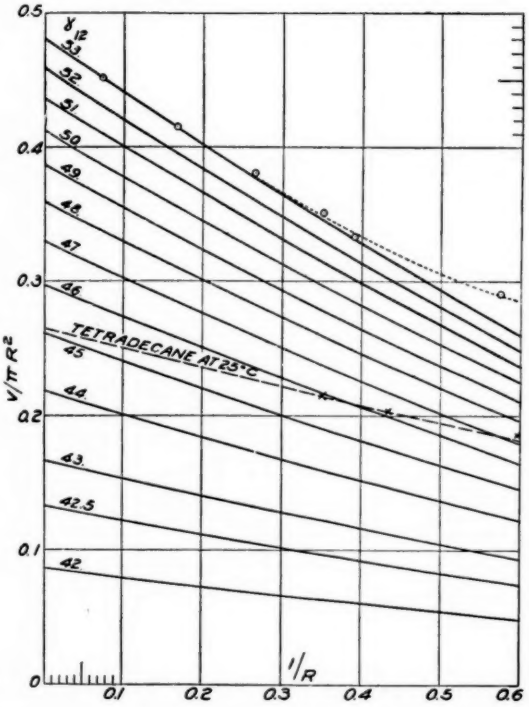

FIG. 4. Calculated curves giving $V/\pi R^2$ (in cm) as a function of $1/R$ (in cm^{-1}) for lenses of petrolatum on water at 20°C taking $\gamma_2 = 31.12$ and the values of γ_{12} marked on the curves. The dashed line is calculated for tetradecane on water at 25°C with $\gamma_2 = 26.9$, $\gamma_{12} = 51.3$. The experimental data for petrolatum are marked by circles and for tetradecane by crosses.

tetradecane from Eastman was found to spread actively on water indicating the presence of hydrophilic substances equivalent to about one percent of stearic acid. Purification was tried by shaking with fuming sulphuric acid and washing with water. About 6–8 treatments gave a sample that did not spread. Agitation with Fuller's earth, and removal of the latter by centrifuging, was found to be far more convenient and effective. The purified material behaves markedly different when placed on water: it does not spread and a large lens shows extraordinary tendencies to break up into small lenses, for example, when touched by a clean wet stirring rod. The points marked by crosses in Fig. 4 give the results of these measurements.

The surface tension γ_2 of tetradecane at 23.5°C by Wilhelmy's method was found to be 27.0 corresponding to 26.9 at 25°C. By choosing various values for γ_{12} and calculating curves for $V/\pi R^2$, it was found that best agreement with the data was obtained with $\gamma_{12} = 51.3$. This curve is shown as a dashed line in Fig. 4. The data for tetradecane on water at 25°C are: $\rho_1 = 0.9970$; $\rho_2 = 0.7615$; $\gamma_1 = 72.0$; $\gamma_2 = 26.9$; $\gamma_{12} = 51.3$; $F_S = -6.2$; $a_1 = 0.3840$; $a_2 = 0.2690$; $a_{12} = 0.667$; $B_1 = 0.2846$; $B_3 = 0.5626$; $A_1 = 0.0908$; $A_2 = -0.4718$; $A_{12} = 0.3754$; $f_1 = 0.080$; $f_2 = 0.53$; $f_{12} = 1.66$; $f = 2.30$; $A_1 = 0.0908\ (1 - 0.004/R)$; $t = 0.265\ (1 + 0.187/R + 0.053/R^2)$; $V/\pi R^2 = 0.265 - 0.147/R + 0.0141/R^2$.

Effect of Adsorbed Hydrophilic Molecules at the Interface of a Free Lens

It is possible by the following technique to introduce known numbers of molecules of certain hydrophilic compounds into the interface between the lens and the water. A large lens (about 10 to 20 cm in diameter) is placed on the surface of water in a wide tray equipped with a horizontal balance to measure surface forces.[8] The movable barrier is pushed back and a definite amount of a benzol solution of a spreadable substance, for example, stearic acid, is placed on the water, taking care that the amount added is insufficient to cover the available water surface. By advancing the barrier, the monomolecular stearic acid film can be compressed and pushed into the lens while the force F can be measured by the balance. If an equilibrium state is reached, measurements of the total area (determined by the barrier), the area of the lens, and the surface concentration of the film on the water give data for calculating the number of molecules introduced into the lens.

Instead of attempting to obtain equilibrium between the hydrophilic molecules on the water surface and those in the interface, it is usually better after introducing a desired number of molecules into the interface to remove the excess of hydrophilic material from the water surface (so that $\gamma_1 = \gamma_w$). The escape of these molecules from the lens is usually such a slow process that it does not cause appreciable loss during measurements of the lens diameter.

The molecules thus introduced into the lens, if their number is not too great, distribute them-

[8] I. Langmuir, J. Am. Chem. Soc. **39**, 1848–1906 (1917). See especially p. 1869.

selves uniformly over the interface under the lens, and lower the interfacial tension γ_{12} (without changing γ_2) and thus cause a change in the radius of the lens. From a family of curves such as that shown in Fig. 4, it is then possible from measurements of R and V to determine γ_{12}.

The lowering of the surface tension of pure water by the presence of adsorbed molecules may be usefully regarded as being due to a spreading force F of the two-dimensional gaseous or liquid adsorbed film. Similarly at the interface between water, w, and a hydrocarbon oil, R, we may put

$$F_{12}=\gamma_{wR}-\gamma_{12}, \tag{42}$$

where γ_{wR} represents the interfacial surface tension between pure water and pure hydrocarbon when no hydrophilic substances are present in the interface.

In this way the two-dimensional equation of state of adsorbed molecules at a water-oil interface can be studied in much the same way as has previously been done at the air-water surface.

If the applied surface pressure is sufficiently increased, the molecules can be crowded into the lens in such numbers that some of them leave the interface and become dissolved in the hydrocarbon phase. The distribution of the molecules between the hydrocarbon phase and the interface for changes in γ_{12} should thus be in accord with Gibbs' equation. In a later paper it is planned to report on these investigations.

Let us consider a hydrocarbon lens which is surrounded by water having an uncontaminated surface, but at whose interface with water there is a known surface concentration σ_{12} of adsorbed hydrophilic molecules. The spreading coefficient F_S, as given by Eq. (1) is then

$$F_S=\gamma_w-\gamma_R-\gamma_{Rw}+F_{12}. \tag{43}$$

Let us denote by F_0 the spreading coefficient for the lens on water when hydrophilic substances are absent so that

$$F_0=\gamma_w-\gamma_R-\gamma_{Rw}. \tag{44}$$

Thus from Eqs. (43) and (44)

$$F_S=F_0+F_{12}. \tag{45}$$

We have seen that for a paraffin oil, lenses are formed which are about 5 mm thick. As σ_{12} is increased by adding hydrophilic molecules to the interface so that F_{12} increases, the thickness of the lens, as given by Eqs. (6) and (45), decreases and must approach zero when F_{12} becomes nearly equal to $-F_0$. Thus at a certain critical concentration of adsorbed molecules, free lenses can no longer exist, for the oil spreads out as a film over the whole of the available water surface (unless it thereby becomes monomolecular in thickness).

Confined Oil Lenses

Let us consider a large free oil lens with an interface containing adsorbed hydrophilic molecules upon an area of clean water in a tray, this area being limited by a movable barrier and a piston. By advancing the barrier the free water surface can be made to disappear so that the lens covers the whole available area. The lens may then be said to be a *confined* lens. If the area is still further decreased, a force F (dynes cm^{-1}) is exerted against the piston. By the same method as was used in the derivation of Eq. (6) and by using Eq. (45) we see that

$$F=F_0+F_{12}+(1/2)g\rho_2 l^2(\rho_1-\rho_2)/\rho_1. \tag{46}$$

By this method of the confined lens it is thus possible to determine F_{12} as a function of σ_{12}. To avoid having the oil creep up onto the piston, it has been found useful to construct a boat-like piston with its edge slightly raised above the water surface. This method for the study of the equation of state of adsorbed molecules at an interface has the following advantages over the free lens method:

(1) It is not limited (as is the free lens method) to the determination of values of F_{12} which are less than $-F_0$.

(2) It permits σ_{12} to be easily and reversibly changed by the movement of a barrier instead of requiring separate experiments involving the production of lenses of different diameters or containing different numbers of hydrophilic molecules.

(3) Because it possesses one more degree of freedom than the free lens method, it permits an independent variation of the film thickness t and so allows any effects dependent on t to be measured.

Duplex Oil Films $F_S > 0$

If the thickness of the oil film used in the confined lens method is less than about 0.1 mm, the last term in Eq. (46) becomes less than about 0.005 dyne cm^{-1} and is therefore negligible. The gravitational effect of film thickness thus disappears. We shall call such films *duplex films*. For these films we then have by Eq. (46)

$$F = F_0 + F_{12}. \tag{47}$$

Since F becomes zero when $F_{12} < -F_0$, we see that by the study of duplex films F_{12} can be determined only when $F_{12} > -F_0$.

The concept of duplex films must evidently be restricted to cases where we are justified in considering that the film has an upper surface and a lower surface (interface) which are distinct from one another. However, in view of the small range of molecular forces, it is to be expected that this condition will be fulfilled until the film becomes at least approximately monomolecular. In a later section we shall discuss the conditions under which monomolecular films may be usefully regarded as being duplex films.

Equation of State of Adsorbed Active Groups at the Interface

The active groups or heads of the molecules of hydrophilic substances present at low concentration in a liquid hydrocarbon on water tend to occupy positions in the interface. The hydrocarbon chains of these hydrophilic molecules, however, being in an environment of other hydrocarbon chains, have no tendency of their own to go to the interface; they are free to move except that one end of the chain must remain attached to the active group at the interface. The thermal agitation of the heads should tend to cause them to become uniformly distributed over the interface. This tendency must manifest itself as a spreading force F_{12} which could be measured by any agent, such as a piston, which interferes with this indefinite spreading. For sufficiently low surface concentration σ_{12} of the heads in the interface, this force F_{12} should be given by the ideal two-dimensional gas law

$$F_{12} = \sigma_{12} kT. \tag{48}$$

In studies of monatomic caesium films on tungsten[9] it has been shown that the finite area occupied by each atom or molecule can be taken into account by modifying this equation to

$$F_{12} = \sigma_{12} kT/(1 - \sigma_{12}/\sigma_M), \tag{49}$$

where σ_M is the maximum concentration corresponding to a close-packed film. If we rewrite this equation in terms of a, the area per molecule instead of the concentration σ we have

$$a = 1/\sigma_{12} \tag{50}$$

and

$$F_{12}(a - a_0) = kT, \tag{51}$$

where a_0 for our present purposes may be regarded as an empirical constant.

It should be noted that this equation is based upon the assumption that there are no attractive or repulsive forces between the heads except those that prevent any two from occupying the same place at the same time.

Of course at higher concentrations (σ_{12}) it is conceivable that attractive forces between the heads might produce large deviations from Eq. (51) and might even cause the heads to condense into a liquid two-dimensional phase within the interface. Let us therefore estimate the magnitude of the forces between the heads and see if they are large enough to cause deviations from Eq. (51).

The dipole moment of the carboxyl group on an aliphatic chain is[10] about 1.4×10^{-18} e.s.u. The vertical component of the dipole moment per molecule for films of fatty acids on water has been found[11, 12] to be about 0.2×10^{-18} e.s.u.

Since the force between electrically charged bodies in a medium of dielectric constant ϵ is only $1/\epsilon$th as great as in free space, the forces between dipoles immersed in water are only 1/80th as great as those given by applying Coulomb's law. This decrease is, of course, due to the orientation of the water molecules, each of which has a dipole moment 1.8×10^{-18}. It is the resulting

---

[9] I. Langmuir, J. Am. Chem. Soc. **54**, 2798–2832 (1932). See Eq. (59).

[10] Smyth and Rogers, J. Am. Chem. Soc. **52**, 1824 (1930).

[11] N. K. Adam and J. B. Harding, Proc. Roy. Soc. **A138**, 411 (1932).

[12] J. H. Schulman and A. H. Hughes, Proc. Roy. Soc. **A138**, 430 (1932).

large attractive force between the water molecules and the carboxyl group that causes the spreading of films of fatty acids on water. Similarly the decrease in the observed dipole moment of the carboxyl group from 1.4 to 0.2 $\times 10^{-18}$ when brought into contact with water is to be looked upon as the effect of the orientation of water molecules, rather than being due principally to an orientation of the carboxyl group itself with respect to the surface as has been suggested by Adam and Harding.

In connection with studies of caesium films on tungsten a general equation has been derived for the spreading force F' resulting from the dipole forces between adsorbed molecules.[9] The equation there given (Eq. (81)) relates to fictitious dipoles resulting from adsorbed ions and their induced images. For the real dipoles of oil films we should multiply the coefficients by 2 and divide by ϵ the dielectric constant so that the equation becomes

$$F' = (2/\epsilon)(3.34\sigma^{5/2}M^2 + 1.53 \times 10^{-5}\sigma^2 T^{1/3} M^{4/3} I), \quad (52)$$

where $I < 0.89$. If we put $M = 1.4 \times 10^{-18}$, $\sigma = 3.3 \times 10^{14}$ corresponding to $a = 30A^2$, $T = 300$ and $\epsilon = 80$, we obtain $F' < 0.7$ dyne cm^{-1} as the effect of the spreading force in modifying F_{12} given by Eq. (51) as a result of the dipole attractions or repulsions between the heads. The value of F_{12} for $a = 30$ and $a_0 = 10$ is 20 dynes cm^{-1}. Considering that the dipoles are probably not so oriented as to produce the maximum attractive or repulsive forces, it appears reasonably certain that the dipole forces in oil films have little effect in modifying Eq. (51) until the heads of the molecules are practically in contact.

Equation of State for Duplex Films

If we ignore the distinction between the upper and lower surfaces of a duplex film and consider the spreading force F for the whole film as given directly by the observed force on the piston, we obtain by combining Eqs. (47) and (51)

$$(F - F_0)(a - a_0) = kT. \quad (53)$$

Taking F and a as variables, this is the equation of a rectangular hyperbola with asymptotes at $F = F_0$ and at $a = a_0$. It should be noted that since negative values of F cannot be observed by the balance method, the portion of the hyperbola below the a-axis cannot be obtained experimentally in the case of duplex films. If, however, we are willing to add a sufficient thickness of pure hydrocarbon to the film to obtain the gravitational effects characteristic of confined lenses, we may determine values of F_{12} less than $-F_0$ by use of Eq. (46) and from these by Eq. (47) can calculate the negative values of F that we cannot observe directly.

Expanded Films of Myristic Acid as Examples of Duplex Films

Fig. 5 contains a family of F–a curves for myristic acid films on 0.01N HCl solution obtained by Adam and Jessop.[13] The ordinates represent the spreading force F in dynes cm^{-1}, and the abscissas are the areas per molecule in A^2. The figures marked on each of the curves give the temperatures at which the measurements were made.

Each curve shows a kink which corresponds to the point J in Fig. 1. The curves to the right of these points J are almost exactly rectangular hyperbolas. The constants F_0 and a_0 in Eq. (53) have been chosen separately for each of these curves to obtain as good fit as possible. The values of F_0 so obtained are found to be practically the same over the whole temperature range, the average value being

$$F_0 = -11.2 \text{ dynes cm}^{-1}. \quad (54)$$

The values of a_0 are found to vary with the temperature in accord with the equation

$$a_0 = 12 + 0.178t, \quad (55)$$

where t is the temperature in degrees Centigrade.

Introducing the values of F_0 and a_0 into Eq. (53), F has been calculated as a function of a for each temperature, and the resulting values have been plotted in Fig. 6. In view of the fact that only three adjustable parameters are involved in Eqs. (53), (54) and (55), the agreement between the curves in Figs. 5 and 6 is remarkably good.

The largest discrepancies between the two families of curves are those for the curve at 34.4°

[13] N. K. Adam and G. Jessop, Proc. Roy. Soc. A112, 362 (1926).

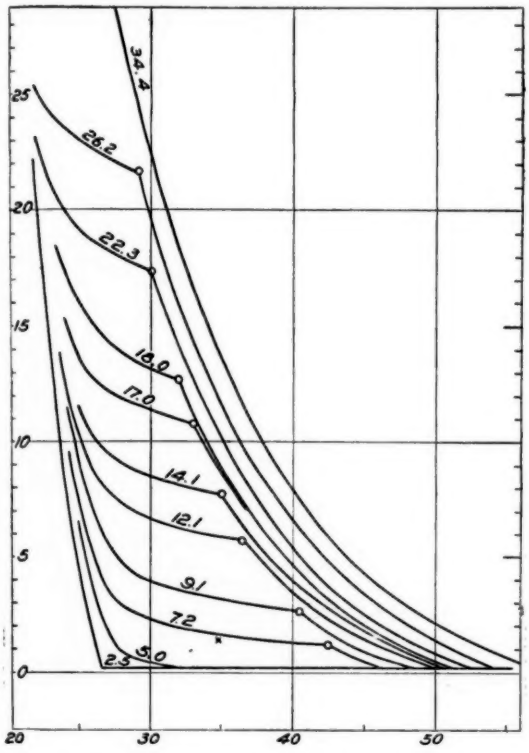

FIG. 5. Experimental F–a curves for myristic acid films on 0.01 N HCl.

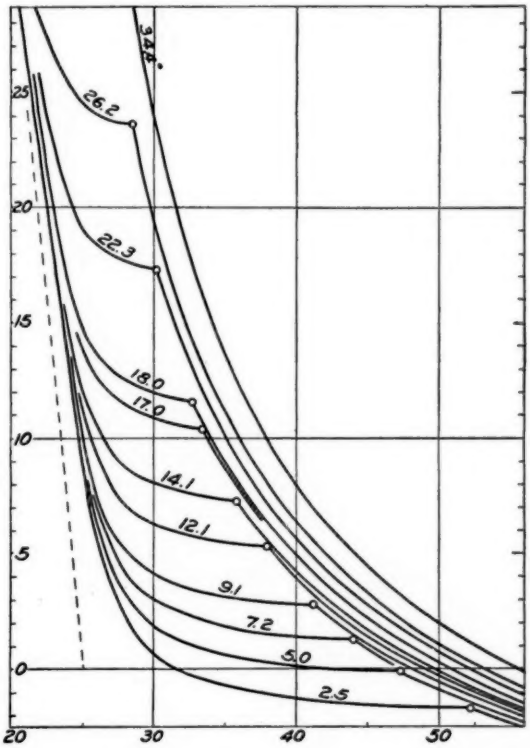

FIG. 6. Calculated F–a curves for myristic acid films.

at values of F greater than 20; these may well be the result of experimental error for these high temperature measurements are difficult. For very low values of F, $F<2$, the slopes of the curves for the observed data are definitely less than those of the calculated curves. With these exceptions the root-mean-square deviation of the observed and calculated curves is only 0.21 dyne cm^{-1}.

A striking feature of these curves is that the F–a curves cut the horizontal axis at a rather definite angle indicating that any horizontal asymptote must lie at negative values of F.

On the whole the agreement seems to be sufficiently good to justify the belief that these expanded films of myristic acid are essentially duplex films. The thickness of the films varies from 14.6A at $a=30$ to 8.8A at $a=50$. These thicknesses are far greater than the range of molecular forces exerted by nonpolar molecules. Since the films are liquid and of a thickness much less than the length of the extended molecule, 22A, the molecules must be inclined at an average angle of about 50° from the vertical when $a=30$ and 66° when $a=50$. The molecules are probably just as free to move as they are in the interior of any liquid except that one end of each molecule is constrained to remain at the interphase. It seems reasonable to assume that this constraint is a matter of minor importance which would lead, at most, to an alteration in F_0, but would not change the character of the phenomenon.

This hypothesis that a liquid monomolecular film of molecules containing long hydrocarbon chains is essentially a duplex film having distinct upper and lower surfaces may be tested in many different ways. In the first place the value of F_0 given by Eq. (54) is in reasonable accord with the value -5.7 which we found for tetradecane. Another test consists of adding to the myristic acid before it is mixed with benzol and spread on water, various proportions of a pure hydrocarbon such as tetradecane. If we are right in considering the film to be a duplex film, the shapes of the F–a curves should remain practically unchanged

except for a small modification due to a slight alteration of F_0. Some preliminary experiments to test this point have shown that the addition of an equal weight of tetradecane to myristic acid produces no appreciable change in the F–a curves. Some variation in F_0 upon the addition of tetradecane may, however, result from the fact that the CH_3 group at both ends of the tetradecane molecule can occupy positions on the upper surface, while in the myristic acid molecule there is only one CH_3 that could take a position in the upper surface. This should have the effect of *reducing* γ_R in Eq. (43). This conclusion is based on several lines of evidence that the field of force around a CH_3 group is less than that for a CH_2 radical. For example, the surface tensions of the isohydrocarbons is less than the *n*-hydrocarbons; the cleavage of crystals of stearic acid, etc., lies along the planes separating the CH_3 groups rather than those separating the CH_2 groups.

Two Phase Duplex Films

Adam's curves for myristic acid in Fig. 5 show a sharp kink at a definite area a_J and at a force F_J, these points corresponding to the point J in Fig. 1.

Such an abrupt change in the direction of a curve must be due to the appearance of a new element in the system such as a new phase.

By measurements of the electric surface potentials Schulman and Hughes* have found some evidence that the film is often observably heterogeneous for areas less than a_J, while for areas less than a_R (see Fig. 1) the film is again homogeneous.

With two phases of constant composition in equilibrium with one another, F should remain constant. It is seen, however, from Fig. 5, that when a is less than a_J each curve has a slope which is definitely not zero. At sufficiently low temperatures, for high values of F, the myristic acid forms condensed films giving curves such as *HGB* in Fig. 1. It would seem probable, therefore, that the new phase which appears at a is a phase of this type consisting of close-packed molecules. A difficulty with this hypothesis, however, is that this new phase should then be one of constant composition with definite properties. This would require that the curve RJ should be a horizontal line.

Adam has demonstrated beyond any reasonable doubt that in condensed films of substances containing long hydrocarbon chains which give curves like *HA* in Fig. 1, the chains are close-packed just as they are in crystals of stearic acid. Myristic acid, however, at low temperatures and especially on pure water gives a break in the curve at G so that the F–a characteristic follows the line GB. Adam regards the area at the point B as being that of the heads.

The strong spreading tendencies of the fatty acids prove that the carboxyl group attaches itself very firmly to water. In the preceding section it was seen that the agreement of the data with Eq. (53) indicates that the forces acting between the carboxyl groups in the expanded films are very weak. This must mean that some of the water molecules become so oriented so as to neutralize the moment of the carboxyl group. Very strong forces must then exist between these carboxyl groups and the water molecules. From this point of view as the film is compressed to an area less than a_B, the decrease in area is due to the progressive squeezing out of these water molecules until at the point G all the water has been removed from the spaces between the carboxyl groups. A suggestion of this kind has also been made by Schulman and Hughes.*

The tendency of fatty acid films to form condensed films increases as the chain length increases. We may assume that the energy involved per molecule, when the chains become close-packed, as at the point G, is proportional to the length of the chain. This energy is a kind of heat of fusion and should be of the same order of magnitude as that involved in the solidification of such substances as stearic acid.

With these facts in mind we may now understand the nature of the curve JR. At the point J the chains of the fatty acid molecules in the film begin to assume the close-packed arrangement in which the molecules have a cross-sectional area of $20.5A^2$. The heads of the molecules, however, because of their hydrated carboxyl groups, cannot space themselves on the surface of the water closer than $25A^2$. The solidification process,

* Reference 12, p. 443.

* Reference 12, p. 449.

therefore, can only proceed to a small extent by forming groups of molecules or micelles of the type represented diagrammatically in Fig. 7.

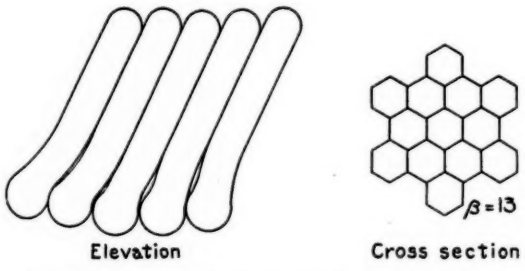

FIG. 7. Diagrammatic representation of a micelle.

The crowding apart of the lower ends of the molecules cannot prevent the upper parts of a few adjacent molecules from arranging themselves as in condensed films, but no large number of molecules can gather together in this way because of the crowding apart of the heads. The new phase that appears at the point J, therefore, consists of micelles containing relatively few molecules. Because the molecular weight of these micelles is not indefinitely large, they therefore exert a pressure which adds itself to that of the phase of single molecules. Strictly speaking, the film between R and J is not a two-phase system, but is a mixture of two two-dimensional gases, one consisting of normal molecules and the other consisting of micelles, each of which contains β molecules. The kink at J is due to the sudden appearance of the micelles at this point. On the basis of these hypotheses we may readily calculate the shape of the curve that we should expect between R and J.

THE SPREADING FORCE F_β DUE TO THE MICELLES

Consider an interface having a total area S between a hydrocarbon liquid and water and let n be the total number of molecules in the interface which act as molecules in a two-dimensional gas, then the area per molecule is given by

$$a = S/n. \tag{56}$$

Now let us consider that the n molecules in the surface exist partly as single molecules and are partly gathered into micelles, each of which contains β-molecules. Let us assume further that an equilibrium exists between the micelles and the single molecules such that the partial spreading force F_1 of the single molecules remains constant as long as the micelles are present. Let S_J be the total area at which the micelles first appear as the area is decreased. We may thus put

$$a_J = S_J/n, \tag{57}$$

where a_J is the area per molecule at the point J (Fig. 1) when the whole surface is covered with single molecules giving a spreading force F_1. Let S_R be the area of the film when it is compressed to such a point that the single molecules disappear so that all the molecules are present as micelles. The number of micelles is then n/β, and each of these covers the area $\beta S_R/n = \beta a_R$. Let us now consider the intermediate stages where $S_R < S < S_J$. Let n_1 be the number of single molecules and n_β the number of micelles. We then have the equation,

$$n_1 + \beta\gamma_\beta = n. \tag{58}$$

We may derive a second equation involving the areas covered by the molecules and by the micelles. Since the partial pressure F_1 remains constant, each of the n_1 single molecules requires the same area a_J as it does when the film area is S_J, whereas each micelle covers the area βa_R. The total surface areas, according to Eq. (56), gives an, and this must be equal to the area required by the single molecules and the micelles. We thus have

$$n_1 a_J + \beta n_\beta a_R = an. \tag{59}$$

Let σ_1 and σ_β be the surface concentrations of the single molecules and of the micelles. We then have

$$\sigma_\beta = n_\beta/S; \quad \sigma_1 = n_1/S. \tag{60}$$

Combining these equations with Eqs. (58), (59) and (56) and then dividing by S we obtain

$$\sigma_1 + \beta\sigma_\beta = 1/a, \tag{61}$$

$$\sigma_1 a_J + \beta\sigma_\beta a_R = 1. \tag{62}$$

Solving these equations for σ_1 and σ_β we find

$$\sigma_\beta = (1/\beta a)(a_J - a)/(a_J - a_R), \tag{63}$$

$$\sigma_1 = (1/a)(a - a_R)/(a_J - a_R). \tag{64}$$

The partial pressure F_β of the micelles in accordance with Eq. (49) may be written

$$F_\beta = \sigma_\beta kT/(1-\sigma_\beta/\sigma_{\beta R}), \tag{65}$$

where $\sigma_{\beta R}$ is the concentration of micelles at the point R. Since the number of micelles is then n/β we have by Eq. (56)

$$\sigma_{\beta R} = n/\beta S_R = 1/\beta a_R. \tag{66}$$

Substituting the values of $\sigma_{R\beta}$ and σ_β from Eqs. (66) and (63) into Eq. (65) we obtain

$$F_\beta = kT(a_J - a)/\beta a_J(a - a_R). \tag{67}$$

Thus between J and R the curves should be given by

$$F = F_J + F_\beta, \tag{68}$$

where F_β is given by Eq. (67).

Examination of the curves in Fig. 5 shows that they are of the type required by this theory. There is a sharp kink at J as the theory would indicate but there is no kink at R where the curve joins the line GB, the approach to this line being asymptotic because of the denominator in the second member of Eq. (67).

The values of β have been calculated from Adam's data of Fig. 5. For this purpose the values of a_R were assumed to lie along a straight line like GB in Fig. 1 with a value of a_B of $25A^2$. Thus

$$a_R = 25 - 0.156F. \tag{69}$$

The values of β obtained in this way from the experimental data on F and F_J by Eqs. (67) and (68) varied from about 9 to 18. For values of a only slightly greater than a_R the accuracy of these determinations of β is naturally not large for it depends too much on the rather arbitrarily assumed value of a_R.

If we may assume that the molecules tend to arrange themselves in a hexagonal lattice like a honeycomb, each molecule should be surrounded by six others and the next ring of molecules should also contain 6. The number of molecules in a micelle may thus naturally be assumed to be 7 or 13. The value $\beta = 13$ is approximately the average of the values found from the data of Fig. 5.

Two-Dimensional Vapor Pressure of the Micelles

The points J in Fig. 5 thus correspond to the two-dimensional vapor pressures of the micelles, that is, to the value F_1, the spreading force due to the single molecules in equilibrium with micelles. If we examine Fig. 5 we see that the points corresponding to J decrease steadily as the temperature is lowered and become zero at a definite temperature of about 6°. This is a very unreasonable behavior for a vapor pressure. When we consider, however, that the true vapor pressure is exerted at the interface, we see that the observed spreading force F does not measure this pressure. The value of F_1 is thus given by

$$F_1 = F_J - F_0. \tag{70}$$

With the data for F_J in Fig. 5 and by using the value of F_0 from Eq. (54) the logarithms of $(F_J - F_0)$ have been plotted against the reciprocals of the absolute temperature. As is usual for vapor pressure curves, a straight line was obtained; this corresponded to the equation

$$\log_{10}(F_J - F_0) = 8.058 - 1950/T. \tag{71}$$

The fact that these vapor pressures measured from F_0 agree with the Clapeyron equation, whereas the uncorrected values do not, affords further justification for regarding these myristic acid films as duplex films.

The values of F_J calculated from Eq. (71) have been used to fix the points J given in Fig. 6 which are marked by small circles. Comparing Figs. 6 and 5, it will be seen that the agreement is probably nearly within the experimental error.

With these values of F_J and a_R, as given by Eq. (69) and by taking $\beta = 13$, the curves in Fig. 6 to the left of points J have been calculated by Eqs. (67) and (68). The general agreement between the slopes of these portions of the curves and those given by the experiments indicates that the value of β is approximately constant and equal to 13. The reasonableness of this value of β thus helps justify the hypothesis that in this two-phase system the condensed phase consists of micelles.

Comparing the curves of Figs. 6 and 5 we see that there are considerable discrepancies at temperatures of 5 and 2.5° and in general at very

TABLE I. *Expanded films of fatty acids on dilute HCl at $F=1.4$ dynes cm^{-1}.*

Acid	1 No. of C atoms n	2 $a_{1.4}$	3 t_0 °C	4 $t_{\frac{1}{2}}$ (obs.)	5 a_0	6 $-F_0$	7 $(-F_0)$ (calc.)	8 $t_{\frac{1}{2}}$ (calc.)
Lauric	12	47.6	14.7	<0°C	14.6	10.4	10.8	−9.0
Tridecylic	13	44.6	13.5	<0	14.4	11.4	12.1	+0.2
Myristic	14	43.7	21.0	9	15.7	13.0	13.4	9.6
Pentadecylic	15	42.1	23.9	19.5	16.2	16.2	14.7	18.8
Palmitic	16	41.5	34.8	28.5	18.1	16.5	16.0	28.2
Margaric	17	42.2	42.2	37.5	19.4	17.5	17.3	37.4
Stearic	18	43.0	52.8	46.	21.3	19.2	18.6	46.6
Heneicosoic	21	46.7	78.0	65.5	25.8	21.6	22.5	74.2
Behenic	22	46.0	75.0	72.5	25.3	21.6	23.8	83.2

low values of F. The probable reason for these deviations will be discussed later.

ADAM'S DATA FOR OTHER FATTY ACIDS

For the other saturated fatty acids Adam has not published full curves such as those of Fig. 5 for myristic acid, but gives merely the area $a_{1.4}$ of the expanded films at a standard small compression of $F=1.4$ dynes cm^{-1} and at some temperature t_0 distinctly above the range at which expansion at this compression occurs. He also gives the temperature $t_{\frac{1}{2}}$ at which half the expansion from the condensed to the expanded film has occurred at $F=1.4$. The data of the first four columns in Table I are those of Adam.[14] The value of $a_{1.4}$ for myristic acid is about 9 percent lower than the value given in his later papers, as shown in Fig. 5, so that exact comparison with our foregoing analysis is not possible.

Taking a_0 as given by Eq. (55) and as tabulated in column 5, we may calculate F_0 by means of Eq. (53) from Adam's data on a and T after placing $F=1.4$. These values, which are given in the 6th column, when plotted against n, lie roughly along a straight line corresponding to

$$F_0=4.8-1.3n. \tag{72}$$

The 7th column gives the values of $-F_0$ calculated by this equation. It is seen that $-F_0$ increases 1.3 dynes cm^{-1} for each additional carbon atom. This agrees approximately with the increment of 1.5 which Harkins[6] found for $-F_S$ between hexane and octane.

The temperatures $t_{\frac{1}{2}}$ as given in the 4th column may be used to generalize Eq. (71) for all saturated normal fatty acids. Referring to Fig. 5, the point marked by a cross just below the curve for 7.2° represents half expansion at $F=1.4$ for it lies about halfway between the intersections with the curves corresponding respectively to JM and GB in Fig. 1. These data thus give about 7.0 for the temperature of half-expansion. The value of F_J at this temperature is evidently about 0.4 lower than $F=1.4$, so that the spreading force F_1 of the micelles, as defined by Eq. (70) is to be taken as $1-F_0$.

Eq. (71) may be written

$$\log_{10} F_1=8.058-B_n/T, \tag{73}$$

where B_n is a constant which depends upon n, the number of carbon atoms in the fatty acid molecule. Taking the values of $-F_0$ from the 7th column of Table I, adding 1 to get $-F_1$, substituting this in Eq. (73) together with the value of T corresponding to $t_{\frac{1}{2}}$ enables us to determine B_n for each acid. These values plotted against n give roughly a straight line corresponding to

$$B_n=1208.+53.n. \tag{74}$$

To show how well these values agree with the experimental data, they have been used in Eq. (73) to calculate (from F_0 in column 7) the temperatures of half-expansion which are given in the 8th column. The agreement with the data of the 4th column is good except for the last two acids where, as Adam points out, the experimental accuracy is much less. The values of B_n in Eq. (74) correspond to a heat of "evaporation" for the micelles of $5.52+0.242n$ kg cal. per mole or $(3.82+1.67n)10^{-14}$ erg per molecule.

The large value for the constant term in these expressions (5.52 kg cal.) suggests that more than

[14] N. K. Adam, Proc. Roy. Soc. **A101**, 521 (1922).

half of the energy of formation of the micelles is due to attractive forces between the carboxyl groups when they are in contact. The increment of 0.242 kg cal. per mole for each CH_2 should correspond roughly with the heat of fusion of the hydrocarbons which is 0.60 kg cal. per CH_2.[14a] Referring to Fig. 7 we see that when 13 hexagons are closely packed, 30 out of the original 78 hexagonal faces are still free. The contribution to the heat of formation of the micelle should thus only be 48/78ths of 0.60 or 0.37 kg cal. per CH_2, even if the solidification were as complete as in a large crystal. The experimental increment 0.242 which is thus 2/3 of the heat of fusion helps justify our hypothesis of the cause of the micelle formation.

It is possible by the methods we have given for myristic acid, applied to the data contained in Eqs. (55), (72), (73) and (74), to construct the whole family of F–a curves for any saturated normal fatty acid. When experimental data are available, it will be interesting to compare them with these predicted curves.

For unsaturated fatty acids on dilute HCl, Adam[14] gives the data contained in the first four columns of Table II. For oleic acid on dilute

TABLE II. *Unsaturated fatty acids.*

Acid	1 n	2 $a_{1.4}$	3 t	4 $t_{\frac{1}{2}}$	5 $-F_0$	6 a_0	7 B_n
Iso-oleic	18	46	35°C	25	18.6	24.9	2016
Oleic(trans)	18	52.5	10	<0	(11.2)	21.7	(1700)
Elaidic(cis)	18	47	10	−0.5	14.0	(21.7)	1875
Erucic(trans)	22	47	10	4.5	16.4	25.2	1892
Brassidic(cis)	22	45	40	34.	19.2	22.6	2073

HCl at 15° Adam and Jessop have given a complete curve[15] which agrees within a standard deviation (S.D.) of 0.24 dyne cm^{-1} with Eq. (53) if we take $a_0=19.9$ and $F_0=-11.2$. For the corresponding saturated acid (stearic) at this temperature, we should have, by Eqs. (55) and (72), $a_0=14.7$ and $F_0=-18.6$. Thus the effect of introducing the double bond in the middle of the hydrocarbon chain has been to increase a_0 by 5.2 and to decrease $-F_0$ by 7.2. The increase in a_0 indicates that the double bond tends to occupy a position on the water surface in accord with the known fact that the effect of a double bond is to increase the solubility of a hydrocarbon derivative in water.

Although for the other unsaturated acids, since only $a_{1.4}$ is given, we cannot determine a_0 and F_0 separately, we may draw certain tentative conclusions.

Taking F_0 for oleic acid to be -11.2 from the more complete later data, we calculate, by Eq. (53), $a_0=21.7$. The difference in $a_{1.4}$ for oleic and elaidic acids is probably due to a change in F_0 rather than to one in a_0. We thus take $a_0=21.7$ for elaidic acid and find the value of F_0 given in the 5th column. For the corresponding acids with 22 carbon atoms, assuming the increment of 1.3 per CH_2 as in Eq. (72), we take a value of $-F_0$ 5.2 units greater than for the 18 carbon acids. For iso-oleic acid with the double bond between the α, β-atoms, F_0 has been taken to be the same as for stearic acid. The variations in the resulting values of a_0 are probably of no significance, since the data for $a_{1.4}$ are uncertain by about 2 units (Adam), but that they are on the average 7.5 ± 2.5 larger than the values given for the saturated acids by Eq. (55) indicates that the general effect of the double bond is to raise a_0.

The values of B_n in the 7th column have been calculated from $t_{\frac{1}{2}}$ and $1-F_0$ by Eq. (73). They should be compared with the values of 2162 for stearic and 2374 for behenic acid given by Eq. (74) for $n=18$ and 22, respectively. The effect of the double bond near the carboxyl group in iso-oleic acid is to lower B_n by 146 which is equivalent to a decrease in n of 2.8. A double bond near the middle of the chain lowers B by an average of 294 (equivalent to a decrease of 5.6 in n) in the case of the cis-compounds elaidic and brassidic acids, while in the trans-compound erucic acid the decrease is 482 which corresponds to the effect of shortening the chain by 9.1 CH_2 groups.

These very large and specific effects of the double bonds near the middles of the chains are in striking contrast with the small changes produced on the JK part of the curve as derived from the data for $a_{1.4}$. This latter part depends only on F_0 and a_0, whereas the value of F_J at any temperature (which determines B) involves all the factors that determine the stability of the

[14a] W. E. Garner, K. Van Bibber and A. M. King, J. Chem. Soc. (1931), 1533.

[15] N. K. Adam and G. Jessop, Proc. Roy. Soc. **A120**, 473 (1928).

micelles. Any irregularity in the chain naturally affects the ease with which the molecules can pack into a micelle.

Compounds with Multiple Chains

In condensed films of such substances as tristearin, glycol dipalmitin, etc., which have two or more chains of equal lengths, each chain occupies the area $20.5A^2$ so that the area for a whole molecule increases in proportion to the number of chains. With expanded films, however, the area depends only on a_0 and F_0 and thus, according to Eq. (53), should not be expected to increase in proportion to the number of chains even if a_0 does so. Adam finds that the area at no compression is 135 for triolein at 15°C, while for tristearin and tripalmitin at 60°C it is 115. He notes that these areas are about 2.4 instead of three times the areas of the "corresponding compounds with single chains."

Adam[16] has given a complete curve for glycol dilaurate at 15°C which agrees within about $SD=0.2$ dyne cm^{-1} with Eq. (53) if we take $a_0=39$ and $F_0=-8.5$. Comparing this with the data for lauric acid in Table I we see that the value of a_0 has been increased very greatly, from 15 to 39, while $-F_0$ has decreased by 2 units. Adam and Jessop's curve for triolein[13] gives best agreement with Eq. (53) (rather poor) with $a_0=90$ and $F_0=-8.5$.

The Effect of Uneven Upper Surface

Films prepared from mixtures of cholesterol and myristic acid[15] on dilute HCl give areas less than the sum of those obtained from the constituents separately.

Cholesterol consists of large compact molecules that form a condensed film with an area of 40.8 and a thickness of 15.3A. An expanded myristic acid film of an area $a=47$ has a thickness of 9.3. In the mixed film the large molecules thus extend through the film and tend to produce humps in the upper surface. If the total area of the upper surface is increased, for example, 10 percent, from this cause, and the surface tension of the upper surface is 50 dynes cm^{-1}, the effect is to increase $-F_0$ by 5 dynes cm^{-1}. This may perhaps be the main cause of the decrease in area of the expanded films containing cholesterol. Similar effects were observed when tripalmitin and other large molecules were used instead of cholesterol. The three chains in tripalmitin being attached at one end must lie closer than if unattached and produce a local thickening of the film.

The micelles present in the JR portion of the curves of expanded films should also tend to cause an uneven upper surface. This effect should be especially marked when F_J is small, that is, at low temperatures, for then the film of single molecules is so thin that the micelles rise above it. It appears probable that the deviations between the curves in Figs. 5 and 6 at low values of a and at low temperatures are due to this cause.

The Effect of Large Head Groups in Decreasing β

For para-dodecyl-phenol a family of curves have been obtained[17] like that for myristic acid. The area at no compression is, however, unusually small ($a=36$). The JK part of the curves at 30°C gives $a_0=16.3$, $F_0=-20$. This large value of $-F_0$ explains the small value of a at $F=0$. The JR portions are far steeper than those of myristic acid and are found to correspond to micelles for which $\beta=5\pm1$. This low value is in accord with the presence of the phenyl group in the head which should restrict the number of chains that can unite in a micelle. The value of B_n is 1970.

A similar example of the effect of a large head group in reducing the value of β is furnished by the data[13] on the α-bromo-fatty acids. For the acid containing 17 carbon atoms, at 15° the JR portion of the curve gives a value $\beta=7$. The JK portion gives $a_0=17.1$; $F_0=-13.7$.

Films of Esters and Vapor Expanded Films

A family of curves is also given for monopalmitin.[17] The JK portions agree well with Eq. (53) ($SD=0.3$) when $a_0=22$ and $F_0=-8.8$. The area at no compression, in accord with these

[16] N. K. Adam, Proc. Roy. Soc. **A126**, 366 (1930).

[17] N. K. Adam, W. A. Berry and H. A. Turner, Proc. Roy. Soc. **A117**, 532 (1928).

values, is large ($a=67$). The values of F_J-F_0 furnish, by Eq. (74), the value $B_n=2052$. When the values of F_J are then calculated by this equation at the four temperatures (from 16 to 37°) at which the experiments were made, the calculated and observed values agree with an S.D. of 0.13 dyne cm^{-1}, although only one adjustable parameter is available in these calculations.

The *JR* portions of the curve are fairly flat. Calculation shows that $\beta=13.5\pm2$. The magnitude of β seems to depend very largely on whether or not the *F–a* curve for the condensed film possesses a *GB* branch (Fig. 1). We have concluded that the line *GB* is due to the hydration of the heads. If there is little or no hydration, the *F–a* curve follows the line *GA*. The fatty acids and particularly the α-bromo acids show a very distinct *GB* line with values of a_B of about 26 which indicate that the carboxyl group has a strong tendency to be hydrated and then occupies an area distinctly greater than 20.5. With the alcohols the point *B* lies at about $a=22$. Thus the larger size of the head in the monopalmitin as compared to the acids is offset by a lower degree of hydration.

The effect of replacing the hydrogen atom in the carboxyl group of the fatty acids by a methyl group is to *lower* the expansion temperature t_i by one or two degrees, while an ethyl group produces a lowering of 15°. This indicates that the tendency to form micelles is decreased very greatly by the presence of an ethyl or higher group in the ester chain. The condensed films of these esters show, however, an area of 20.5 so that the fact that the—COO—group must be pulled away from the water in the formation of the micelles (as in the condensed films) explains the lesser stability of the micelles.

Another interesting feature of these ester films is that the *GB* section of the curve is wholly absent in the condensed films and as a result of this lack of hydration the values of β are very large (the *JR* lines are flat). This means that the expanded film passes to the condensed state more nearly as a definite change of phase instead of by the growth of micelles. The curves for propyl palmitate give $a_0=12$, $F_0=-4.8$, $B_n=2000$, and $\beta=60$. For ethyl palmitate[13] similar data give $a_0=12$, $F_0=-5.7$, $B_n=2059$ and $\beta=55$.

The small values of $-F_0$ for these esters are presumably due to a lack of sufficient flexibility of the molecule in the neighborhood of the—COO—group to allow both chains to assume a steep angle to the water surface. With glycol dilaurate and triolein the larger value of $-F_0=8.5$ results from the additional linkages between the two chains by which greater flexibility can be attained.

The marked effect of attachment to the water in the middle of a chain in decreasing $-F_0$ is best illustrated by the data which Adam and Jessop have given[13] for films of oleic acid on acidulated water containing potassium permanganate. The oxidation of the double bond gives strong attachment to the water near the middle of the chains. The curve at 15° yields $a=27.1$ and $-F_0=2.2$, which is the lowest value derivable from any of Adam's curves.

The films which Adam has called *vapor expanded* films are evidently merely those which are characterized by very low values of $-F_0$. At low compressions the curve then extends to such large values of a that the film becomes so thin that the molecules lie nearly flat on the surface before F falls to zero. Thus the films can no longer be considered duplex films and it is not surprising that they should merge into true gaseous films without the abrupt change of slope that characterizes typical (liquid) expanded films.

Factors which Determine a_0

In the foregoing analysis of the experimental data a_0 has been treated as an empirical constant, although its derivation from Eq. (49) would suggest that a_0 should have the value of a which corresponds to a close-packed film. The empirical values of a_0 are usually less than this.

The fact that no two molecules in a monomolecular film can be in the same place at a given time indicates the existence of repulsive forces of very short range. Such forces yield a term a_0 which should correspond to the value of a for a condensed film (at least for fairly concentrated films).[9]

We have seen, however, particularly in our discussion of Eq. (74) that in the formation of the micelles there is evidence of short range attractive forces between carboxyl groups. Such forces

should tend to counteract the effect of the repulsive forces at contact and thus tend to *decrease* the value of a_0. We should therefore not attach too much significance to the actual values of a_0 but may well interpret the differences in a_0 for different substances as indications not only of the relative sizes of the active groups, but also of the magnitude of the forces between them.

Flexibility of Hydrocarbon Chains

Adam has summarized[16] the evidence that the chains are flexible. The fact that the upper and lower surfaces of duplex films of a thickness of only 5–10A^2 can act nearly independently just as in a thicker film of liquid is perhaps still more convincing evidence.

In a series of papers Staudinger[18] and his coworkers have developed a theory of the viscosity of solutions of high polymeric compounds which is based on the assumption of long rigid molecules. It would seem that such theories require revision. Perhaps it is the shearing stress in a liquid during viscosity measurements that pulls a very long molecule into a nearly straight line and thus, in part, justifies the theoretical derivation of the equations.

Note on Antonoff's Rule

Antonoff's rule[19] states that for true equilibrium $F_S=0$. As Harkins and others have pointed out, this cannot be true in general. For example, for a pair of liquids A and B there are two spreading coefficients: for lenses of A on B, $F_{SA}=\gamma_B-\gamma_A-\gamma_{AB}$, while for lenses of B on A, $F_{SB}=\gamma_A-\gamma_B-\gamma_{AB}$. Both spreading coefficients can be zero only when $\gamma_{AB}=0$, i.e., when the liquids are miscible.

It is nevertheless a fact that F_S is extremely close to zero for very large numbers of organic liquids placed on water and *in equilibrium* with it, so that as a useful empirical rule Antonoff's rule is justified.

If the molecules of a vapor of an organic liquid, when they strike a water surface, form an adsorbed film which nearly completely covers the surface, then some molecules must condense on top of those already adsorbed. We then have two cases to consider:

(1) The molecules in the 2nd layer may have a shorter life t (before evaporating again) than the life t_0 of molecules on the surface of the organic liquid.

(2) The life t of the molecules may be equal to or greater than t_0.

In the 1st case the 2nd layer of molecules will not become complete so that $F_S<0$, while in the 2nd case the 2nd layer and therefore presumably a 3rd and 4th layer, etc., will grow in presence of saturated vapor until the water is covered by a liquid film and therefore $F_S=0$.

According to the principle of independent surface action[20] which the writer has so often employed, the properties of a surface depend primarily on the atoms or groups of atoms actually forming the surface and depend on the underlying layers only insofar as they alter the actual surface atoms. Thus in general the properties of the upper surface of an adsorbed monomolecular film are nearly the same as those of the substance in bulk. This may be illustrated by some examples.

Carbon tetrachloride vapor forms an adsorbed monomolecular film on water which tends to become nearly complete before the vapor becomes saturated. The properties of the upper surface of the film thus approximate to that of liquid carbon tetrachloride, so that the life t of molecules of CCl_4 which may condense on the film is about the same as that of molecules on liquid CCl_4. Thus the film grows in thickness which means that $F_S=0$.

Orientation of the molecules in the adsorbed film may make t for the second layer very different from t_0. Thus lenses of molten palmitic acid on water, although in equilibrium with it, do not spread indefinitely. This is due to the fact that the orientation and tight packing of the molecules in the film on the water has the effect of preventing the carboxyl groups of any vapor molecules incident on the surface from coming into contact with other carboxyl groups. On the other hand a molecule striking a surface of liquid palmitic acid can more easily penetrate the less tightly packed surface layer and thus its carboxyl

[18] H. Staudinger and E. Ochiai, Zeits. f. physik. Chemie **A158**, 35 (1931).

[19] Antonoff, J. Chim. Phys. **5**, 372 (1907). Bartell, Case and Brown, J. Am. Chem. Soc. **55**, 2769 (1933).

[20] I. Langmuir, Chem. Rev. **6**, 467 (1929); also Colloid Symposium Monographs **3**, 48 (1925).

can meet other carboxyls. Thus t for molecules in the 2nd layer of the adsorbed film is less than t_0 and therefore $F_S<0$.

A corollary of this point of view is the conclusion that if, for two immiscible liquids A and B, A is strongly adsorbed (from a saturated vapor) on B then the vapor of B cannot be strongly adsorbed on A (since both F_{SA} and F_{SB} cannot be zero).

The frequency with which strong adsorption occurs and the relatively small effects on the lives t produced by orientation is thus the fundamental reason that Antonoff's rule is so often applicable.

Of course there are numerous cases such as that of the higher hydrocarbons and water where only a negligible adsorption of either vapor by the other liquid occurs. Such cases are usually those yielding large negative values for F_S.

Molecular Symmetry and the Reduction of the Secular Equation

HENRY EYRING, ARTHUR A. FROST AND JOHN TURKEVICH, *Frick Chemical Laboratory, Princeton University*

(Received September 15, 1933)

A method is given for expressing a bond eigenfunction of any multiplicity in terms of a linear independent set. The independent sets for the multiplicities corresponding to one bond and to two bonds for an arbitrary number of electrons are given. A method recently given for obtaining matrix components for singlet bond eigenfunctions is generalized to include all multiplicities. Group theory is applied to the bond eigenfunctions for symmetrical molecules to reduce the secular equation and examples are worked out for all multiplicities. The possible reasons for the approximate additivity of bond energies for molecules is examined in connection with the chemist's custom of ignoring all but the strongest bonds.

INTRODUCTION

IN the calculation of activation energies for reactions involving complicated molecules it is important to know at least approximately how nearly the experimental bond strength corresponds to a simple exchange integral between the paired electrons. In the many reactions for which this is approximately the case the electrons not actually changing partners may be ignored or considered as causing only small steric effects. The binding energy for a few typical molecules is given here. We hope later to extend the cases examined to include more complicated molecules and to supplement these considerations by calculations of the integrals involved.

REDUCTION OF BOND EIGENFUNCTIONS TO A LINEARLY INDEPENDENT SET

Rumer[1] has shown how a linearly independent set of singlet bond eigenfunctions may be chosen. Points representing the atomic eigenfunctions are drawn as a polygon without reentrant angles. Straight lines representing bonds are then drawn. Only bond eigenfunctions for which no bonds cross are included in the linearly independent set. To express any singlet eigenfunction in terms of this linear independent set we require but one relationship. This may be expressed diagrammatically as follows:

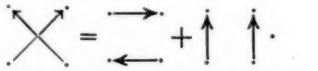

(1)

This relationship holds not only for bond eigenfunctions involving four electronic eigenfunctions but for those involving an arbitrary number providing the bonding not indicated in our diagram is identical for all three bond eigenfunctions. This same relationship holds even when an arbitrary number of the electronic eigenfunctions are connected by no bonds, i.e., for all multiplicities having as many as two bonds. For multiplets higher than singlets one additional relationship is required. If n bond eigenfunctions are identical except for a single bond in each and if these n unequal bonds added together vectorially have a resultant equal to zero then the sum of the bond eigenfunctions is zero. Diagrammatically this is simply

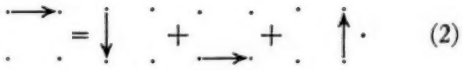

(2)

These two relationships enable us to express any bond eigenfunction in terms of a linearly independent set. Both propositions are readily verified by expressing the bond eigenfunctions in terms of Slater functions. A recent article by Rumer, Teller and Weyl[1a] is of interest in this connection.

If our $2n$ electronic eigenfunctions (n an integer) be thought of as arranged in the polygon described above, a linearly independent set of one bond eigenfunctions is formed by $2n-1$ of the $2n$ eigenfunctions around the perimeter which then requires but one bond to form a closed figure.

[1] G. Rumer, Nach. d. Ges. d. Wiss zu Göttingen, M. P. Klasse, p. 337 (1932).

[1a] Rumer, Teller and Weyl, Nach. d. Ges. d. Wiss. zu Göttingen, M. P. Klasse, p. 449 (1932).

Since any other bond will form a closed figure it is clear all other bond eigenfunctions can be expressed in terms of the set selected, and as there are $(2n-1)$ independent eigenfunctions we have a linearly independent set. An equally satisfactory set corresponds to the $2n-1$ bonds connecting a particular electronic eigenfunction with each of the others.

A linear independent set of two bond eigenfunctions corresponds to the $n(2n-3)$ ways that two bonds can be drawn on the perimeter, never of course using the same electronic eigenfunction in both bonds of the pair. Our two propositions enable us to express any other two bond eigenfunction in terms of this set. The independent set for more than two bonds will involve bonds not falling on the perimeter and is, therefore, slightly more difficult to describe. The two propositions given are, however, all that are required to single out a satisfactory set for any number of bonds.

Kimball and Eyring[2] defined an operator which acting on all the antisymmetric Slater functions for which M_s (the z component of spin) is zero gives the particular bond eigenfunction with $M_s=0$. To form a bond function with $M_s\neq 0$ proceed exactly as before. Take the linear combination of all Slater functions, with the proper M_s, which associate opposite spin eigenfunctions with each pair of electronic eigenfunctions bound together. Give the Slater function the positive sign if it associates negative spins an even number of times (or not at all) with the first letters in each bond as written, otherwise give it a negative sign. The proof that the functions so formed are eigenfunctions for the operator S^2, the total angular momentum, proceeds exactly as in the case $M_s=0$.[3]

The secular equations for a particular independent set of bond eigenfunctions is the same for each value of M_s except for a constant factor multiplying every term in the equations. This factor is smallest for the largest possible M_s for each multiplet. This factor of course divides out of the secular equations and we get the same eigenvalue repeated in a multiplet for each M_s.

[2] G. E. Kimball and H. Eyring, J. Am. Chem. Soc. **54**, 3876 (1932).

[3] H. Eyring and G. E. Kimball, J. Chem. Phys. **1**, 239 (1933).

Calculation of Matrix Components Between Bond Eigenfunctions of all Multiplicities

Bond eigenfunctions with a different number of bonds belong to different multiplets and are noncombining for the energy operator considered in which magnetic terms are neglected. Consider two eigenfunctions with the same number of bonds

$$\psi_1=a-b\ c-d\ e-g\ f\ h\ i-j\ k\ l\ m\ n,$$

$$\psi_2=a-c\ b-d\ e-f\ g\ h\ i\ j\ k-l\ m\ n.$$

Now to calculate the matrix component write down the electronic eigenfunctions in order

$$\begin{array}{c} a\ \ b\ \ c\ \ d\ \ e\ \ f\ \ g\ \ h\ \ i\ \ j\ \ k\ \ l\ \ m\ n \\ +\alpha_1\ \beta_1\ \beta_1\ \alpha_1\ \beta_i\ \alpha_i\ \alpha_i\ \alpha\ \alpha_f\ \beta_f\ \alpha_s\ \beta_s\ \alpha\ \alpha \end{array}$$

and below each letter an α or β is written. We shall call this array of α's and β's a sequence. Assign an α or β to an electronic eigenfunction in the following way. If there is a bond in the first eigenfunction between two letters neither of which form part of a bond in the second eigenfunction write α_f under one letter and β_f under the other. The letters $i\ j$ are an example. For a similar bond in the second eigenfunction, as $k\ l$, do the same except use the subscript s. If either eigenfunction has more than one such bond the matrix component is zero to the approximation of first order exchange integrals. If of two letters forming a bond in one of the eigenfunctions for example $e-g$ only one, e, is bonded in the second eigenfunction write α_i under the unbonded letter and β_i under the bonded one. Now continue assigning successively α_i and β_i to the chain of letters connected to these by bonds (connected first in one function and then in the other) until you again come to one which forms part of a bond in one function but not in the other. Here the chain terminates. We shall use the word chain for such a series of atoms to distinguish them from a cycle defined below. The chain $g\ e\ f$ is an example. If there is another chain of this sort do the same using the subscript j. Continue until all chains have been assigned. Now if a letter forms part of a bond in both functions, for example a, write α_1 below it and write β_1 below the letter to which it is bound, b in our example, and below the companion of b

in the second function write α_1 alternating thus around the cycle until you return to the initial letter. Such a cycle in the example is *abcd*. A cycle may contain as few as two letters or as many as all of them. Now if there is a second cycle proceed exactly in the same way using the subscript 2 and so on until all the cycles have been assigned. Finally below letters which are not bonded in either eigenfunction write α without any subscript. We next write a + or − sign before our sequence of α's and β's depending on whether to the totality of first letters of bonds in the two functions an even or odd number of β's have been assigned. In this example four β's have been assigned so the sign is +. In general if β's have been assigned p times this sign is $(-1)^p$.

From our sequence we may now tell immediately how many Slater eigenfunctions are common to the two eigenfunctions. If the subscript f or s occurs obviously there are none. If these subscripts do not occur there are 2^m where m is the largest subscript used for numbering the cycles. This is because for each cycle there was really an arbitrary choice of α or β to be assigned to the first letter while outside of cycles there was no choice. The coefficient of the coulombic integral is zero if the subscript f or s occurs otherwise it is $(-1)^p 2^m$. The corresponding coefficient of the energy W in the secular equation is always just the negative of the coefficient of Q.

Case I

If either the subscript f or s occurs on an α as many as two times in a sequence the matrix component is identically zero.

Case II

If both f and s occur as subscripts on but one bond only the four exchange integrals occur which may be formed by taking one of the letters from each of these two bonds. The two integrals corresponding to letters to which like spins have been assigned occur with a plus sign the other two with minus signs. It is to be understood in addition that these quantities are multiplied by the factor $(-1)^p 2^m$. Thus for the two eigenfunctions written down the matrix component is $2(ik+jl-kj-il)$ since $(-1)^p 2^m = 2$.

Case III

Next consider the case where either the subscript f or s does not appear while the other subscript appears only on a single bond. If the bond $k-l$ in eigenfunction ψ_2 is replaced by $g-h$ we have such an example. The sequence would then differ from the former one only in having β_i assigned to h while to k and l are assigned α's without subscripts. The value of $(-1)^p 2^m$ is unchanged. For this case the only terms appearing will be exchange integrals between one of the two letters in this bond (when the subscript f has been assigned) and a second letter from a chain. All such integrals where like spins have been assigned in the sequence enter with the coefficient 1 while the others have the coefficients −1. All are multiplied by the factor $(-1)^p 2^m$ as before. For the two eigenfunctions just described the matrix component is

$$(-1)^{p+1} 2^m (if+ig+ej+jh-ie-ih-jf-jg).$$

Case IV

Finally consider the case where neither the subscript f or s appears. An example is obtained if in eigenfunction ψ_2 we replace the bond $k-l$ by $i-j$. The sequence would then differ from the one written down in that to both k and l would be assigned α's with no subscripts and the subscripts associated with i and j would be changed from f to 2. Again it is to be understood that the coefficients given below are all to be multiplied by $(-2)^p 2^m$. The coefficients of the coulombic integral Q and all exchange integrals between letters to which opposite spins with identical subscripts are assigned is then 1; integrals between letters with like spins and like subscripts have coefficients −2; those between letters with positive spin and no subscripts have the coefficient −1; those between letters in cycles and any letter outside the cycle have the coefficient $-\frac{1}{2}$; any integral between a letter in one chain and a second letter outside this chain but not in a cycle with spins alike has the coefficient −1, if the spins are unlike the coefficient is zero.

This gives the general scheme for all multiplicities. For singlets the sequence contains only cycles and the rules reduce to the very simple form already given.[3, 4, 5] The proof of the rules given follow from the sequence by inspection

using considerations of the type found in the article[3] just referred to.

We now consider the simplifications arising in secular equations from molecular symmetry.

General Group Theoretical Considerations

We shall state the few group theory propositions required without proof and refer the reader to standard treatises for more detail.[6, 7, 8] If we have a molecule containing like atoms symmetrically placed certain bonds are equal and the matrix components in the secular equation are entirely unchanged by any rotation or interchange of atoms which simply changes like bonds into like bonds. These operations can be expressed as a group of permutations which acting on any bond eigenfunction changes it into another bond eigenfunction which may or may not be a member of our linear independent set. It can in any case be readily expressed in terms of such a set. The effect of such a permutation on our linear independent set of bond eigenfunctions can be expressed as a matrix and the sum of the terms on the principal diagonal, called its character, is denoted by χ_i. Now the group of operations breaks up into classes such that all members of a class C_i, have the same character χ_i. We denote by h_i the number of members in this class. If all the members of a class C_i be multiplied into the members of a class C_j we get a relationship of the type $C_iC_j=\Sigma_k c_{ijk}C_k$ (3) where c_{ijk} is some integer or zero. The identity, c_1 always constitutes a class by itself; so that χ_1 is the degree of our representation, being simply the number of functions operated upon. For a particular group there is only a limited number of irreducible representations possible, i.e., representations for which no linear combinations of the functions can be found such that they break into two or more sets not transforming into each other for any of the group operations. These may be found by using the relationship $h_ih_j\chi_i\chi_j=\chi_1\Sigma_k c_{ijk}h_k\chi_k$ (4) in connection with the set of relationships (3).[6, 9] The possible choices of the characters in (4) which are consistent with (3) fix the characters of the irreducible representations. Examples will be given later.

Now in molecular problems for each multiplicity we have a linear independent set of bond eigenfunctions as a representation of the group corresponding to the molecular symmetry. This representation, unless especially chosen, is in general reducible for a symmetrical molecule. By taking suitable linear combinations we may break up our representation into equivalent irreducible representations of the group any one of which may fail to appear or may appear once or more times. There is a simple way of determining how often each irreducible representation will appear, however. If for each class we multiply the character, χ_i', of our reducible representation by the character of the irreducible representation in question, χ_i, and multiply this by the number of members of the class, h_i, the sum of all such quantities divided by the number of members in the group, N, gives the number of times, n, the irreducible representation will appear $1/N\Sigma_i h_i\chi_i'\chi_i=n$ (5). One other theorem is frequently useful. The average value over all members of the group of the square of the character of the irreducible representation equals the sum of the squares, G, of the number of times each irreducible representation will appear in the reduced representation. $1/N\Sigma_i h_i\chi_i'^2=G$ (6).

The advantage of using irreducible representations is that they are non-combining and if a particular one of degree χ_1 occurs but once all χ_1 roots are equal; so that only a linear equation must be solved to get the energy. If a particular irreducible representation occurs l times we must solve an equation of the l-th degree.

Having determined a particular irreducible representation is to appear, very simple means suffice to obtain it. Beginning with any bond eigenfunction from the reducible representation we apply an operation to it and add to it the eigenfunctions which give the proper character for this class. Should this turn out to be impossible this eigenfunction does not occur in this representation and we start with a new one. Having found eigenfunctions which transform

[4] H. Eyring and G. E. Kimball, J. Chem. Phys. **1**, 626 (1933).

[5] L. Pauling, J. Chem. Phys. **1**, 280 (1933).

[6] A. Speiser, *Theorie der Gruppen*, 2nd edition.

[7] E. Wigner, *Gruppentheorie.*

[8] H. Weyl, *The Theory of Groups and Quantum Mechanics*, tr. by H. P. Robertson.

[9] H. Bethe, Ann. d. Physik **3**, 133, 19 (1929).

properly for a member of one class we adjust it to have the proper character for a member of a second class adding functions which do not spoil the first transformation. This is repeated for a member of each class. In some cases it was found easier to start with the most general representation which had the proper character for the first class and specialize it for successive classes. For the identical representation we begin with any eigenfunction and add together all the quantities obtained by operating on it with each member of the group. The linear independence of two representations of the same irreducible representation (equivalent representations) is readily investigated by expressing them in terms of the linear independent set.

Ammonia

We assume the molecule has one three-fold axis of symmetry and three planes of symmetry. We take the three electronic eigenfunctions on the nitrogen atom as b, d, f and assume they are bonded respectively to the three hydrogen eigenfunctions a, c and e. Our symmetry operations are then C_1 : identity; C_2 : $(ac)(bd)$, $(ae)(bf)$, $(ce)(df)$; C_3 : $(ace)(bdf)$, $(aec)(bfd)$. The relationships (3) are $C_2^2=3C_1+3C_4$; $C_4^2=2C_1+C_4$ and $C_2C_4=2C_2$. These with Eq. (4) give for the characters of the classes of the three irreducible representations:

	C_1	C_2	C_3
Γ_1	1	1	1
Γ_2	1	−1	1
Γ_3	2	0	−1

We take as the linear independent set for the singlets the Rumer set of bond functions: $a-f\ b-c\ d-e$, $a-b\ c-d\ e-f$, $a-f\ b-e\ c-d$, $a-d\ b-c\ e-f$ and $a-b\ c-f\ d-e$. The group of operations transform these five eigenfunctions among themselves with only one new eigenfunction appearing $d-a\ b-e\ c-f$ which by the method of resolving crossed bond functions is readily shown to be just the negative of the sum of the five Rumer functions. We write for the five Rumer eigenfunctions ψ_1 to ψ_5 respectively and ψ_6 for the other eigenfunction. The members of the group are represented by the letters E, A, B, C, D, F respectively. When the operations act on the eigenfunctions in the first line of the table we get the eigenfunctions in the line with the operation.

E	ψ_1	ψ_2	ψ_3	ψ_4	ψ_5	5
A	ψ_6	ψ_2	ψ_5	ψ_4	ψ_3	1
B	ψ_6	ψ_2	ψ_3	ψ_5	ψ_4	1
C	ψ_6	ψ_2	ψ_4	ψ_3	ψ_5	1
D	ψ_1	ψ_2	ψ_4	ψ_5	ψ_3	2
F	ψ_1	ψ_2	ψ_5	ψ_3	ψ_4	2

Here the operations in the first column acting on the first row of eigenfunctions give the subsequent rows with the character given in the last column. Using proposition (5) we find there are two irreducible representations of Γ_1; one of Γ_2 and one of Γ_3. These are found almost by inspection to be respectively: $\psi_1+\psi_6$, ψ_2; $\psi_1-\psi_6$; and $\psi_3-\psi_4$ with $\psi_5-\psi_4$, the latter of course being a two-dimensional representation. The five energies are, respectively, $Q+\alpha-\frac{3}{2}\beta-\frac{3}{2}\gamma-\delta \pm[(2\alpha-2\delta)^2+(3\delta-\frac{3}{2}\gamma-\frac{3}{2}\beta)^2]^{\frac{1}{2}}$; $Q-3\alpha$; and two equal energies with the value $Q-\alpha-2\delta$. Here the interchange integrals $ab=cd=ef=\alpha$; $ac=ae=ce=\beta$; $bd=bf=df=\gamma$; $ad=af=bc=be=cf=de=\delta$.

Triplet States

Next consider the triplet terms. These are two bond eigenfunctions and the method of selecting the linear independent set of nine eigenfunctions has been described. In specifying the bond eigenfunctions only the bonded electronic eigenfunctions are written down. Also to further simplify the notation a bond will be indicated by simply writing the two bonded eigenfunctions next to each other leaving a space between atoms not bound together. Thus $ab\ cd$ indicates the bond eigenfunction with a bonded to b and with c bonded to d it being understood that e and f are unbound. A line will be used, however, for one bond eigenfunction to prevent confusing this notation with that for interchange integrals. The linear independent set is then $ab\ cd$, $ab\ ef$, $cd\ ef$, $ab\ de$, $af\ bc$, $af\ cd$, $af\ de$, $bc\ de$, $bc\ ef$. By going through precisely the same sort of considerations as for singlets these eigenfunctions break up into two representations of Γ_1, $\phi_1=ab\ cd+ab\ ef+cd\ ef$

and $\phi_2 = af\,bc + af\,bd + cb\,de + cb\,df + ed\,fb + ed\,fa$; one representation of Γ_2, $\phi_3 = ab\,de + dc\,be + ab\,cf + dc\,af + ef\,ad + fe\,cb$; and three representations of Γ_3, $\phi_4 = ab\,cd + ab\,fe$ with $\phi_5 = ab\,cd + cd\,fe$, $\phi_6 = ac\,bd + fb\,ae$ with $\phi_7 = ac\,bd + ec\,df$, and finally $\phi_8 = ab\,cf + ab\,de + ef\,cb + ef\,da$ with $\phi_9 = dc\,be + dc\,af + ef\,cb + ef\,da$.

These energies lie considerably higher than the lowest singlet and so are not particularly interesting. The matrix components can be readily calculated by the scheme outlined.

Quintet States

For the quintet states we can conveniently take for the five linearly independent single bond functions $[a-b]$, $[a-c]$, $[a-d]$, $[a-e]$ and $[a-f]$. Proceeding as before we get one representation of Γ_1, $\Omega_1 = [a-b]+[c-d]+[e-f]$; two representations of Γ_3, $\Omega_2 = [a-e]+[a-f]+[b-f]+[b-e]$ with $\Omega_3 = [c-e]+[c-f]+[d-f]+[d-e]$ and $\Omega_4 = [e-f]+[b-a]$ with $\Omega_5 = [e-f]+[d-c]$.

Septet States

These states correspond to no bonds and there is a single eigenfunction for each M_s corresponding to this multiplicity, namely the sum of all Slater functions for each M_s. For the largest M_s this eigenfunction is simply the single Slater function with all spins positive and the energy is $Q-3(\alpha+\beta+\gamma+2\delta)$. This is the highest possible energy for such a system if all the interchange integrals are negative.

It is interesting to consider under what circumstances the lowest energy for the system corresponds to the energy which would be calculated from ψ_2, the bond function chemists ordinarily assume. This happens when $\delta = \frac{1}{2}(\beta+\gamma)$ and of course for the much more specialized case when these three integrals are zero. The results given for ammonia apply to all cases of three equivalent bonds, such as might be expected in $C \equiv N$, unless in addition we have symmetry about the plane perpendicular to the triple bond as for example in the case of the nitrogen molecule.

Nitrogen

The additional symmetry in nitrogen over ammonia just doubles the number of group operations and also the number of classes; so that proceeding exactly as in the case of ammonia we find the characters of the six irreducible representations given in the following table.

	C_1	C_2	C_3	C_4	C_5	C_6
Γ_1	1	1	1	1	1	1
Γ_2	1	1	−1	1	−1	−1
Γ_3	1	−1	−1	1	1	−1
Γ_4	1	−1	1	1	−1	1
Γ_5	2	0	2	−1	0	−1
Γ_6	2	0	−2	−1	0	1
h_i	1	3	1	2	3	2

The last line of the table gives the number of operations in each class. The operations of classes C_1, C_2, C_4 are the same, respectively, as C_1, C_2, C_3 for ammonia. The other classes may be specified by one operation taken from each; $C_3(ab)(cd)(ef)$; $C_5(ad)(bc)(ef)$; $C_6(adebcf)$. Each of the irreducible representations of ammonia have split into two representations; the first one into the first pair and so on. Exactly the same eigenfunctions form irreducible representations for nitrogen as for ammonia but with the difference that certain eigenfunctions now belong to different representations and are non-combining. The energies are exactly as written for ammonia if we remember that now $\beta = \gamma$. The following is the assignment of eigenfunctions to representations for nitrogen. For the singlets Γ_1, $\psi_1+\psi_6$ and ψ_2; Γ_3, $\psi_1-\psi_6$; Γ_5, $\psi_3-\psi_4$ with $\psi_5-\psi_4$. Triplets Γ_2, ϕ_1, and ϕ_2; Γ_4, ϕ_3; Γ_5, ϕ_8 with ϕ_9; Γ_6, ϕ_4 with ϕ_5 and ϕ_6 with ϕ_7. Quintets Γ_1, Ω_1; Γ_5, Ω_4 with Ω_5; Γ_6, Ω_2 with Ω_3.

Methane

The group of twenty-four symmetry operations includes all the rotations of a regular tetrahedron into itself plus the interchange of two hydrogen atoms, the rest of the molecule remaining fixed. The method of procedure is precisely the same as before. The five irreducible representations have the characters given in the table.

	C_1	C_2	C_3	C_4	C_5
Γ_1	1	1	1	1	1
Γ_2	1	−1	1	1	−1
Γ_3	2	0	2	−1	0
Γ_4	3	1	−1	0	−1
Γ_5	3	−1	−1	0	1
h_i	1	6	3	8	6

The four hydrogen eigenfunctions are indicated by the letters b, d, f, h and they are supposed bound, respectively, to the four carbon eigenfunctions a, c, e, g. The five classes are identified by the five permutations given in order: identity; $(eg)(fh)$; $(ae)(bf)(cg)(dh)$; $(ceg)(dfh)$; $(aceg)(bdfh)$. The representations for the fourteen singlet states are then: three representations of Γ_1, $\psi_1 = \text{II}$ and $\psi_2 = \text{III}+\text{V}+\text{XIX}$ and $\psi_3 = \text{IV}+\text{VI}+\text{VIII}+\text{XI}+\text{XII}+\text{XIV}$; one of Γ_2, $\psi_4 = \text{IV}-\text{VI}-\text{VII}-\text{IX}+\text{X}+\text{XIII}$; two of Γ_3, $\psi_5 = \text{V}-\text{III}$ with $\psi_6 = \text{V}-\text{XIX}$ and $\psi_7 = \text{XI}+\text{XII}-\text{IV}-\text{VI}$ with $\psi_8 = \text{XI}+\text{XII}-\text{XIV}-\text{VIII}$; one representation of Γ_4, $\psi_9 = \text{VI}-\text{IV}$, $\psi_{10} = \text{VIII}-\text{XIV}$, $\psi_{11} = \text{XII}-\text{XI}$; and finally one representation of Γ_5, $\psi_{12} = \text{I}-\text{XX}$, $\psi_{13} = \text{XV}-\text{XVII}$, $\psi_{14} = \text{XVI}-\text{XVIII}$. The bond eigenfunctions indicated by the Roman numerals are: $\text{I} = ah\ bc\ de\ gf$; $\text{II} = ab\ cd\ ef\ gh$; $\text{III} = ah\ bg\ cf\ de$; $\text{IV} = ab\ ch\ dg\ fe$; $\text{V} = ad\ bc\ eh\ fg$; $\text{VI} = af\ be\ cd\ hg$; $\text{VII} = ah\ bc\ dg\ ef$; $\text{VIII} = ah\ bg\ cd\ fe$; $\text{IX} = ab\ ch\ de\ fg$; $\text{X} = af\ bc\ de\ gh$; $\text{XI} = ab\ cd\ eh\ gf$; $\text{XII} = ad\ bc\ ef\ hg$; $\text{XIII} = ah\ be\ cd\ fg$; $\text{XIV} = ab\ cf\ de\ hg$; $\text{XV} = ah\ be\ cf\ dg$; $\text{XVI} = ad\ be\ ch\ fg$; $\text{XVII} = af\ bg\ ch\ de$; $\text{XVIII} = af\ bc\ dg\ eh$; $\text{XIX} = af\ be\ ch\ dg$; $\text{XX} = ad\ bg\ cf\ he$. The last six can be expressed in terms of the first fourteen but nothing is gained by this after linear independence of the eigenfunctions for each representation has been established.

The lowest energy lies in the symmetrical eigenfunctions, Γ_1, which involves the solution of the cubic:

$$\begin{vmatrix} 4\alpha-3(\beta+\gamma)-6\delta-W & 3\alpha-(9/2)(\beta+\gamma)-3W/4 & 12\alpha-(27/2)(\beta+\gamma)-9\delta-3W \\ 3\alpha-(9/2)(\beta+\gamma)-3W/4 & -9\alpha-18(\beta+\gamma)+9\delta-9W/2 & 9\alpha-(63/2)(\beta+\gamma)+18\delta-9W/2 \\ 12\alpha-(27/2)(\beta+\gamma)-9\delta-3W & 9\alpha-(63/2)(\beta+\gamma)+18\delta-9W/2 & 36\alpha-72(\beta+\gamma)-27W/2 \end{vmatrix} = 0.$$

α is the energy of one of the four exchange integrals corresponding to principal bonds; β corresponds to the interaction between hydrogen atoms; γ to the interaction between two bond electrons on carbon and δ to the interaction of an electron on hydrogen with one on carbon to which it is not bound. Examining the cubic it can be seen that if $\delta = (\beta+\gamma)/2$ one root of the equation, the lowest, is the upper principal diagonal element. This is the energy corresponding to ψ_1 the bond function regularly assigned to methane. This eigenfunction is, therefore, probably a rather good approximation. The letter W as written includes only the interchange energy.

The energy corresponding to Γ_2 is $Q-2\alpha-6\beta$ where Q is the coulombic binding. The four energies for Γ_3 correspond to taking the plus and minus sign each twice in $Q-(2/3\alpha+5/3(\beta+\gamma)+4\delta) \pm 2/3[\alpha^2+1/4(\beta+\gamma)^2+6\delta^2+2(\beta+\gamma)\alpha-6\alpha\delta-3(\beta+\gamma)\delta]^{\frac{1}{2}}$. For Γ_4 we have a triple root with energy $Q-2\beta-2\gamma-4\delta$ and for Γ_5 we have a triple root $Q-2(\alpha+\beta+\gamma+\delta)$.

These results offer some justification for Woods[10] use of the lowest bond eigenfunction in an approximate calculation. For more accurate results a cubic should of course be used. Van Vleck's[11] very interesting papers on methane treat the whole question from a somewhat different point of view.

Instead of using the symmetry group on the bond functions one could first apply it to get representations in terms of Slater functions with subsequent separation of the multiplets. This was carried through for certain of the cases given here but there seemed to be no real advantage and the labor of calculating the final matrix components is greatly increased. The method as outlined seems readily applicable to all symmetrical systems of bond functions.

F. Seitz, A. Sherman and A. E. Stearn have considered this problem from a somewhat different point of view and we wish to thank them for helpful joint discussions.

[10] H. J. Woods, Trans. Faraday Soc. **28**, 877 (1932).

[11] J. H. Van Vleck, J. Chem. Phys. **1**, 177 (1933); **1**, 219 (1933).

On the Quantum Mechanical Stability of a Benzol Molecule

M. MARKOV, *Physical Institute, University of Moscow*

(Received August 28, 1933)

The Heitler-London-Rumer treatment of valence bonds is applied to the benzol molecule, considered as a system of six trivalent nitrogen-like CH groups. Partial solution of the secular equation of the thirty-fourth degree shows that this model of the benzol ring is thermodynamically unstable relative to three acetylene molecules, in disagreement with experiment. The method does not take cognizance of the directional properties of valence bonds (Slater-Pauling). *Editors.*

AT the first attempt to approach the interpretation of the stability of a benzol molecule from the standpoint of Heitler-London's homopolar bending it is natural to start from the simplified model of a benzol molecule, namely, to assume that the benzol ring consists of six nitrogen-like atoms; that is, to take each of the CH groups that enter symmetrically into the structural formula of benzol as a single nitrogen-like trivalent atom.

The indication of the nitrogen-likeness of the CH molecule may be found, for instance, in the work of R. S. Mulliken,[1] who gives for the reaction of formation of CH the following formula:

$$C(1s^2 2s^2 2p^2)+H(1s)\rightarrow CH(1s^2 2s^2 2p^3)+D,$$

where D is the heat of dissociation and $1s^2$, $2s^2$, $\cdots$, etc., are the current notations in the systematics of spectra. Thus, we replace all CH in the benzol molecule by nitrogen atoms in their fundamental states.

Following the usual method for solving such problems it is necessary to start from "eigenvalue problem" in the space of valency functions: $(\lambda-W)\varphi=0$. In case of a cyclic chain of six trivalent atoms 1, 2, 3, 4, 5, 6 the operator W is equal to $T_{12}+T_{23}+T_{34}+T_{45}+T_{56}+T_{61}$, and T_{xy} is a differential operator of the kind[2] $T_{xy}=D_{xy}D_{yx}-3$. In other words the "exchange integrals" between the neighboring atoms are put equal to 1 and the interaction between the noncontiguous atoms is neglected.

Further, it is necessary to select independent valency functions φ_i; "to build a basis"; i.e., to select a complete set of independent functions φ_i each of them being a product of symbols of the kind $([xy];[xz]\cdots)$. The symbol $([xy])$ corresponds to a valency bond between the atoms x and y and, moreover, to a valency bond having a definite sense (from x to y); i.e., to a valency arrow.

If one uses the methods developed by G. Rumer the building of the basis does not present any difficulty even in the case of such a complicated system as a benzol molecule. To build the basis one has according to Rumer[3] to proceed as follows. Atoms are arranged arbitrarily along a circumference[4] and linked up by valency *arrows;* each of the figures of this kind having no intersecting arrows then corresponds to an independent valency state, and all other figures with intersecting arrows (as shown for the general case by Rumer) represent superpositions of independent valency states. For example:

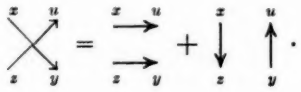

If the brackets of the kind $([xy])$ correspond to the valency arrows directed from X to Y,

[1] R. S. Mulliken, Phys. Rev. **40**, 55; **41**, 49 (1932).

[2] M. Born, *Ergebnisse der Exakten Naturwissenschaften* Vol. **10**, 1931.

[3] G. Rumer: *Zur Theorie der Spinvalenz,* Nachrichten von der Gesellschaft der Wissenschaften zu Göttingen. 1932. No. 27.

[4] Generally along the convex side of the closed curve.

we can write the same in symbols: $[xy][zu]=[xu][zy]+[xz][yu]$.

In our case there are thirty-four independent valency states. They are given in Fig. 1.

Operating on the valency functions by the operator W, using the notations of the valency functions of Fig. 1, and expressing the result by independent valency states, we obtain:

$$Wa_1=20a_1+18b_1+3l_1-8c_4+j_1+3k_1,$$

$$Wc_1=16c_1-2i_2-6d_2-6d_6-18m_2-4a_4,$$

$$Wd_1=16d_1+12m_1-4m_2+i_1-2c_2-2c_6-2l_2+6b_3-6b_2+2k_3,$$

$$Wb_1=10b_1+a_1-a_4+8m_1-8m_2+2d_3-2d_2+2d_5-2d_6,$$

$$Wl_1=22l_1-8d_6+8d_3+2c_1-2c_4+3a_1-3a_4+12b_1+4m_1-4m_2,$$

$$Wk_1=22k_1-8d_2+8d_5+2c_1-2c_4+3a_1-3a_4+12b_1+4m_1-4m_2,$$

$$Wj_1=30j_1-18a_4+18a_1,$$

$$Wi=18i_1-9c_4-9c_6-9c_2,$$

$$Wm_1=6m_1+4b_1-4b_2+4b_3-c_4-c_6-c_2.$$

Thus, generally speaking, we get a matrix of the thirty-fourth order. But as the operator W commutes with the cyclic operator Z, there is the possibility of reducing the order of the matrix. By the cyclic operator we understand the operator which acting on any function $\varphi_i(a_i; b_i; c_i \cdots)$ represented in Fig. 1 changes it into φ_{i+1} if $i<n$ $(i=1, 2 \cdots n)$ and into $+\varphi_1$ or $-\varphi_1$ if $i=n$.

Transforming the operator Z to the principal axes, we get:[5]

$$Z(a_1+\sigma a_2+\sigma^2 a_3+\sigma^3 a_4+\sigma^4 a_5+\sigma^5 a_6)=\sigma^5(a_1+\sigma a_2+\sigma^2 a_3+\sigma^3 a_4+\sigma^4 a_5+\sigma^5 a_6),$$

$$Z(a_1+\sigma^2 a_2+\sigma^4 a_3+a_4+\sigma^2 a_5+\sigma^4 a_6)=\sigma^4(a_1+\sigma^2 a_2+\sigma^4 a_3+a_4+\sigma^2 a_5+\sigma^4 a_6),$$

$$Z(a_1+\sigma^3 a_2+a_3+\sigma^3 a_4+a_5+\sigma^3 a_6)=\sigma^3(a_1+\sigma^3 a_2+a_3+\sigma^3 a_4+a_5+\sigma^3 a_6),$$

$$Z(a_1+\sigma^4 a_2+\sigma^2 a_3+a_4+\sigma^4 a_5+\sigma^2 a_6)=\sigma^2(a_1+\sigma^4 a_2+\sigma^2 a_3+a_4+\sigma^4 a_5+\sigma^2 a_6),$$

$$Z(a_1+\sigma^5 a_2+\sigma^4 a_3+\sigma^3 a_4+\sigma^2 a_5+\sigma a_6)=\sigma(a_1+\sigma^5 a_2+\sigma^4 a_3+\sigma^3 a_4+\sigma^2 a_5+\sigma a_6),$$

$$Z(a_1+a_2+a_3+a_4+a_5+a_6)=1(a_1+a_2+a_3+a_4+a_5+a_6).$$

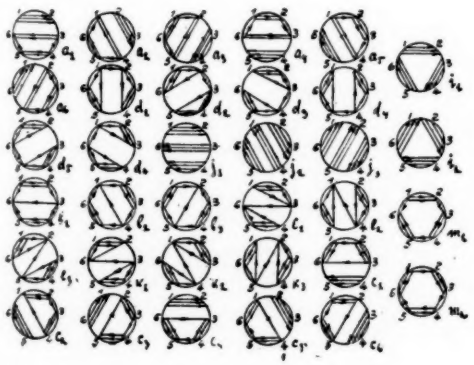

FIG. 1.

Denoting linear combinations of the kind a_i by A_i, C_i, etc., we have in case of c_i and d_i also:

$$ZC_1=\sigma^5 C_1, \quad ZD_1=\sigma^5 D_1,$$

$$ZC_2=\sigma^4 C_2, \quad ZD_2=\sigma^4 D_2,$$

$$ZC_3=\sigma^3 C_3, \quad ZD_3=\sigma^3 D_3,$$

$$ZC_4=\sigma^2 C_4, \quad ZD_4=\sigma^2 D_4,$$

$$ZC_5=\sigma C_5, \quad ZD_5=\sigma D_5,$$

$$ZC_6=1C_6, \quad ZD_6=1D_6.$$

[5] $\sigma^3=-1$.

In case of b_i:

$$Z(b_1+\sigma b_2+\sigma^2 b_3) = -\sigma^2(b_1+\sigma b_2+\sigma^2 b_3),$$

$$Z(b_1-\sigma^2 b_2-\sigma b_3) = \sigma(b_1-\sigma^2 b_2-\sigma b_3),$$

$$Z(b_1-b_2+b_3) = -1(b_1-b_2+b_3).$$

Denoting the corresponding combinations of the kind b_i by capital letters B_i etc. for l_i; k_i; j_i we get:

$$ZL_1=-\sigma^2 L_1; \quad ZK_1=-\sigma^2 K_1; \quad ZJ_1=-\sigma^2 J_1;$$

$$ZL_2=\sigma L_2; \quad ZK_2=\sigma K_2; \quad ZJ_2=\sigma J_2;$$

$$ZL_3=-1L_3; \quad ZK_3=-1K_3; \quad ZJ_3=-1J_3;$$

and finally:

$$Z(i_1+i_2)=1(i_1+i_2); \quad Z(m_1+m_2)=1(m_1+m_2);$$

$$Z(i_1-i_2)=-1(i_1-i_2); \quad Z(m_1-m_2)=-1(m_1-m_2).$$

Thus our matrix of the thirty-fourth order may be decomposed into six matrices: one of the ninth, two of the seventh, two of the third, and one of the fifth order. Each of these matrices corresponds to a definite eigenvalue λ_i of the operator W. Acting with the operator W on the functions denoted by capital letters we obtain the following matrices:

$$\begin{vmatrix} 6-\lambda & 0 & 0 & 1 & 0 \\ 0 & 18-\lambda & 0 & 9 & 0 \\ 0 & 0 & 20-\lambda & 8 & 0 \\ 54 & 6 & 4 & 16-\lambda & 12 \\ 24 & 3 & 0 & 4 & 16-\lambda \end{vmatrix} = 0, \quad (1)$$

$$\begin{vmatrix} 20-\lambda & -8 & 0 \\ -4 & 16-\lambda & 6 \\ 0 & 2 & 16-\lambda \end{vmatrix} = 0 \quad (2)$$

$$\begin{vmatrix} 20-\lambda & -8 & 0 \\ -4 & 16-\lambda & 6 \\ 0 & 2 & 16-\lambda \end{vmatrix} = 0, \quad (3)$$

$$\begin{vmatrix} 10-\lambda & 0 & 0 & 0 & 1 & 0 & -2 \\ 12 & 22-\lambda & 0 & 0 & 3 & 2 & -8\sigma \\ 0 & 0 & 30-\lambda & 0 & 18 & 0 & 0 \\ 12 & 0 & 0 & 22-\lambda & 3 & 2 & 8\sigma^2 \\ 36 & 6 & 2 & 6 & 20-\lambda & 8 & 0 \\ 0 & 0 & 0 & 0 & 4 & 16-\lambda & -6 \\ -12 & 4\sigma^2 & 0 & -4\sigma & 0 & -2 & 16-\lambda \end{vmatrix} = 0, \quad (4)$$

$$\begin{vmatrix} 10-\lambda & 0 & 0 & 0 & 1 & 0 & -2 \\ 12 & 22-\lambda & 0 & 0 & 3 & 2 & 8\sigma^2 \\ 0 & 0 & 30-\lambda & 0 & 18 & 0 & 0 \\ 12 & 0 & 0 & 22-\lambda & 3 & 2 & -8\sigma \\ 36 & 6 & 2 & 6 & 20-\lambda & 8 & 0 \\ 0 & 0 & 0 & 0 & 4 & 16-\lambda & -6 \\ -12 & -4\sigma & 0 & 4\sigma^2 & 0 & -2 & 16-\lambda \end{vmatrix} = 0, \quad (5)$$

$$\begin{vmatrix} 6-\lambda & 0 & 8 & 0 & 0 & 0 & 0 & 1 & 0 \\ 0 & 18-\lambda & 0 & 0 & 0 & 0 & 0 & 9 & 0 \\ 24 & 0 & 10-\lambda & 0 & 0 & 0 & 1 & 0 & 4 \\ 12 & 0 & 12 & 22-\lambda & 0 & 0 & 3 & 2 & 8 \\ 0 & 0 & 0 & 0 & 30-\lambda & 0 & 18 & 0 & 0 \\ 12 & 0 & 12 & 0 & 0 & 22-\lambda & 3 & 2 & 8 \\ 0 & 0 & 36 & 6 & 2 & 6 & 20-\lambda & 8 & 0 \\ 54 & 6 & 0 & 0 & 0 & 0 & 4 & 16-\lambda & 12 \\ 48 & 3 & 24 & 4 & 0 & 4 & 0 & 4 & 16-\lambda \end{vmatrix} = 0. \qquad (6)$$

When using the mirror symmetry K_i and L_i the order of the latter matrix may be lowered by a unit, and we obtain

$$\begin{vmatrix} 6-\lambda & 0 & 8 & 0 & 0 & 0 & 1 & 0 \\ 0 & 18-\lambda & 0 & 0 & 0 & 0 & 9 & 0 \\ 24 & 0 & 10-\lambda & 0 & 0 & 1 & 0 & 4 \\ 24 & 0 & 24 & 22-\lambda & 0 & 6 & 4 & 16 \\ 0 & 0 & 0 & 0 & 30-\lambda & 18 & 0 & 0 \\ 0 & 0 & 36 & 6 & 2 & 20-\lambda & 8 & 0 \\ 54 & 6 & 0 & 0 & 0 & 4 & 16-\lambda & 12 \\ 48 & 3 & 24 & 4 & 0 & 0 & 4 & 10-\lambda \end{vmatrix} = 0 \qquad (6')$$

and $\lambda_9 = 22$.

As the energy of three N_2-like molecules is equal to -9 we are interested only in matrices whose roots lie in the region of negative λ and especially in the region lower than -9, for only these values for the energy secure mechanical and (in case $\lambda < -9$) thermodynamical stability of the benzol molecule as well.[6]

It is quite evident that all the matrices with the exception of the last one have no roots in the region $\lambda < -9$. In fact, the proper values $\lambda_1; \lambda_2 \cdots \lambda_n$ of matrices in the general case (in case of complex matrix elements a_{ik}) lie only within a certain closed region (in a complex plane) made up by circles K_i $(i = 1, 2, \cdots n)$ with centers in a_{ii} and radii:

$$R = \Sigma' |a_{ik}|,$$

where Σ' means the sum over all k with exception of $k = i$.[7] Transforming our matrices in a suitable way (by multiplying rows and columns by certain numbers) we can slightly narrow the region of proper values of these matrices deduced directly from 1, 2, 3, 4, 5, 6.

The proper values of the transformed matrix of the fifth order lie between $-6 < \lambda_i < 36$, of the third between $6 < \lambda_i < 28$, of the seventh between $-8 < \lambda_i < 40$, of the eighth between $-17 < \lambda_i < 54$. Matrices (2) and (3), (4) and (5) have the same roots. The root in question hence can arise only from the last matrix (6'), which when transformed may be written:

[6] The minus sign before the "exchange integral" indicates attraction.

[7] S. Gerschgorin: *Über die Abgrenzung der Eigenwerte einer Matrix*, Bulletin de l'Academie der Sciences de U. S. S. R., 1931.

$$\begin{vmatrix} 6-\lambda & 0 & 16 & 0 & 0 & 0 & 6 & 0 \\ 0 & 18-\lambda & 0 & 0 & 0 & 0 & 9 & 0 \\ 12 & 0 & 10-\lambda & 0 & 0 & 3 & 0 & 12 \\ 2 & 0 & 4 & 22-\lambda & 0 & 3 & 2 & 8 \\ 0 & 0 & 0 & 0 & 30-\lambda & 18 & 0 & 0 \\ 0 & 0 & 12 & 12 & 2 & 20-\lambda & 8 & 0 \\ 9 & 6 & 0 & 0 & 0 & 4 & 16-\lambda & 12 \\ 8 & 3 & 8 & 8 & 0 & 0 & 4 & 16-\lambda \end{vmatrix} = 0.$$

The direct substitution of definite values of λ_i shows that the lowest proper value of this matrix lies between -8 and -9; hence in the model chosen by us the benzol molecule is stable mechanically but not thermodynamically.

We may suppose that this thermodynamical instability is the result of the incompleteness of our model of the benzol molecule. We have assumed the nitrogen-like atoms replacing CH in our model of the benzol ring to be in the state ^4S; we have further assumed the benzol model to be flat while we had to refer to it as to a space one, in fact it is known that N does not enter NH_3 in its fundamental state and that NH_3 (as the result of the absence of spherical symmetry of N) has not a plane structure, but a pyramidal one.

In conclusion I wish to offer my best thanks to Professor Rumer for the suggestion of the problem and for his continued help in this work.

On the Theory of the Distribution of Electrolytes Between a Solid Crystalline and a Liquid Phase

A. P. RATNER, *Chemical Laboratory, State Radium Institute, Leningrad*

(Received July 31, 1933)

A short discussion of the nature of distribution equilibria between mixed crystals and aqueous solutions is given. From the general theory of the thermodynamical potential and the activity theory of strong electrolytes, equations are deduced giving the influence of the composition of the liquid phase on the distribution ratio and the dependence of the partition constant on the properties of the pure components. The relative importance of the various factors in these equations, depending on the concentrations and properties of the components, is discussed. The deduced equations are in agreement with the experimental data.

THE conception of solid solution was first introduced into science by J. H. van't Hoff in the year 1890.[1] In support of such a view of solid mixtures he had already pointed out the distribution between solid and liquid solutions. If solid mixtures are really solutions the distribution of a substance between a solid and a liquid phase must take place according to the Berthelot-Nernst distribution law—$C_s/C_L = K_N$, where C_s and C_L are the concentrations of the micro-component in the solid and liquid phases, respectively, in case the following three requirements are fulfilled: (1) the solutions must be dilute enough with respect to the distributing substance in order that the variations in its content do not affect the thermodynamic properties of the solutions; (2) true equilibrium between phases and throughout each phase must be attained; and (3) the distributing substance must be in the same molecular state in both phases.

Since then a great number of investigations have been published concerning the question, but with very discordant results.[2] The cause of the discrepancies lie in the difficulty of attaining equilibrium, because of the extreme slowness of diffusion in crystals at ordinary temperatures; for the same reason inhomogeneous crystals once formed "freeze in" and do not spontaneously become uniform. Many investigators have paid much attention to this circumstance and have even considered the equilibrium conception, as well as the thermodynamical laws, inapplicable to the crystalline mixtures.[3]

But thermodynamics is not bound to any particular mechanism that fulfills its requirements. Diffusion is only a very convenient method for attaining equilibrium and does not affect the fundamental thermodynamical properties such as internal energy, entropy, etc. Therefore it is clear that the practical absence of diffusion in crystals at ordinary temperatures is only a matter of experimental method of attaining equilibrium and not of the inapplicability in principle of thermodynamics to the crystalline mixtures.

In fact in recent years Professor V. Chlopin and his collaborators[4] have worked out several methods of attaining equilibrium between mixed crystals and solutions, based on the recrystallization phenomenon. During the process of recrystallizaton each molecule of salt passes many times through the solution and, if this process is repeated often enough, an equilibrium between crystals and solution is established, and all the resulting crystals grow up from a solution of constant composition. Such crystals are quite homogeneous, and the Berthelot-Nernst distri-

[1] J. H. van't Hoff, Zeits. f. physik. Chemie **5**, 322 (1890).

[2] G. Bruni, *Feste Lösungen und Isomorphismus*, Leipzig, 1908, where the early literature is given. See also G. Tammann, Zeits. f. anorg. Chemie **87**, 1 (1919); G. Tammann and A. Svorykin, Zeits. f. anorg. Chemie **173**, 75 (1928); G. Meyer, Rec. Trav. Chim. Pays-Bas **42**, 304 (1923).

[3] See Tammann, reference 2.

[4] For a summary see: V. Chlopin, A. Polessitsky, A. Ratner and P. Tolmatscheff, Ber. **64**, 2653 (1931); see also R. Mumbrauer, Zeits. f. physik. Chemie **A156**, 113 (1931).

bution law is strictly valid for them. The true character of equilibrium attained is proved by the fact that the value of the distribution constant is the same independently of the side from which the equilibrium is attained, i.e., whether the distributing salt (usually a radio-element in concentrations of the order of 10^{-10} mol./cc) was added to the solution, or to the crystals at the beginning. The same result may be attained also more conveniently, especially at ordinary temperatures, by means of a rapid crystallization from a supersaturated solution with powerful stirring. Under such conditions, the recrystallization of minute crystals goes on very fast, and the equilibrium is reached in the process of growth of the crystals from the submicroscopical dimensions. In order to attain the equilibrium by crystallization from a supersaturated solution without such stirring, the crystallization must take place very slowly for otherwise instead of the simple form of the distribution law, the differential form or the so-called Doerner-Hoskins formula is followed. This formula is $\ln x = \lambda \ln y$, where x and y are the percents of the micro and macrocomponents, respectively, remaining in the solution. In that case, the concentration ratio remains constant for each surface layer of the growing crystals, but not for the crystal, as a whole. The same formula holds also for crystallization by slow evaporation, but the value of λ varies depending on the rate of evaporation and stirring, reaching, when the latter is good enough, the value of the partition factor $D = K_N C_L'/d$, where K_N is defined as above, and C_L' is the concentration of the macrocomponent in its saturated liquid solution.

These experiments have shown the possibility of attainment of an equilibrium state between a solid and a liquid solution, and have furnished a basis for further theoretical treatment of this subject. Such treatment is required in the first place in order to find the influence of the composition of phases on the value of the distribution constant. Such an influence was found experimentally by Professor V. Chlopin and his coworkers,[5] but the relations are too complicated to be made clear by purely experimental methods.

Since the work of van't Hoff and Roozeboom,[6] the question has not been subjected to theoretical treatment, except in two works, one by K. Herzfeld on thermodynamics of the formation of mixed crystals[7] and the other by L. Imre on the absorption view of the distribution.[8]

In the first work for which the distribution was only of secondary importance, the influence of the activity coefficients, so important in concentrated salt solutions, were lost sight of completely. Also the equation obtained is very complicated, because of the correction terms which have no importance for the distribution phenomena.

The second work deals only with the cases where the Doerner-Hoskins equation is valid, and L. Imre thinks, that in this case we are dealing with quite another phenomenon than the distribution attained by recrystallization, and that, due to the greater speed of the process, the adsorption equilibrium "freezes in" and that the work of "building on" (Anlagerung) and not that of "building into" (Einlagerung) is the more important. But these assumptions seem not to be true, for the range of rates of crystallization is the same for both cases. Which of the two forms of the distribution law holds depends not on the rate of crystallization, but on other conditions? If the number of crystals finally present is small compared with the number of crystallization centers originally formed, the crystals are homogeneous and the simple form of the distribution law is valid. But if the number of crystals is in the main the same during the entire process of crystallization, as in the evaporation experiments, or if their number diminishes by binding together of subcrystallites, and not by repeated recrystallization, the differential form of the distribution law holds, and if diffusion is eliminated, the value of λ is the same as that of the partition factor D. When the crystallization takes place without stirring, the equilibrium is not attained due to the slowness of diffusion and the observed values of λ lie nearer to 1 than corresponding values of D. Thus we have no reason to use different laws for different cases of crystallization and to take into account

[5] V. Chlopin and A. Polessitsky, Zeits. f. physik. Chemie **A145**, 57 (1929); V. Chlopin and A. Ratner, Comptes Rendus Acad. Sciences U. S. S. R. 723 (1930).

[6] B. Roozeboom, Zeits. f. physik. Chemie **8**, 504 (1891).

[7] K. Herzfeld, Zeits. f. Physik **16**, 84 (1923).

[8] L. Imre, Zeits. f. physik. Chemie **A164**, 364 (1933).

the work of "building on" instead of "building into" even when the Doerner-Hoskins formula is followed. L. Imre himself takes as the base of his calculation the values of heat of solution of the components when calculating the value of λ from his equation. But the heat of solution corresponds to the work of bringing the salt into the solution from the volume of the crystal and not from its surface, in other words, to the work of "building into" and not of "building on." Obviously the right order of the value found for λ based on those heats of solution speaks against L. Imre's ideas of "freezing in" of absorption equilibrium rather than for them. Because of these considerations I took as a starting point for my work the thermodynamical treatment of the equilibrium state based on the general theory of chemical potentials and on modern activity theory of strong electrolytes and not the kinetics of crystallization. This allowed me to find definite connections between the value of D, the composition of the solution and the properties of the pure components.

Theoretical Part

Notation

In this work the following notations are used: x = mol fraction; c = concentration in grams per liter; m = molality; L = solubility product; a_+, a_- = activities of the ions; a = activity of the electrolyte as a whole = $a_+^{\nu+}a_-^{\nu-}$; γ_+, γ_- = activity coefficients of the ions; γ = activity coefficient of the electrolyte; μ = Gibbs's chemical potential; $\mathfrak{y}$ = chemical potential in the standard state chosen in the usual way for a solute;[9] d = specific weight of the crystals; D = partition factor = $K_N C'/d = C_s C'/C_L d$. The subscripts s and L refer to solid and liquid phases, respectively. The superscript $'$ refers to the macrocomponents.

Deduction of the Formulae

According to the main statements of the theory of the chemical potential its value for the distributing substance at equilibrium must be the same in both phases:

$$\mu_L = \mathfrak{y}_L + RT \ln a = \mu_s. \tag{1}$$

[9] Lewis and Randall, *Thermodynamics*, McGraw-Hill Book Co., New York, 1923, p. 259.

As in the solid phase we have a very dilute solution we can write for μ_s

$$\mu_s = \mathfrak{y}_s + RT \ln x_s^{\nu+}. \tag{2}$$

The $x_s^{\nu-}$ is omitted for the anion is common for both components and the only one in crystals. From (1) and (2) we obtain:

$$\ln (x_s^{\nu+}/a_+^{\nu+}a_-^{\nu-}) = (\mathfrak{y}_L - \mathfrak{y}_s)/RT. \tag{3}$$

For the saturated solution of the microcomponent in pure water, we can write

$$\mu_{0s} = \mathfrak{y}_L + RT \ln a_0. \tag{4}$$

Substituting $\mathfrak{y}_L$ in (3) from (4) we obtain finally:

$$x_s^{\nu+}/a_+^{\nu+}a_-^{\nu-} = (1/a_0)e^{(\mu_{0s}-\mu_s)/RT}. \tag{5}$$

The right-hand side of this equation does not depend on the composition of the liquid phase; therefore we have in it the main expression for the distribution constant of an electrolyte between a solid and a liquid phase.

For the most important case practically, i.e., when the solid phase is a pure salt isomorphous with the microcomponent, the Eq. (5) can be transformed into another form more convenient for comparison with experiment. This may be done by multiplication of both sides of the Eq. (5) by the activity of the microcomponent, the same in all the solutions and equal to a_0, the activity in pure saturated solution since they are all in equilibrium with the pure solid macrocomponent. Taking into account that a_-' and a_- is the same quantity, for it refers to a common ion in a common solution, and expressing the activities through molalities, we obtain:

$$\frac{x_s^{\nu+}m_+'^{\nu+}}{m_+^{\nu+}}\frac{\gamma_+'^{\nu+}}{\gamma_+^{\nu+}} = \frac{a_0'}{a_0}e^{(\mu_{0s}-\mu_s)/RT} = D_0. \tag{6}$$

The quantity D_0 may be called the "true partition constant," for on one hand, it does not depend on the composition of the liquid phase and on the other hand it is connected with the partition factor D, which is usually employed to express the experimental results, and as a characteristic of the course of the fractional crystallization. We can divide the Eq. (6) into two:

$$\frac{x_s^{\nu+}m_x'^{\nu+}}{m_+^{\nu+}}\frac{\gamma_+'^{\nu+}}{\gamma_+^{\nu+}} = D_0 \tag{6a}$$

and

$$D_0 = (a_0'/a_0)e^{(\mu_{0s}-\mu_s)/RT}, \qquad (6b)$$

the first of which expresses the dependence of the concentrations of the components in both phases on one another, and the second the dependence of the value of D_0 upon the properties of the pure components.

Discussion of the Results

The left-hand side of Eq. (6a) consists of two factors: $x_s^{\nu_+}m_+'^{\nu_+}/m_+^{\nu_+}$ represents the law of distribution of an electrolyte as it would be if the solutions were ideal, and the second $\gamma_+'^{\nu_+}/\gamma_+^{\nu_+}$ containing the activity coefficients, gives the correction due to deviations of the solutions from ideal. We can see from it, that in ideal or very dilute solutions the first term must be constant regardless of the composition changes of the solution. For the case $\nu_+=1$, as in all hitherto studied systems, the first factor becomes identical with the partition factor D.

Up till now in all the works on the distribution of radioelements, between solid and liquid phases, it was admitted, that because of the very minute concentrations used (of the order of 10^{-10} mol/cc or even less) we can consider their solutions as ideal and neglect the activity coefficients. But that supposition is only partly true; namely, in that the variations in the content of the radioelements do not influence the activity coefficients of the components, and this is the reason for good constancy of the partition factor at constant composition of the solution obtained. But as the activity coefficient of an electrolyte depends on the total ionic strength of the solution and not upon the concentration of the given electrolyte, and we usually deal with more or less concentrated salt solutions, the γ_+ is very far from unity and depends very much on the composition of the liquid phase.

But, as it is seen from the Eq. (6a) the second factor consists not of γ_+ only, but of the ratio γ_+'/γ_+, and that ratio can be considered as equal to unity, or at least as independent of the composition in a limited range, even in fairly concentrated solutions, for the ions of the components are of the same valency and do not differ very much in dimensions for otherwise they could not form isomorphous crystals.

The range of the probable constancy of D becomes even larger if we take into consideration that γ_+ of the Eq. (6a) is the activity coefficient of the microcomponent when added to the solution of the macrocomponent and not in a solution of the same concentration of itself only. As some of the factors that determine the deviations of the behavior of electrolytes from the ideal depend on all the ions in solution (electric field in the solution, dielectric constant) and some upon the particular ion under consideration (polarizability, degree of ionization, side chemical reactions) we may expect that generally the value of the activity coefficient of an ion, when added to a much larger quantity of another ion would lie nearer to the value of γ for the latter at the same ionic strength, than the value of pure microcomponent.[10] Also, the changes of the activity coefficient of microcomponent in such solutions lie nearer to the corresponding changes of the activity coefficient of the macrocomponent than they would to such changes in a pure solution of the microcomponent. Obviously the difference of the behavior of the components must be the smaller, and the constancy of the ratio of the γ's the better, the more dilute the solution is and the more alike the ions of the components are.

Turning now to the comparison of the Eq. (6a) with the experimental data, we meet with the lack of knowledge of the activity coefficients in such mixed solutions. But the above considerations show a way for approximate proof of this equation, namely, by taking D instead of D_0 and comparing then the deviations from constancy caused by this substitution with what may be expected from the electrochemical properties of the components.

In the Tables I, II and III are collected all the available data on the variation of the distribution constant with the composition of the liquid phase.

---

[10] So it is generally, but not always for the above factors change the activity coefficients in different directions, and we may find sometimes that as a result of their interaction the activity coefficient of the microcomponent would get farther from that of macrocomponent instead of approaching it. Such is the case for HCl in concentrated solutions of LiCl (see J. Hawkins, J. Am. Chem. Soc. **54**, 4480 (1932).

TABLE I. $Pb(NO_3)_2-Ra(NO_3)_2$ *at 25°.**

Composition of the solution		K_N	D
1.82 m $Pb(NO_3)_2$		18.2	2.19
1.01 " "	1.09 m HNO_3	41.9	2.81
4.55 " "	7.12 " $NaC_2H_3O_2$	26.3	4.55
	3.29 " $HC_2H_3O_2$		

* V. Chlopin and A. Ratner, reference 5.

TABLE II. $BaBr_2-RaBr_2$ *at 0°.**

Composition of the solution		K_N	D
3.11 m $BaBr_2$		52.8	12.4
2.92 " "	0.27 m HBr	57.7	13.2
2.84 " "	0.43 " "	59.1	12.8
2.67 " "	0.64 " "	58.3	11.9
2.42 " "	1.03 " "	68.4	12.6
1.72 " "	2.22 " "	116.0	15.4
1.27 " "	2.92 " "	146.0	14.2
0.74 " "	4.00 " "	173.4	9.8
0.42 " "	4.81 " "	243.0	7.8

* V. Chlopin and B. Nikitin, Zeits. f. anorg. Chemie **166**, 311 (1927).

TABLE III. $Ba(NO_3)_2-Ra(NO_3)_2$.*

Composition of the solution		$t°$	K_N	D
0.411 m $Ba(NO_3)_2$		25°	46.0	1.49
0.367 " "	0.530 m $BaCl_2$	"	21.7	1.56
0.195 " "	0.585 " HNO_3	"	85.2	1.31
0.674 " "	3.34 " $NaC_2H_3O_2$	"	25.5	1.34
	0.13 " $HC_2H_3O_2$			
0.400 " "	0.209 " $HgCl_2$	"	44.7	1.39
0.416 " "	1.18 " glucose	"	56.1	1.60
0.189 " "		0°	154.0	2.31
0.080 " "	0.423 " HNO_3	"	334.0	2.12
0.185 " "	0.202 " $BaCl_2$	"	64.0	2.24

* V. Chlopin, A. Ratner and P. Tolmatscheff, unpublished.

As it may be seen from the tables, the constancy of D is in full accord with the above considerations, the worst in the case of lead nitrate as macrocomponent, because of the large solubility of lead nitrate and the great difference in properties between lead and radium ions and the best for the sparingly soluble barium nitrate whose cation is very much more similar to the radium ion. In the last case the constancy of D is fairly good (within 20 percent) though the K_N values vary many times.

But not only the degree of constancy of D, but also the direction of deviations from it is in full accord with what could be expected from the properties of the components. Thus in the case of lead nitrate which is much more associated electrolytically than barium and radium salts[11] and gives nondissociated basic acetates on addition of HNO_3 or $NaC_2H_3O_2$ the activity coefficient of lead γ_+' falls a great deal faster than that of radium, the ratio γ_+'/γ_+ falls too, and as D_0 must remain constant, D must rise, which is the case. For barium salts the conditions are reversed, for radium salts must be more associated than those of barium because of the larger polarizability of radium, and we see in Tables II and III that D in these systems decreases slightly but systematically in all cases on addition of corresponding acids. So it seems that the Eq. (6a) is wholly confirmed by the experiment.

Expressing the activities through molalities, we can write Eq. (6b)

$$D_0=(L_0'/L_0)(\gamma_0'/\gamma_0)e^{(\mu_{0s}-\mu_s)/RT}.$$

The first factor on the right-hand side of this equation, which would have been the only one if both phases were ideal mixtures, gives the connection between the partition factor and the solubilities of the components. The existence of such a connection was admitted by all chemists who had worked with the fractional crystallization and it was thought to be so direct that conclusions in regard to the identity of the solubility of the components[12] were made from an unsuccessful attempt of fractional crystallization. But an exact investigation, experimental or theoretical, on the existence and form of such a connection was still lacking, and in recent years there has been accumulated material contradicting it, at least in such exact form as it was assumed before.[13]

It follows from Eq. (6b) that this connection consists of a proportionality to the ratio of the solubility products but is masked by the influence of the non-ideal behavior of the solutions expressed in the liquid by the activity coefficients, and for the solid in the term $e^{(\mu_{0s}-\mu_s)/RT}$. These influences, especially that of the liquid phase,

[11] Plake, Zeits. f. physik. Chemie **A162**, 24 (1932).

[12] M. Curie, *Traite de Radoactivite*, Gauther, Villard, Paris, 1910. V.I. p. 174.

[13] V. Chlopin, Zeits. f. anorg. Chemie **143**, 97 (1923); O. E. Erbacher, Ber. **63**, 141 (1930); A. Polessitsky, Zeits. f. physik. Chemie **A161**, 325 (1932).

may change the value of D_0 many times and thus the above-mentioned experimental facts are explained.

The comparison of the Eq. (6b) with experiment is even more difficult than that of Eq. (6a) for we meet again with the absence of data for the ratio γ_+'/γ_+, but here we need the constancy of that ratio as well as its absolute value. Further the term $e^{(\mu_{0s}-\mu_s)/RT}$ is also undeterminable as yet, for the theoretical calculation of lattice energies is not exact enough and its computation from the heats of solution of the mixed crystals also fails because of the absence of such determinations through a sufficiently large range of concentrations. We could pass over all these difficulties by means of a determination of the partition constant for a weakly soluble macrocomponent at different temperatures, but even with data now available we can judge of the validity of the Eq. (6b) by comparing the values of D with the ratios a_0'/a_0 for all the systems, for which the solubilities of the components are known.

These data for $t=20°C$ are given in Table IV in the first column of which the systems considered are given, the microcomponent being placed in brackets. The solubilities of radium salts are taken from the work of O. Erbacher,[14] and the values of activity coefficients necessary for the figures of the fourth column were evaluated approximately by a graphical extrapolation, using Lucass'[15] data on alkaline earths chlorides for the halide systems, and Gellbach and Heppke's[16] on barium bromide, and the author's determinations at 70° on the nitrates (by vapor pressure methods, unpublished).

TABLE IV.

System	m_0	m'_0/m_0	a'_0/a_0	D
$Ba(Ra)Br_2$	3.50	1.91	60	11
$Ba(Ra)Cl_2$	1.71	2.07	16.5	4.5
$Ba(Ra)(NO_3)_2$	0.33	0.83	1.14	1.6
$Ba(Pb)(NO_3)_2$	0.33	0.20	0.12	0.16
$Pb(Ra)(NO_3)_2$	1.66	4.15	11.9	2.5
$Pb(Ba)(NO_3)_2$	1.66	5.03	8.32	2.4

[14] O. Erbacher, Ber. **63**, 141 (1930).

From Table IV we see that the partition factors show an unmistakable parallelism to the activity ratios, though they are by no means equal to the theoretical values, the discrepancy increasing with increased solubility of the macrocomponent. At the same time, it is difficult to speak even of a parallelism between the solubility ratios and the partition factors.

We may go slightly further for the system $Ba(Pb)(NO_3)_2$ due to the determination of the heats of solution of mixed crystals of barium and lead nitrates made by G. Tamman,[17] which enables us to compute at least the sign and order of magnitude of $\mu_{0s}-\mu_s$. This computation gives the value of 400–600 cal., from which

$$D_0=a_0'/a_0e^{(\mu_{0s}-\mu_s)/RT}=0.30.$$

The γ_+'/γ_+ for this system is equal approximately to 1.30 and the experimental value of D_0 is approximately 0.20. The agreement between these values may be considered as quite satisfactory, taking into account the very approximate character of the calculations.

At this point I wish to take the opportunity to acknowledge my gratitude to Professor V. Chlopin for his advice and continued attention throughout this work.

[15] Lucass, J. Am. Chem. Soc. **47**, 743 (1925).

[16] Gellbach and Heppke, J. Am. Chem. Soc. **48**, 1504 (1926).

[17] G. Tammann and Krings, Zeits. f. anorg. Chemie **130**, 229 (1923).

Correlation of Heat Capacity, Absolute Temperature and Entropy

GEORGE A. LINHART, *Riverside Junior College, Riverside, California*

(Received August 7, 1933)

Correlation of heat capacity, absolute temperature and entropy: Starting with the two assumptions that at very low temperature the heat capacity is proportional to the entropy, and that at relatively high temperature it approaches a limiting value (C_∞), very simple relations are obtained between the heat capacity and the absolute temperature, and between the entropy and the absolute temperature of a given substance, by the introduction of a simple algebraic function which satisfies the two assumptions. The validity of these relations is substantiated by the excellent agreement of the observed and the calculated values for the heat capacities and for the entropies of a considerable number of substances, ten of which are given in this paper.

IN establishing the relation of heat capacity, absolute temperature and entropy of a given substance at constant pressure, two assumptions are made: first, the heat capacity C is proportional to the entropy S as the absolute temperature approaches zero; second, the heat capacity C approaches a limiting value C_∞ at relatively high temperature. These assumptions may be expressed analytically as follows:

(a) $$(\partial C/\partial S)_p = K(T \to 0),$$

and

(b) $$(\partial C/\partial S)_p = 0(T \to \infty).$$

Making use of the thermodynamic equation,

$$(\partial S/\partial T)_p = C_p/T,$$

gives

$$\left(\frac{\partial C}{\partial S}\right)_p = \left(\frac{\partial C}{\partial T}\right)_p \cdot \left(\frac{\partial T}{\partial S}\right)_p = \left(\frac{\partial C}{\partial T}\right)_p \cdot \frac{T}{C_p}. \quad (1)$$

Arithmetical experience with a large number of heat capacity data shows that the left-hand member of Eq. (1) may be replaced by a very simple function, namely,

$$(\partial C/\partial S)_p = K(1 - C/C_\infty), \quad (2)$$

so that Eq. (1) becomes,

$$(\partial C/\partial T)_p = K(1 - C/C_\infty)C/T. \quad (3)$$

The right-hand member of Eq. (2) obviously satisfies the two assumptions (a) and (b).

The integrated form of Eq. (3) is,

$$\log C/(C_\infty - C) = K \log T + \log k, \quad (4)$$

which may also be written in the forms,

$$C = C_\infty k T^K/(1 + kT^K) \quad (5)$$

or,

$$C = C_\infty k e^{K \log T}/(1 + ke^{K \log T}). \quad (6)$$

In testing the validity of Eq. (4), the following method was used.

First, the experimental values for C were plotted against the corresponding logarithms of the absolute temperatures, and the curves representing Eq. (6) sketched in.

Second, the best value for C_∞ was in each case located on the curve. This was easily attained, since the curve is symmetrical with respect to the inflection point, as may be readily shown by placing the second derivative of C with respect to $\log T$, of Eq. (6) or (7), equal to zero; at this point, $C = C_\infty/2$.

Third, the best values for K and for $\log k$ were obtained from the straight line plot of Eq. (4), where K is the slope and $\log k$ is the intercept on the $\log C/(C_\infty - C)$ axis.

Fourth, with the aid of these quantities, the values for C "calculated" may be readily obtained by means of Eq. (4).

DISCUSSION OF C_∞

From the analogy of the specific heat of a "perfect monatomic gas," the older school of physical chemists reached the conclusion that C_∞ for all solids at constant volume should be $3R$ (5.966), calories per gram atom of substance. Any excess of this value was attributed to the work done by virtue of the expansion of the

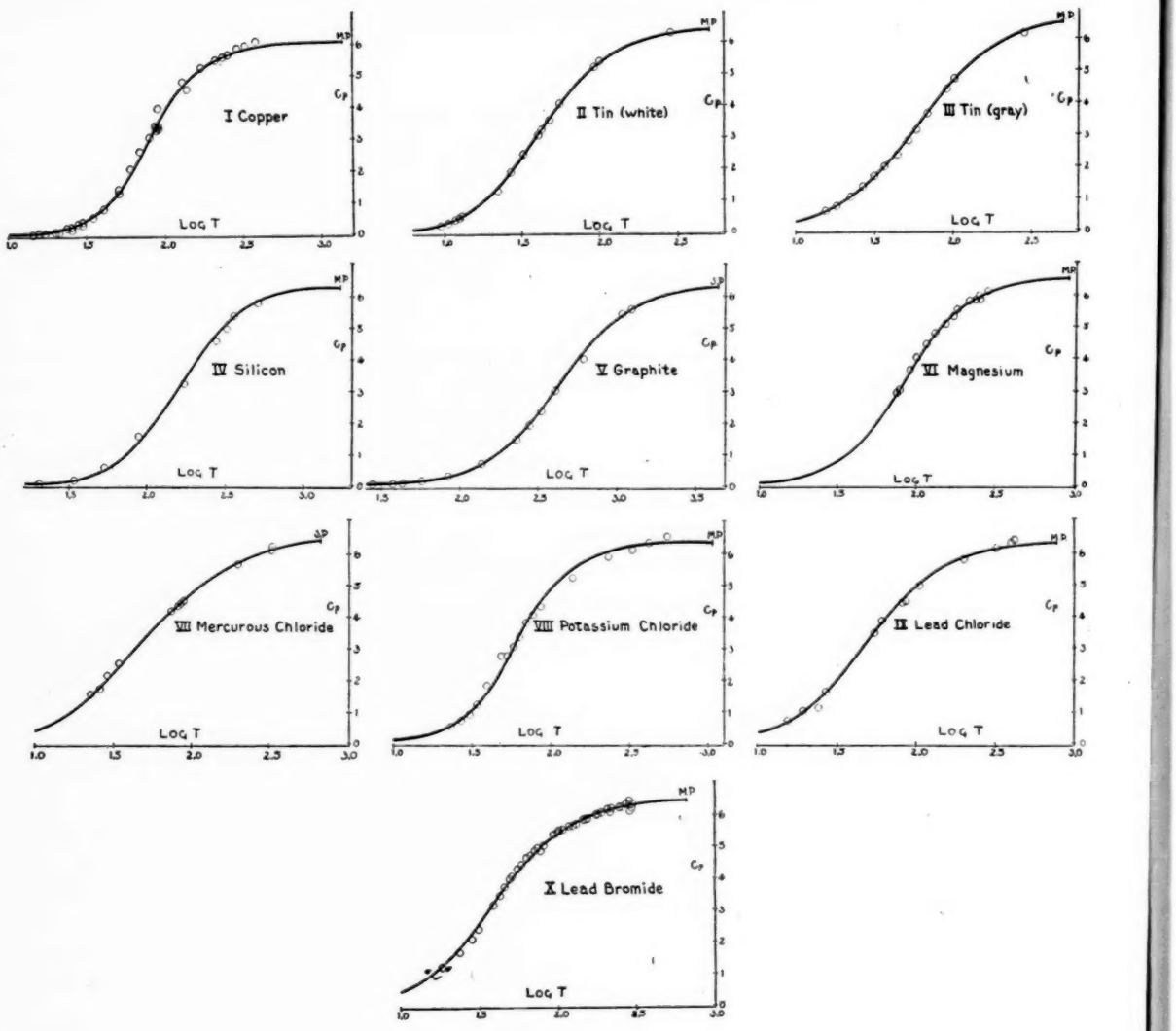

FIG. 1.

substance. Modern investigators have found, however, that the rather large excess of $3R$ calories near the melting point cannot be accounted for in this manner. Some suggest that at the upper temperature, or near the melting point of the substance, the electrons themselves may acquire an appreciable heat capacity; but the specific heat data in the region of the melting point are still meager and of insufficient accuracy to warrant calculation of the heat capacity of the electrons. Investigations in this field are now being conducted by Jaeger and Bottema,[1] and their results will very likely lead to definite conclusions.

Similar investigations in the neighborhood of the absolute zero are now being carried on by Keesom and his associates.[2] When sufficient data have been accumulated in these two fields they will be analyzed in a similar manner.

THE GRAPHS

The graphs are self-explanatory. The letters M.P. denote the melting point; the letters S.P. denote the sublimation point. It is of interest

[1] Jaeger and Bottema, Proc. Acad. Sci. (Amsterdam), 1932.

[2] Keesom, Proc. Acad. Sci. (Amsterdam), 1932.

TABLE I. *Summary of entropies from 0 to 298° absolute, and constants.*

	S_p		C_∞	K	log k
Copper	8.10	8.18	5.97	2.900	−5.49550
Tin (white)	12.22	11.17	6.40	2.074	−3.41445
Tin (gray)	10.82	9.23	6.70	1.700	−3.03844
Silicon	4.25	4.70	6.30	2.316	−5.15068
Graphite	1.45	1.30	6.40	1.820	−4.79222
Magnesium	8.55	8.30	6.60	2.050	−3.94848
Mercurous chloride	23.88	23.20	6.50	1.480	−2.52140
Potassium chloride	20.50	19.70	6.40	2.380	−4.23445
Lead chloride	34.86	33.20	6.40	1.769	−2.99838
Lead bromide	39.02	39.75	5.50	1.840	−2.96575

to note that the experimental points follow the calculated curves very closely, and that the average deviations do not exceed the average experimental variations.

CONCLUSION

In conclusion it may be mentioned that the heat capacities of all substances, measured by the thermoelectric method, conform statistically to Eq. (6). The ten substances given in this paper were taken at random from a group of about three times that number. It is also interesting to find that the entropies calculated from the integrated form of Eq. (2) between 0 and 298° absolute are practically identical with those given in the thermodynamic literature, which have been obtained by the mechanical integration of the areas under the $C-\log T$ curves. A comparison of these values is given in Table I. In the second column are given the values for the entropies from 0 to 298° absolute calculated from the integrated form of 2,

$$S=2.3(C_\infty/K)\log C_\infty/(C_\infty-C), \qquad (7)$$

and in the third column are given the values as recorded in the thermodynamic literature; these have been obtained by mechanical integration.

It is seen that in every one of the ten substances the observed values agree with the calculated values within experimental error.

Note: References to the data used in this paper may be found in the International Critical Tables, Vol. V. The data recorded in that volume are not, however, the original values and are therefore not suitable for investigational purposes. For an extensive and interesting discussion of specific heat data at constant volume, the reader is referred to an article by F. Schwers, Phys. Rev. **8**, 117 (1916).

The Thermal Decomposition of Propyl Mercaptan

H. AUSTIN TAYLOR AND EDWIN T. LAYNG,[1] *New York University*

(Received August 24, 1933)

The thermal decomposition of normal propyl mercaptan over a temperature range from 405 to 435°C and pressures from 100 to 300 mm is homogeneous on a poisoned glass surface. The reaction is complex showing an induction period with auto-accelerating rate, ending finally in a pseudo-equilibrium involving propylene, hydrogen sulphide and isopropyl mercaptan. The energy of activation of the induction period is about 40,000 calories and that of the later reaction 39,000 calories. A mechanism, has been proposed which involves primarily the formation of propyl sulphide reacting further to form a sulphonium hydrosulphide as an unstable intermediate.

FROM a recent study of the decomposition of ethyl mercaptan Trenner and Taylor[2] concluded that the mechanism involved a series of consecutive reactions leading to an equilibrium in which ethylene and hydrogen sulphide preponderate. The marked similarity in the decomposition of ethyl sulphide suggested a parallel mechanism and the same intermediate was tentatively assigned to both reaction schemes. The isolation of this intermediate could not be accomplished as definite proof of the conclusions drawn. Propyl mercaptan being homologous with the ethyl derivative a similarity in their decompositions might logically be expected whilst the individual rates of the consecutive reactions might be such as to allow the isolation of the intermediate compound for further study. Although this has not been achieved the work has served to verify, amplify or in some ways modify the conclusions previously drawn.

EXPERIMENTAL

The sample of normal propyl mercaptan used was from the Eastman Kodak Company and was carefully dried and fractionated to give a product boiling in agreement with the findings of Ellis and Reid[3] from 67.4 to 67.6°C at 763 mm.

A. Static method

The apparatus used in the work was practically identical with that used by Trenner and Taylor. The reaction vessel of Pyrex glass had a capacity of 279 cc. The total free volume outside the furnace was less than two percent of this value and was maintained by auxiliary heaters at 65°C to prevent condensation of mercaptan. As was found with ethyl mercaptan the induction periods in the decomposition of the propyl mercaptan were somewhat erratic in duration on a clean surface but after three or four samples were successively decomposed, the products of each being removed by five minutes pumping with a "hyvac" oil pump, the induction periods as well as the entire decomposition rates could be reproduced at will. The results for various pressures and temperatures will be presented later.

B. Dynamic method

To obtain a qualitative knowledge of the products of reaction particularly during the early stages, as substantiation of the proposed mechanism, several dynamic experiments were made. The propyl mercaptan was maintained at a temperature of 78°C with ethyl alcohol constantly refluxing, to exert a constant vapor pressure on a calibrated capillary connected with the reaction tube in the furnace. The temperature was measured by a platinum resistance thermometer located in the center of the reaction tube. Passing out of the reaction tube the gases were carried through three traps. The first trap was immersed

[1] Abstract from a thesis presented in partial fulfillment of the requirements for the degree of Doctor of Philosophy at New York University, June, 1933.

[2] Trenner and Taylor, J. Chem. Phys. **1**, 77 (1933).

[3] Ellis and Reid, J. Am. Chem. Soc. **54**, 1674 (1932).

in a Dewar flask containing ice and salt at −19°C; the second was immersed in solid carbon dioxide and toluene and the third in liquid air. This latter trap was connected to a mercury manometer and gas burette. The pressure on the reservoir side of the calibrated capillary was thus constant at 1066 mm, the rest of the system being maintained at atmospheric pressure. That the system should be entirely free from oxygen, it was first swept out with helium. During a run as the helium was displaced it was allowed to blow off at atmospheric pressure, whilst any small quantities remaining would not interfere with a qualitative analysis of other gases produced by reaction.

Results

Since there are no data available on the vapor pressure of propyl mercaptan and since the apparatus for the static experiments lent itself admirably to this determination the values given in Table I were obtained.

Table I.

Temperature		Vapor pressure	
284.6°K	318.1°K	84.0 mm	351.0 mm
289.9	323.3	97.5	425.0
295.8	328.2	141.0	509.5
301.7	333.3	182.4	600.0
307.5	340.57 (calc'd)	233.0	760
313.0		284.2	

Fig. 1 shows these results graphically where the logarithm of the pressure is plotted against the reciprocal of the absolute temperature. The straight line may be represented by the following equation:

$$\log p = -1647/T + 7.7190.$$

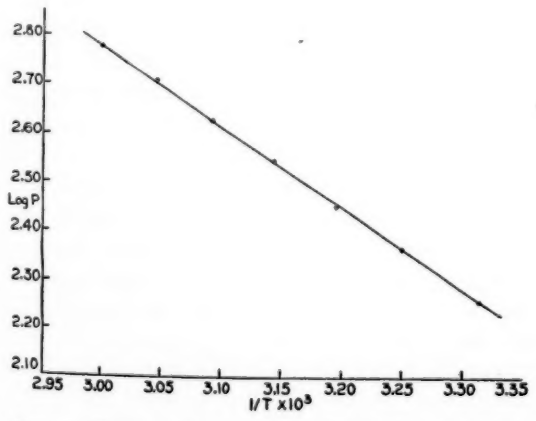

Fig. 1. Vapor pressure curve of propyl mercaptan.

A. Static method

By this method data on the rate of decomposition were obtained at varying pressures from 100 to 350 mm and at temperatures from 405 to 435°C. Fig. 2 illustrates graphically the rates obtained at initial pressures of 101, 152, 199, 300 and 351 mm at 405°C. It will be observed that

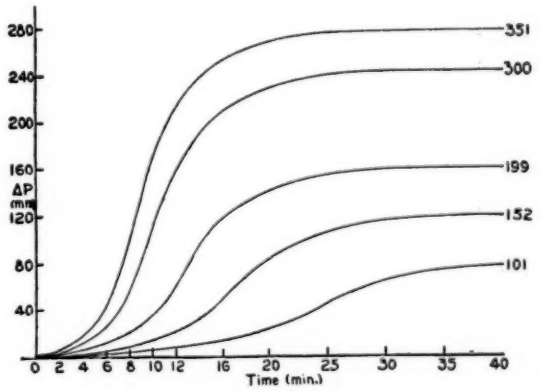

Fig. 2. Decomposition rate curves of propyl mercaptan at pressures of 101, 152, 199, 300 and 351 mm at 405°C.

the curves are identical in form to those obtained by Trenner and Taylor for ethyl mercaptan. Since it was there shown that the point of inflection was of considerable importance, its exact location was made experimentally by taking pressure readings every fifteen seconds in the neighborhood of the approximate position of maximum rate previously determined. Table II gives the location of the points of inflection at the various pressures and temperatures studied. The last two columns will be referred to later in the discussion.

The peculiar behavior of the induction period previously mentioned, suggesting heterogeneity, the effect of an increased surface was tested. Results again identical with those for ethyl mercaptan were found. The first reaction after the chamber had been filled with short lengths of Pyrex tubing and very thoroughly evacuated showed practically no induction period. In subsequent reactions this became progressively

TABLE II.

Init. press. P (mm)	Time to inflection (min.)	Press. increase	Press. unreacted P_I	P_I/P
		Temperature 405°C		
351	8.75	132	219	0.624
300	10.00	107.6	192.4	0.641
199	12.75	71.8	127.2	0.638
152	17.50	60.7	91.3	0.601
101	25.00	41.5	59.5	0.589
		Temperature 415°C		
351	5.50	134	217	0.618
304	6.12	107.5	196.5	0.646
202	9.00	85	117	0.585
149	13.00	63.5	85.5	0.574
99	19.00	44.7	54.3	0.554
		Temperature 425°C		
351	3.75	132	219	0.624
297	4.00	111.9	185.1	0.624
200	5.75	88	112	0.560
147	9.00	63.6	83.4	0.569
101	12.00	45.5	55.5	0.550
		Temperature 435°C		
347	2.50	133	214	0.617
298	2.75	109	189	0.634
202	3.75	85.9	116.1	0.581
150	6.00	67.2	82.8	0.552
100	8.00	43.8	56.2	0.562

TABLE III.

Init. press. (mm)	Press. increase	Percent decomp.	t_{25}	t_{50} (min.)
		Temperature 405°C		
351	276	78.6	1.13	2.55
300	243	81.0	1.26	2.91
199	164	82.0	1.42	3.30
152	126	82.8	1.72	4.27
101	86	85.3	1.85	4.35
		Temperature 415°C		
351	279	79.5	0.76	1.75
304	247	81.3	0.80	1.84
202	166	82.3	0.97	2.32
149	125	83.9	1.30	2.75
99	86	86.0	1.56	3.42
		Temperature 425°C		
351	283	80.7	0.50	1.15
297	242	81.5	0.55	1.29
200	165	82.5	0.62	1.62
147	125	85.0	0.92	2.47
101	87	87.0	1.12	2.78
		Temperature 435°C		
347	281	81.2	0.36	0.85
298	244	81.7	0.37	0.85
202	168	83.2	0.42	1.02
150	130	87.0	0.60	1.77
100	89	89.0	0.91	2.10

longer eventually reaching a constancy to duplicate that found for the empty vessel. This same "aging" effect was shown also when finely powdered glass was used to increase the surface. It is apparent therefore that the reaction is one which may be catalyzed under suitable conditions but that under the conditions prevalent in this work is strictly homogeneous. The slope of the rate curves subsequent to the inflection was always constant even for reactions in a new vessel before aging. This fact would suggest that the secondary reactions are always homogeneous. That the primary reaction becomes homogeneous may be connected with the observed darkening of the reaction bulb by a dark brown deposit which could be distilled slowly under vacuum and which therefore could not be carbon but in all probability was a complex polysulphide.

An examination of the end-points of the reaction shows a variation with temperature and pressure. The greatest percentage decomposition occurred at the highest temperature and lowest initial pressure; the least percentage decomposition at the lowest temperature and highest pressure. This variation is apparent from the data in Table III and would suggest the existence of an equilibrium similar to that established by Trenner and Taylor for ethyl mercaptan, ethylene and hydrogen sulphide. In an attempt to verify the existence of this equilibrium for propylene and hydrogen sulphide a mixture of 350 mm of the latter and 355 mm of the former were allowed to react at 435°C. Such a mixture should be equivalent to 350 mm propyl mercaptan which decomposed under these conditions with a pressure increase of 81.2 percent. If the suggested equilibrium existed, the mixture should react with a pressure decrease of 18.2 percent. Actually a maximum decrease of only 10 percent was obtained after twelve hours, after which time the pressure began to increase again very slowly. Duplicate runs always showed the same tendency though quantitative reproducibility was small suggestive of some heterogeneity in the complicating reactions.

The effects of foreign gases were determined in eleven cases with oxygen, ethylene, propylene, sulphur dioxide, carbon dioxide, nitrogen, helium.

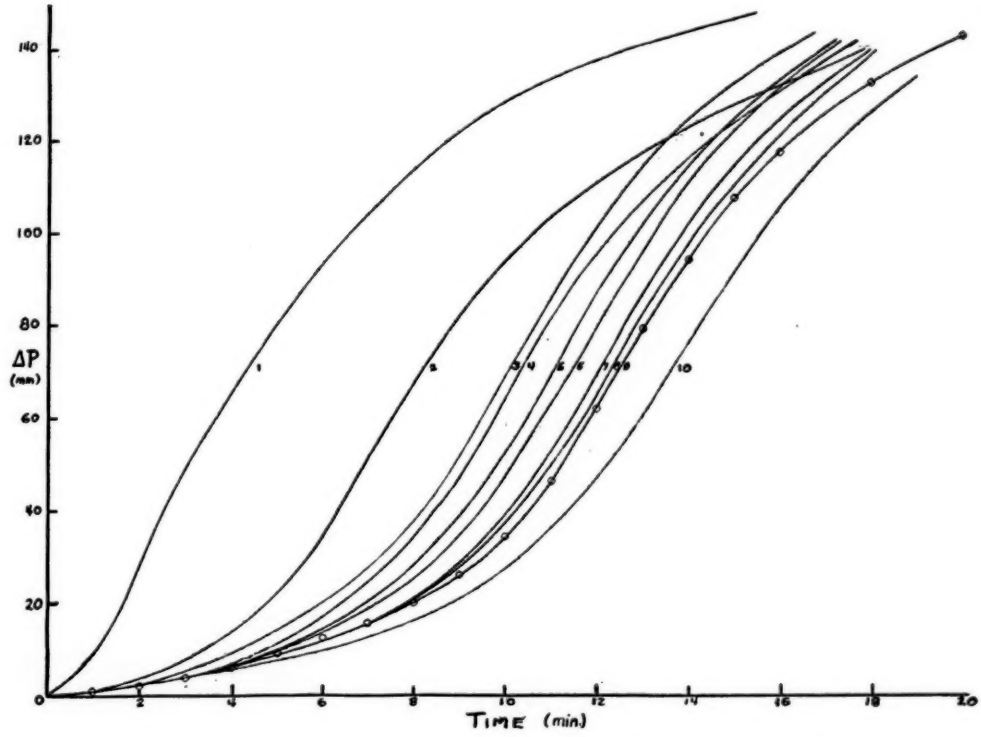

FIG. 3. Foreign gas effect. Initial pressure of PrSH = 200 mm. Temp. = 405°C

1. 5 mm O_2
2. 102 mm C_2H_4
3. 102 mm CO_2
4. 100 mm C_3H_6
5. 100 mm N_2
6. 100 mm H_2S
7. 100 mm C_2H_6
8. 100 mm H_2
9. Normal
10. 101 mm NH_3

hydrogen sulphide, ethane, hydrogen and ammonia. In each instance, oxygen excepted, 100 mm of gas were added to 200 mm of mercaptan vapor. With oxygen only 5 mm were used because of the pronounced effect it had on the length of the induction period. Fig. 3 shows eight of the eleven cases studied, the normal rate curve being included for comparison. The curve for sulphur dioxide is practically coincident with that for carbon dioxide, whilst helium was apparently without effect. The striking feature of Fig. 3 is the parallelism of the curves beyond the inflection in each case, ethylene and propylene excepted, the sole differences lying in the lengths of the induction periods. The more specific effects of the products of decomposition were determined by allowing a sample of mercaptan partially to decompose and then adding a fresh sample and following the reaction to the end. By knowing from previous experiment the shape of the reaction rate curve for the initial sample, the rate curve for the injected sample may be synthesized by subtracting the ordinates of the curve for the initial sample alone from those of the actual observed curve. Three such tests were made and checked: first, the fresh reactant was added before the original sample had reached the maximum reaction rate, that is, early in the induction period; second, the addition made at the point of inflection; and third, injecting the second sample when the first had practically completely decomposed. The results of these three tests are condensed on one diagram in Fig. 4 for the sake of simplifying comparison. The points where the injections were made have been taken as origins for axes for the injected sample. The continuous curve marked "normal" represents the course of decomposition of 181 mm of mercaptan at 405°C. The first injection of 172 mm was made when the original 181 mm had

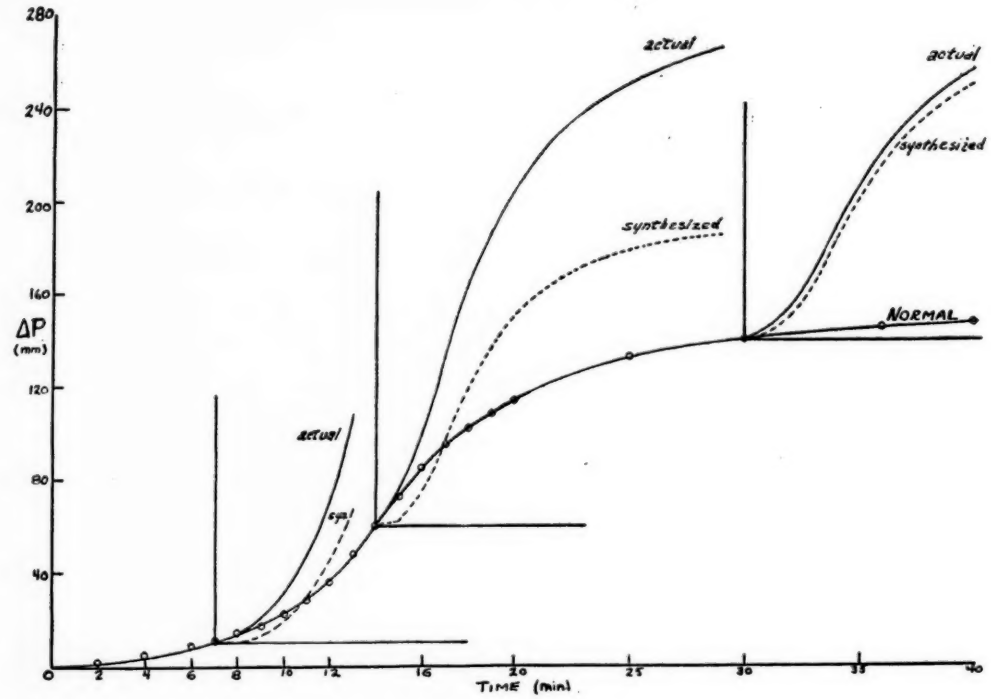

FIG. 4. Composite diagram of the effects of three separate additions of propyl mercaptan to 181 mm already partially decomposed at 405°C. Sample 1 of 172 mm injected after 7 min. Sample 2 of 177 mm injected after 14 min. and sample 3 of 181 mm, after 30 min.

reacted for seven minutes. The curve labelled "actual" represents the course of decomposition of the combined samples. By subtracting the ordinates of the normal curve from those of the actual curve the synthesized curve for the injected sample is found and is shown dotted in the diagram. In the second case 177 mm were injected after 181 mm had decomposed 14 minutes and in the third case 181 mm were injected at the thirtieth minute of decomposition of the original 181 mm. It should be noted that the induction period of the injected sample is in each instance shorter than that of the original sample. The most marked shortening occurs however in the sample injected at the point of inflection of the original sample.

It was shown by Trenner and Taylor that the decompositions of ethyl mercaptan and ethyl sulphide proceeded analogously and were in all probability intimately connected. Since propyl sulphide boils at 142°C it was impossible with the present apparatus to make any extended study of its decomposition due to the inability of keeping the stopcocks and capillaries at this elevated temperature. Nevertheless by maintaining the capillaries at 75°C a few observations at initial pressures between 30 and 60 mm and at temperatures between 435 and 455°C were made. Examples of the curves obtained are shown in Figs. 5 and 6. The lower curve in Fig. 5 is for the decomposition of 31 mm of propyl sulphide at 435°C. The shape is essentially the same as that found for low pressures of mercaptan. Although the marked flattening at these pressures appears to mask the presence of the induction period the fact is that the curve is practically all induction period, the rate of reaction never becoming sufficiently great to produce a noticeable point of inflection. There is no doubt that at higher pressures the curves would show the same hysteresis shape that mercaptan shows. This can be seen from Fig. 6 where curve 1 is for 30 mm of mercaptan and curve 2 for 31 mm of sulphide both at 435°C where the mercaptan curve is so flattened as to indicate an apparently smooth decomposition free from induction.

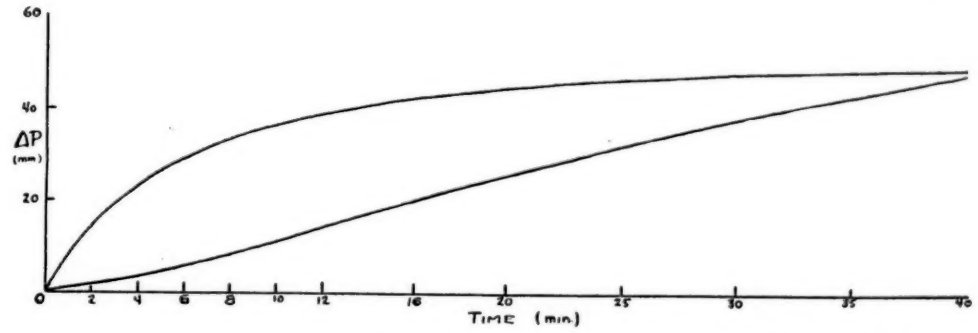

FIG. 5. Decomposition rate curves of propyl sulphide (lower) and propyl sulphide and hydrogen sulphide (upper).

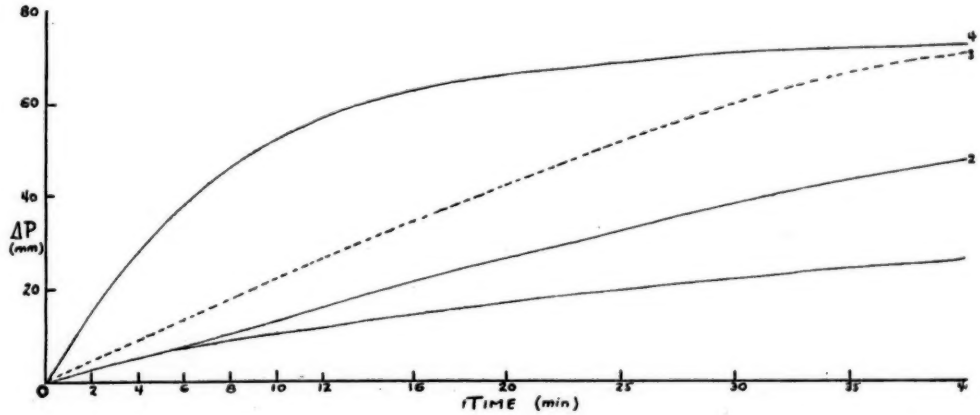

FIG. 6. Rate curves for the decomposition of (1) propyl mercaptan, (2) propyl sulphide, (4) a mixture of both. Curve (3) for comparison is the result of adding the ordinates of (1) and (2).

Since with ethyl sulphide it was shown that the presence of hydrogen sulphide completely removed the induction period a comparison was made in this case with propyl sulphide. Fig. 5 shows the result at 435°C, the upper curve representing the pressure change with time of 30 mm each of propyl sulphide and hydrogen sulphide. The lower curve for comparison is that of 31 mm propyl sulphide alone. The shape of the former curve is entirely different from that of the latter; there is no induction period, the reaction beginning at maximum rate. It should be noted in passing that hydrogen sulphide alone is stable at 435°C.

Since mercaptans are in reality substituted hydrogen sulphides it might be expected that mixtures of sulphides with mercaptan would behave as did mixtures with hydrogen sulphide. In Fig. 6 are given the results observed at 435°C for a mixture of 32 mm propyl sulphide and 31 mm propyl mercaptan indicated by curve 4. Curves 1 and 2 as already stated are for 30 mm mercaptan and 31 mm sulphide alone, respectively. The dotted line, curve 3, is simply the sum of the ordinates of curves 1 and 2 and is thus the pressure change which would be expected for the mixture if each constituent reacted individually. The marked difference between the observed curve 4 and the "theoretical" curve 3 must surely indicate an interaction in some way between the sulphide and mercaptan as between the sulphide and hydrogen sulphide. Similar results were found also at 445° and 455°C.

B. Dynamic method

Experiments were made at temperatures of 405°, 435° and 440°C. The contact times under the conditions previously given were calculated

to be 0.97, 0.93 and 0.92 minute, respectively, at these temperatures, all estimated to be well within the induction period of a reaction with an initial pressure of 760 mm.

In the first run at 405°C all of the reaction products condensed in the first trap at −19°C as a colorless liquid which distillation proved to be unchanged mercaptan. There had been therefore practically no reaction. At 435°C the majority of the products condensed again in the first trap, there being, however, a small amount of liquid in the carbon dioxide trap. This latter proved to be only liquid hydrogen sulphide by the usual tests. The liquid in the first trap was washed with sodium hydroxide, most of it dissolving. The alkali-insoluble, oily residue was separated by extraction with ether and the ether removed by distillation. An amount of a brownish liquid remained, too small to be tested but having the disagreeable odor of propyl sulphide. The alkali-soluble portion was acidified with dilute hydrochloric acid liberating a lemon colored liquid which practically all distilled in the range for propyl mercaptan leaving a small amount of a tarry residue which showed no boiling point but seemed to decompose at about 200°C.

At 440°C the first trap at −19°C contained a large amount of a brown liquid, the second at −78°C, a considerable quantity of a colorless liquid, the liquid air trap was empty and no uncondensed gases were collected in the gas burette. The contents of the first trap were treated as before. The alkali-insoluble portion, again a brownish oily liquid with an odor of propyl sulphide, was treated with mercuric chloride solution to yield a finely divided crystalline precipitate of buff color, which was taken to be the white addition compound of propyl sulphide and mercuric chloride colored with traces of polysulphides, the presence of which was indicated by a distillation with decomposition above 200°C. The alkali-soluble portion proved again to be unchanged mercaptan contaminated also with polysulphides which decomposed about 200°C. The colorless liquid in the carbon dioxide trap proved to be hydrogen sulphide and hydrocarbons. The hydrogen sulphide was allowed partially to distill off and the trap then connected to an Orsat gas analyzer. A large fraction of the gas was absorbed by sodium hydroxide, another large fraction by bromine water and the small remainder by absolute alcohol. The gas removed by sodium hydroxide was undoubtedly hydrogen sulphide. The bromine water would remove propylene whilst absolute alcohol would take up propane. Boiling points will substantiate these conclusions since that of hydrogen sulphide is −59°C, that of propylene −47°C and of propane −44.5°C. Lower paraffins and olefines are excluded since they would not condense at −78°C. It must be admitted that higher hydrocarbons would be retained but their probability of formation seems remote.

Discussion of Mechanism

The marked analogy between the foregoing data and those found by Trenner and Taylor for ethyl mercaptan would suggest a similar mechanism of decomposition for propyl mercaptan. The presence of the induction period is indicative of at least two reactions occurring during the decomposition and most obviously a distinction can be made between the two portions of the reaction up to and succeeding the point of inflection. That this latter is a comparable point for all the cases studied can be seen from a perusal of the last column of Table II in which the ratio of the pressure of mercaptan undecomposed to the initial pressure is constant and independent of the temperature. This fact makes it possible to study separately the course of the reaction in its later stages with the point of inflection as origin for this portion. It was on this basis that the fractional lives given in Table III were calculated. Because of the variable end-point of the reaction at different pressures and temperatures, an approximate correction has been applied to make the times more comparable from case to case. To do this the end-point of the reaction at the highest pressure for each temperature was chosen as standard and all the other end-points at this temperature corrected to this value by multiplying each by the ratio of the percentage increase of this standard reaction to that of the particular reaction to be corrected. The quarter and half lives so found will be seen to show approximate constancy with, however, a definitely rising trend with decrease in initial pressure at each temperature. This would lead one to

suspect that this secondary portion of the reaction constituted a pure unimolecular reaction which deviated from unimolecularity around 300 mm. It is probable however as will be shown that even this portion of the overall rate curve is not typical of a simple reaction and that therefore these fractional lives are themselves complex.

The energy of activation of this secondary part of the reaction calculated from the above fractional lives by means of the Arrhenius equation is found to have an average value of 39,000 calories. In a similar manner using the times taken to reach the points of inflection the energy of activation of the induction period may be calculated to be on the average 40,000 calories. The agreement between these two values is striking when it is considered that an error of one-hundredth of a minute in the fractional life will change the value of the energy of activation by almost 1000 calories. The agreement also has as a consequence the impossibility of separating the primary and secondary reactions by a temperature variation. The energy of activation of the reaction of mixtures of propyl mercaptan and propyl sulphide was calculated, using the quarter life, to be 39,500 calories, also in striking agreement with the previous values.

On the basis of these facts it is possible to postulate a probable mechanism for the reaction which will account for all the observations and at the same time suggest where complicating side reactions might mask a complete understanding of the reaction. It will be convenient to consider the reactions postulated individually, for since the mechanism formally resembles that of Trenner and Taylor for ethyl mercaptan some amplification is possible.

In the first place the induction period is viewed as being due to the bimolecular reaction of two propyl mercaptan molecules to give propyl sulphide and hydrogen sulphide without volume change:

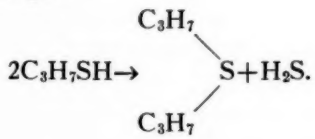

Well known as a heterogeneous reaction on metallic sulphide surfaces it is probable that a clean glass surface would catalyze it and cause the observed erratic values in the length of the induction period. That hydrogen sulphide is formed early in the reaction has been shown by the results from the dynamic method at 435°C where it was further shown (the second case) to be present without any accompanying propylene or other hydrocarbon. Furthermore it may be recalled a small amount of an alkali-insoluble portion was also found. To split hydrogen sulphide from a mercaptan without forming any olefine would seem to require the above reaction which is in keeping with numerous previous findings.

For the next step, the observation that both hydrogen sulphide and propyl mercaptan were capable of removing completely the induction period of the decomposition of propyl sulphide, must mean that a definite chemical reaction occurs in which an addition compound is formed. Trenner and Taylor suggested such an intermediate formed from ethyl sulphide and hydrogen sulphide. Since propyl mercaptan has been shown to remove the induction period of the sulphide and since it must still be present in considerable quantities early in the reaction, there would appear to be two competitors for the propyl sulphide formed in the first step as shown by the following equations:

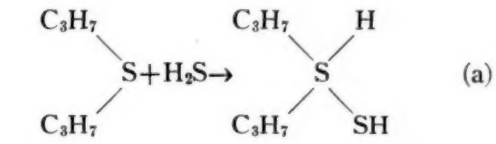

(a)

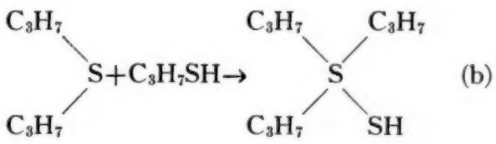

(b)

The intermediate in Eq. (a), analogous to that which Trenner and Taylor postulated and attempted unsuccessfully to prepare in quantity, appears at first sight to be improbable. It is however, only by comparison with the compound in Eq. (b) that its possibility becomes apparent, for this latter compound would simply be tripropyl sulphonium mercaptan. Now although no such compounds are definitely reported in the literature there is every indication that they do

exist. There has been reported[4] an analogous selenium compound $(C_2H_5)_2Se.SeH$. The sulphonium halides and hydroxides are well known, the latter being strong bases. Bernthsen and Sudborough[5] state specifically "trimethyl sulphonium hydroxide . . . gives salts with acids even with hydrogen sulphide, these latter closely resemble the alkali sulphides." Crum-Brown and Blaikie[6] succeeded in preparing trimethyl sulphonium sulphide $[(CH_3)_3S]_2S$ from equivalent amounts of trimethyl sulphonium hydroxide and hydrogen sulphide. Attempts to concentrate an aqueous solution by drying over phosphorus pentoxide were successful only to a certain point however, beyond which decomposition to dimethyl sulphide occurred.

In view of these facts a synthesis of triethyl sulphonium hydrosulphide was attempted.[7] Triethyl sulphonium bromide was treated with sodium hydrosulphide in absolute alcohol at 35°C. After some time the mixture assumed a yellow color and smelled strongly of mercaptan. A fractional distillation yielded ethyl mercaptan and diethyl sulphide. The presence of these compounds is in reality positive evidence that the desired sulphonium hydrosulphide had first been formed but decomposed rapidly. A second attempt using liquid hydrogen sulphide as solvent was unsuccessful because of the small solubility of sodium hydrosulphide. A substitution of ammonium hydrosulphide for the latter, however, despite its solubility in liquid hydrogen sulphide, showed no apparent reaction with the sulphonium bromide. Finally an attempt to prepare the analogous compound $(C_2H_5)_3S-SC_2H_5$ by treating sodium mercaptide with triethyl sulphonium bromide in absolute alcohol was without success. This inability to isolate the suggested compound indicates, in view of the existence of other parallel compounds, its marked instability, such that its immediate decomposition might be expected particularly under the experimental conditions used in the mercaptan decomposition studies.

The third step in the series would then involve the decomposition of the sulphonium hydrosulphide into propylene and hydrogen sulphide:

$$(C_3H_7)_3S-SH \rightarrow 3C_3H_6+2H_2S.$$

The rapidity of this reaction with its large pressure increase would most certainly counterbalance the pressure decrease in the second step of the scheme, namely, the formation of the intermediate. No pressure decrease was ever observed.

On the basis of this mechanism the production of polysulphides which are always found as a "tarry" residue receives a plausible explanation. The sulphonium hydrosulphide referred to above, being essentially a complex mercaptan can undergo the reaction in Step I to form complex sulphides by loss of hydrogen sulphide from two molecules. These complex sulphides in the presence of more mercaptan or of hydrogen sulphide would unite to form new mercaptans still more complex, a cyclic chain of reactions which could produce large molecules of high sulphur content. There is evidence from the dynamic runs that such tarry materials contain both mercaptan and sulphide linkages since part is soluble in alkali and part insoluble.

The absence of an induction period in the decompositions of propyl sulphide-hydrogen sulphide and propyl sulphide-propyl mercaptan mixtures as also its presence in propyl mercaptan alone is well accounted for. The initial step in the latter involves the formation of propyl sulphide and hydrogen sulphide; a reaction with no volume change giving therefore an induction in the rate of pressure increase. With the mixtures the formation of the intermediate and its subsequent rapid decomposition can immediately occur. In fact under the experimental conditions the rate of pressure increase must actually measure the rate of the bimolecular association with a pressure decrease in terms of the larger pressure increase of the much more rapid, probably unimolecular, decomposition of the intermediate. It is this counterbalancing of effects that probably gives to the fractional lives of the

---

[4] Pieroni and Coli, Gazz. chim. ital. **44**, II, 353 (1914).

[5] Bernthsen and Sudborough, Organic Chemistry, pp. 93, 752. D. Van Nostrand Co. (1930).

[6] Crum-Brown and Blaikie, J. prakt. Chim. **23**, 400 (1881).

[7] The experimental work was kindly performed by Dr. Nelson R. Trenner to whom thanks are due.

later portions of the reaction the falling values with increasing pressure.

The decreased induction periods in the injection tests also receive explanation in this same way. Since propyl sulphide or some substances with similar thio-ether linkages, possibly of the polysulphide type, are produced in the decomposition of the initial mercaptan sample, the rate of the association reaction, Step II, would be increased by the addition of the injected mercaptan, and hence the overall rate of pressure increase, giving a decreased induction for the injected sample. The suggested mechanism would necessitate that the concentration of propyl sulphide formed from propyl mercaptan by Step I should be greatest at the point of inflection. This is in line with the observation that the decrease in the induction period is greatest for the sample injected at the point of inflection.

Finally, with regard to the equilibrium existing at the "end-point" of the decompositions, it has been pointed out that mixtures of propylene and hydrogen sulphide did not yield results in line with expectations from propyl mercaptan. This was shown to be due to the instability of propylene at these elevated temperatures. Duffey, Snow and Keyes have recently[8] studied the equilibrium between isopropyl mercaptan, propylene and hydrogen sulphide in presence of various catalysts at 275–300°C by a dynamic method. The rule of addition to unsaturated compounds would suggest that the $-SH$ group in hydrogen sulphide would add to the least hydrogenated carbon atom in propylene thus giving isopropyl mercaptan. It is this same equilibrium then, that should eventually be reached in normal propyl mercaptan decomposition. Keyes and coworkers experienced difficulty in overcoming propylene polymerization in presence of many of their catalysts, such that the same end-point was not reached from the two sides of the equilibrium. The amount of isopropyl mercaptan present at equilibrium from the decomposition reaction was always greater than that from the combination reaction.

To ascertain whether this propylene polymerization would account for the difficulties in the present work, a quantity of propylene was introduced into the reaction vessel at 435°C. A very slow reaction with a pressure decrease occurred. After twenty-four hours this decrease having reached a maximum, the pressure began to increase indicating depolymerization and decomposition. This is in keeping with the findings of Wheeler and Wood[9] who find similar polymerization followed by cracking. It would seem therefore, that a shift in the previously observed "end-point" of the propyl mercaptan decomposition should be noticeable after a long period of time due to the propylene reactions. To this end 300 mm of mercaptan were maintained at 435°C. After half an hour the pressure had increased 244 mm changing only one millimeter in the next half hour with no further change during the second hour. This is the value previously quoted as the "equilibrium end-point." After seven hours the pressure had decreased five millimeters corresponding to propylene polymerization. No further change was noted after twelve hours but about twenty-four hours from the beginning of the reaction the pressure again slowly increased continuing thus for four days to apparent constancy at a value twenty-eight millimeters more than the previous "end-point," thus confirming the belief that the propylene decomposition was responsible for the lack of agreement in the equilibrium studies from the two sides of the reaction. From the experiments the decomposition rate is five times as rapid as the combination reaction, consequently the time of contact of propylene-hydrogen sulphide mixtures must be five times that for the mercaptan thus giving opportunity for considerable propylene decomposition. This does not invalidate, however, the idea that the "end-points" quoted in this paper represent pseudo-equilibrium values since all the reactions showed a constancy for at least two hours; it merely explains why the same "end-points" cannot be reached from the reverse side.

The main steps therefore in the complete mechanism may be represented as follows:

[8] Duffey, Snow and Keyes, Paper presented at the Washington meeting of the Am. Chem. Soc. March, 1933.

[9] Wheeler and Wood, J. Chem. Soc. 1819 (1930).

Step I $2C_3H_7SH \rightarrow (C_3H_7)_2S + H_2S$

Step II $(C_3H_7)_2S + H_2S \rightarrow$ 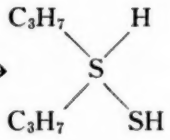

and $(C_3H_7)_2S + C_3H_7SH \rightarrow$ 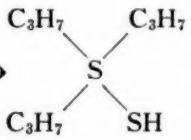

Step III 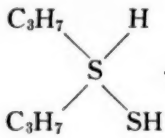 $\rightarrow 2C_3H_6 + 2H_2S$

and 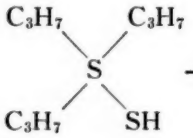 $\rightarrow 3C_3H_6 + 2H_2S$

Step IV $C_3H_6 + H_2S \rightleftarrows (CH_3)_2CHSH$

Step V $C_3H_6 \rightarrow$ polymerization $\rightarrow$ decomposition.

The mathematical difficulties in the solution of the differential equations for the kinetics of such a complex series of reactions prevent elucidation of individual rate constants. It may be noted, however, that Step III must be very considerably faster than either I or II, that Step I mainly controls the length of the induction period and that Step II controls that portion of the reaction arising at the point of inflection.

The Dielectric Constant and Absorption of Several Organic Fluids at 1.82 m

W. T. SZYMANOWSKI, *Department of Physics, University of Pittsburgh*

(Received July 29, 1933)

For the further test of Debye's theory of anomalous dispersion, dielectric constants and absorptions were measured at $\lambda = 1.82$ m for the following fluids: ethyl alcohol, *n*-propyl alcohol, isopropyl alcohol, isobutyl alcohol, *n*-butyl alcohol, amyl alcohol, chlorobenzene, quinoline and nitrobenzene. The resonance method for undamped waves was used. The results are generally in good agreement with Debye's theory as well as with the results of Mizushima and others for fluids whose polarizations for infinite dilution do not differ greatly from those at normal concentration, as for the alcohols and chlorobenzol. For fluids like quinoline and nitrobenzene, the agreement is far from satisfactory. For these, however, when Malsch modification of Debye's theory is taken into account, a somewhat improved check is found, that for the dielectric constant being satisfactory, but that for the absorption of energy, while improved, being still far from satisfactory.

INTRODUCTION

DEBYE'S dipole theory of anomalous dispersion in the region of short electric waves has been lately confirmed by several authors. However, certain discrepancies have been found as in the case of glycerine by Bock [1] and Mizushima.[2] These have been attributed to three possible causes. (1) Debye's equations neglect the possible effects of associations of molecules. (2) The Debye equations are based on Mossotti's hypothesis for the internal field. (3) The calculation of the relaxation time is based on the assumption of a spherical molecule and therefore, on the validity of Stokes' formula. The third assumption does not seem, however, to cause very great discrepancies between theory and experimental data since Johnston and Williams[3] obtained for nitrobenzene, a highly associated fluid, a value of the right order for the molecular radius calculated from the relaxation time obtained by extrapolation to infinite dilution.

The purpose of this paper is the collection of further data on dielectric constants for wave-lengths of the order of a few meters, especially for associated fluids for the sake of a further test of Debye's dipole theory.

[1] R. Bock, Zeits. f. Physik **31**, 534 (1925).

[2] San-Chiro Mizushima, Bull. Chem. Soc. Japan **1**, 47, 83, 115, 143, 163 (1926); Phys. Zeits. **28**, 418 (1927).

[3] J. H. L. Johnston and John Warren Williams, Phys. Rev. **34**, 1483 (1929).

EXPERIMENTAL METHOD

A simple resonance method was used. Two UX 852 Radiotron tubes, as in Fig. 1, generated short electric waves. The resonance circuit consisted of a small loop, a variable condenser C_v, and, connected in parallel with the latter, a Pyrex glass vessel C_x with short platinum or tungsten lead-in wires, containing the liquid under investigation. The aperiodic circuit consisted of a loop of wire, a Weston thermocouple and a galvanometer. To eliminate any systematic error, preliminary measurements were made: (1) with two different condensers, one a variable

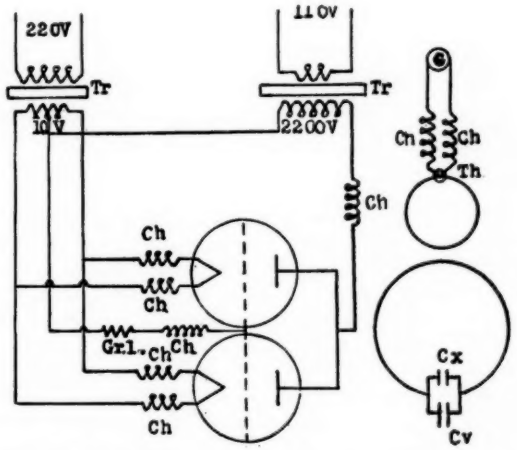

FIG. 1. Wiring diagram. *Tr*, transformer; *Ch*, choke coils; *Gr*, grid leak; *Th*, thermocouple; C_x, Pyrex vessel; C_v, variable condenser.

glass condenser, the other a variable cylindrical air condenser. Both had linear characteristics and the two sets of measurements gave the same results within the limits of experimental error, which amounted to a few percent. (2) The measurements were made under different coupling conditions. (3) Vessels of different capacity were used, their capacities being as 1 : 1.4 : 2. In this way, it was possible to measure the dielectric constants of the investigated fluids through a wide range, and also to eliminate systematic errors by repeating single sets of measurements with different vessels.

Calibration curves showing condenser setting for each vessel, as a function of the dielectric constant, were obtained with the aid of benzene-acetone and acetone-water solutions of known dielectric constants. These curves were approximately linear. A curve showing absorption of energy by the liquid in the cell C_x of Fig. 1 was determined by a method similar to Mizushima's in which KI solutions in acetone of known concentration and conductivity were used. The deflections α of the galvanometer at the point of resonance were noted for each vessel containing a fluid of a given conductivity at a given temperature. The ratios of these deflections to the deflections at resonance point without the fluid in the vessel $k=\alpha/\alpha_0$ were the ordinates of the absorption curves, whose abscissae were the corresponding conductivities in ohm^{-1} cm^{-1}. To correct for the apparent increase in capacity due to the conductivities of the fluids, correction curves for each vessel were drawn in a way similar to Mizushima's. At the wave-length used in this investigation, acetone had not yet shown any effect of anomalous absorption at room temperature. Distilled water, however, showed a marked anomalous absorption.* A corresponding smaller effect was also observed in the water-acetone solutions used for the calibration of the vessels, therefore, the calibration curve of the vessels with greater capacity had to be corrected for the small apparent increase in capacity due to this effect.

A wave-length of $\lambda=1.82$ m was chosen. By this choice, difficulties involved in using a thermostat with a resonating circuit for short electric waves were avoided, and data at a wave-length other than those already reported (Mizushima used $\lambda=3.08$, 9.5, and 50 m) were obtained. Further, it was expected that the anomalous dispersion and absorption effects would be marked enough at this wave-length for the substances under investigation, without using extremely low temperatures. The wave-length was measured in a parallel wire Lecher system. The fluids were cooled and then allowed to warm up slowly. In the meantime, the temperature of the fluid $t°$, the condenser setting S, and the galvanometer deflection α were noted. The same observations were made during the cooling of the heated fluids. Before and after each set of measurements, and without fluid in the cell, the condenser setting S_0 and the galvanometer deflection α_0 were carefully determined. Although the condenser allowed a sharp determination of the resonance point, the effects of the anomalous absorption in the investigated fluids flattened the resonance curve appreciably and caused errors ranging from one to three percent. This accuracy, however, was thought to be sufficient for the purpose of this investigation, since it was of the same order of Mizushima's. The resonance curve did not have any irregularities.

Results

Alcohols

All alcohols used in this investigation were C.P. products of the Eastman Kodak Research Laboratories, with the exception of ethyl alcohol which was purified and distilled from a technical product.

Ethyl alcohol

Fig. 2 shows the dielectric constant and absorption curves for an interval of 0–50°C.

* Although this seems to be surprising, many measurements made in different coupling conditions and with acetone-water solutions of different concentrations showed always this absorption effect. A marked heating of distilled water was also observed at this frequency, if the vessel were put between two plates in a resonating circuit.

That this absorption was not a normal absorption effect but an anomalous one must be concluded from the galvanometer deflection data at different temperatures. These deflections showed an increase with temperature elevation which expressed in equivalent conductivity ranged from about 11.4×10^{-5} to 6.5×10^{-5} ohm^{-1} cm^{-1} for a temperature interval of about 15–30°C.

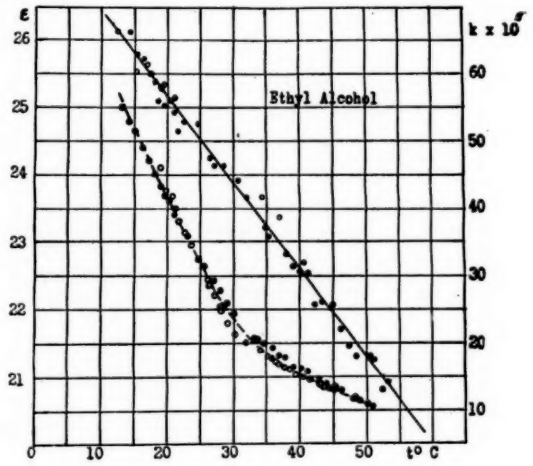

FIG. 2. Variation with temperature of dielectric constant ϵ (——) and absorption k (- - - -) for ethyl alcohol at $\lambda = 1.82$ m.

These data may be compared in Table I with the values computed from Debye's equations:[4]

$$\epsilon'_{\text{calc.}} = \epsilon_0 + \frac{\epsilon_1 - \epsilon_0}{1 + [(\epsilon_1+2)/(\epsilon_0+2)]^2\omega^2 t^2} \tag{1}$$

$$\epsilon''_{\text{calc.}} = (\epsilon_1 - \epsilon_0)\frac{[(\epsilon_1+2)/(\epsilon_0+2)]\omega t}{1 + [(\epsilon_1+2)/(\epsilon_0+2)]^2\omega^2 t^2} \tag{2}$$

$$t = 4\pi\eta a^3/KT \tag{3}$$

where:

T = absolute temperature; η = viscosity;

$t°$ = temperature in °C; K = Boltzmann constant;

t = relaxation time; $\omega = 2\pi \times$ frequency;

a = molecular radius;

ϵ_0 = dielectric constant at high frequency = square of the refractive index for the D lines;

ϵ_1 = dielectric constant for zero frequency;

$\epsilon'_{\text{obs.}}$ = real part of the complex dielectric constant interpolated from Fig. 2 at $\lambda = 1.82$ m;

$\epsilon'_{\text{calc.}}$ = calculated value for the real part of the dielectric constant for $\lambda = 1.82$ m from Eq. (1);

$\epsilon''_{\text{obs.}}$ = imaginary part of the complex dielectric constant $= 4\pi\sigma/\omega$ where σ is the electrical conductivity corresponding, as shown by a calibration curve, to the observed ratio k of Fig. 2;

$\epsilon''_{\text{calc.}}$ = imaginary part of the generalized dielectric constant calculated from Eq. (2).

[4] P. Debye, *Polar Molecules*, p. 97, 1929, Chem. Cat. Co., New York.

TABLE I. *Ethyl alcohol.**

$a = 1.8 \times 10^{-8}$ cm; $\lambda = 1.82$ m.

t°C	η (poise)	ϵ_0	ϵ_1	$\epsilon'_{\text{obs.}}$	$\epsilon'_{\text{calc.}}$	$\epsilon''_{\text{obs.}}$	$\epsilon''_{\text{calc.}}$
50	0.00701	1.8	21.2	21.3	21.11	1.20	1.47
40	0.00831	1.82	22.7	22.6	22.52	1.69	1.97
30	0.00992	1.83	24.25	23.9	23.93	2.57	2.74
20	0.0119	1.85	25.8	25.15	25.15	4.48	3.80
10	0.0145	1.86	27.0	26.45	25.86	6.88	5.24
0	0.0177	1.88	28.4	27.72	26.28	9.10	7.10

* Debye's Eqs. (1) and (2) were used in obtaining $\epsilon'_{\text{calc.}}$ and $\epsilon''_{\text{calc.}}$ in Tables I through IV.

The computations were made under the assumption of a molecular radius $a = 1.8 \times 10^{-8}$ cm. The values for ϵ_0 and ϵ_1 at 30°, 40°, and 50°C were extrapolated from Mizushima's data. The experimental values of $\epsilon'_{\text{obs.}}$ and k at 0°C were also extrapolated from the curves in Fig. 2. The same extrapolation procedure was used in all the following tables. From Table I, we can see that the theoretical values check well the experimental ones as was found by Mizushima for other wave-lengths. However, considerable discrepancies are noted when the computations are carried out under the assumption of $a = 2.0 \times 10^{-8}$ cm as calculated from critical point data,[5] the van der Waals constant b being taken as $16/3\pi Na^3$.

n-Propyl alcohol

The absorption curve shows a maximum at around 5°C. The dielectric constant starts to decrease in the region of 20°C (Fig. 3). For an assumed molecular radius $a = 2.2 \times 10^{-8}$ cm as calculated from critical data, a comparison of experimental and theoretical values is shown in

TABLE II. *n-Propyl alcohol.*

$a = 2.2 \times 10^{-8}$ cm; $\lambda = 1.82$ m.

t°C	η (poise)	ϵ_0	ϵ_1	$\epsilon'_{\text{obs.}}$	$\epsilon'_{\text{calc.}}$	$\epsilon''_{\text{obs.}}$	$\epsilon''_{\text{calc.}}$
50	0.011305	1.87	18.35	16.2	17.77	1.80	2.96
40	0.01405	1.89	19.65	16.85	18.57	2.95	4.26
30	0.0178	1.90	20.9	17.42	18.82	4.48	5.67
20	0.0226	1.92	22.2	17.4	18.35	7.54	7.92
10	0.0292	1.94	23.5	15.35	16.73	10.1	9.97
0	0.0388	1.95	24.8	12.6	13.73	10.6	11.42

[5] Landolt and Bornstein, Tables, 5th Edition. VI.

Table II. The check is not as good as for ethyl alcohol. The general characters of the theoretical and experimental curves, however, are the same.

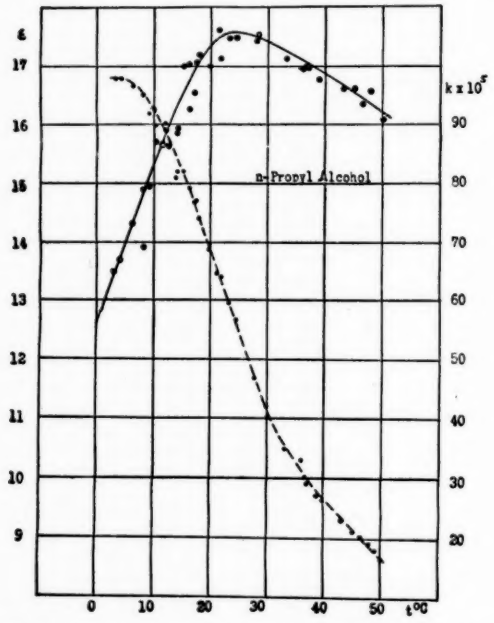

FIG. 3. Variation with temperature of dielectric constant ϵ (——) and absorption k (- - - -) for n-propyl alcohol at $\lambda = 1.82$ m.

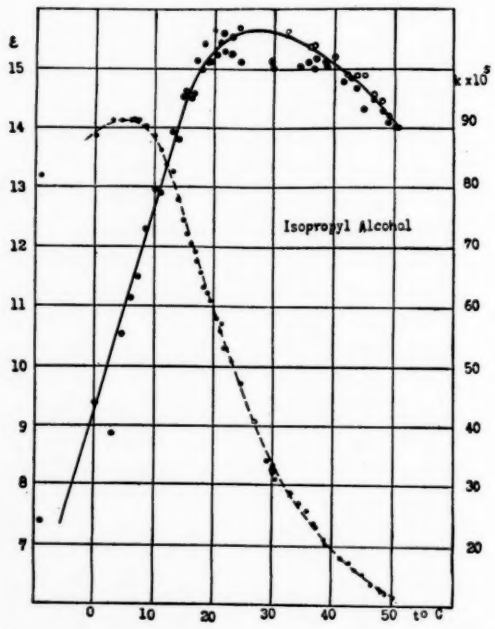

FIG. 4. Variation with temperature of dielectric constant ϵ (——) and absorption k (- - - -) for isopropyl alcohol at $\lambda = 1.82$ m.

Isopropyl alcohol

We do not have sufficient data for ϵ_0 and ϵ_1 at different temperatures to compare the theoretical and the experimental values; however, since the viscosity of isopropyl alcohol is but little different from that for n-propyl alcohol, we expect, according to Debye's theory, the maximum of absorption and the decrease of the dielectric constant to be in the same region as for n-propyl alcohol. Fig. 4 shows this to be the case.

Isobutyl alcohol

In Fig. 5 we find a maximum for the absorption at about 15°C and a decrease of the dielectric constant at about 30°C. Calculating the molec-

TABLE III. *Isobutyl alcohol.*
$a = 2.3 \times 10^{-8}$ cm; $\lambda = 1.82$ m.

t°C	η (poise)	ϵ_0	ϵ_1	$\epsilon'_{obs.}$	$\epsilon'_{calc.}$	$\epsilon''_{obs.}$	$\epsilon''_{calc.}$
50	0.0161	1.88	17.4	13.25	16.19	2.14	4.12
40	0.0212	1.90	18.25	13.7	15.92	3.54	5.71
30	0.0287	1.93	19.15	13.6	14.74	5.56	7.51
20	0.0391	1.95	20.0	11.9	12.33	8.00	8.92
10	0.0555	1.97	21.0	8.6	8.92	8.45	9.20
0	0.0804	1.99	21.8	5.4	5.88	6.82	7.88

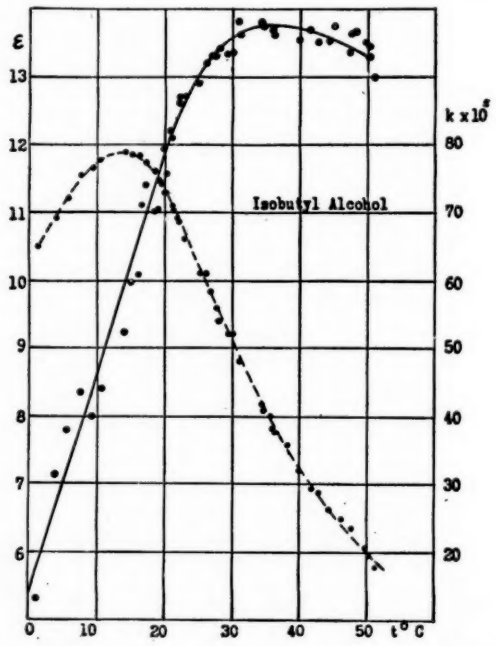

FIG. 5. Variation with temperature of dielectric constant ϵ (——) and absorption k (- - - -) for isobutyl alcohol at $\lambda = 1.82$ m.

ular radius from critical data, we obtain $a=2.3\times10^{-8}$ cm. With this value, Table III was computed and the experimental values compared with the theoretical ones. In general the check is good except for the higher temperatures.

n-Butyl alcohol

Here again we do not have sufficient data for ϵ_0 and ϵ_1 at different temperatures in order to compare theoretical and experimental values as for isobutyl alcohol; however, since the viscosity of *n*-butyl alcohol is less than that of isobutyl alcohol, we expect a shift of both the absorption and the dielectric constant curves towards lower temperatures. This is the case, as may be seen from a comparison of Figs. 5 and 6.

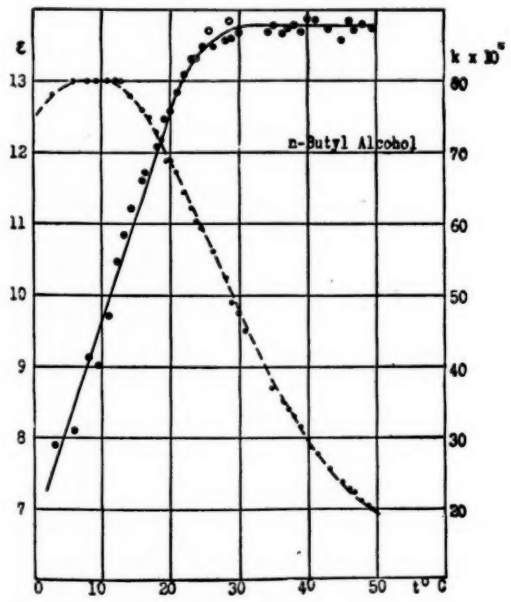

FIG. 6. Variation with temperature of dielectric constant ϵ (——) and absorption k (- - - -) for *n*-butyl alcohol at $\lambda=1.82$ m.

Amyl alcohol

Here η is greater than that of the above-mentioned alcohols; therefore, a shift towards higher temperatures for the maximum of absorption and for the bend in the dielectric constant curve must be expected. Fig. 7 shows this to be the case. The maximum absorption occurs

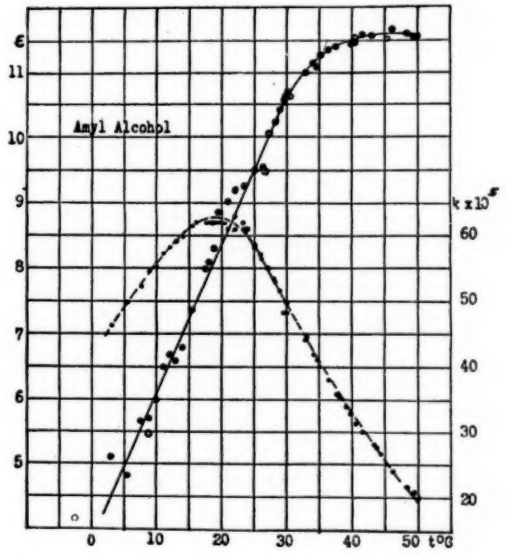

FIG. 7. Variation with temperature of dielectric constant ϵ (——) and absorption k (- - - -) for amyl alcohol at $\lambda=1.82$ m.

at about 20°C and the bend in the dielectric constant curve starts at about 40°C. We are not in possession of sufficient critical data in order to compute the molecular radius. It is expected, however, to be much greater than that of the above-mentioned alcohols. Assuming $a=2.5\times10^{-8}$ cm, Table IV was computed. The check is, in general, good.

TABLE IV. *Amyl alcohol.*

$a=2.5\times10^{-8}$ cm; $\lambda=1.82$ m.

t°C	η (poise)	ϵ_0	ϵ_1	$\epsilon'_{obs.}$	$\epsilon'_{calc.}$	$\epsilon''_{obs.}$	$\epsilon''_{calc.}$
50	0.01864	1.91	13.85	11.6	12.58	2.13	3.69
40	0.02434	1.94	14.6	11.55	12.16	3.60	4.95
30	0.03235	1.96	15.3	10.7	11.00	5.46	6.24
20	0.0437	1.98	16.0	8.4	9.02	6.84	7.00
10	0.0610	2.00	16.8	6.1	6.56	6.11	6.84
0	0.0876	2.02	17.5	3.9	4.58	4.58	5.73

Chlorobenzene

A C.P. product from the Eastman Kodak Research Laboratories was used. For chlorobenzene the molecular radius computed from critical data is $a=2.4\times10^{-8}$ cm. From Eq. (1) we compute for 18°C and for $\lambda=1.82$ m $\epsilon'_{calc.}=5.7$. On the other hand, the experimental

value is $\epsilon'_{obs.} = 5.61$. The discrepancy is still not great. No anomalous absorption was observed at this temperature.

Quinoline

A C.P. product from the Eastman Kodak Research Laboratories was used. For quinoline sufficient critical data are not known for the computation of the molecular radius. We have here to compute it from the experimental dielectric constant in a manner similar to that used by Mizushima for glycerine and to consider whether or not this value is reasonable. Putting in Eq. (1) the observed experimental value of the dielectric constant for quinoline at 18°C, $\lambda = 1.82$ m; namely, $\epsilon'_{obs.} = 8.74$, we obtain as the molecular radius $a = 2.3 \times 10^{-8}$ cm. This value seems to be small, since the benzene molecule has a radius of about 2.3×10^{-8} cm and quinoline has a benzene and a pyridine ring. We can see, therefore, that for such a degree of association as is in quinoline, the simple Debye equations do not check the experimental data. Quinoline shows a small anomalous absorption corresponding to a conductivity of about 4×10^{-5} ohm^{-1} cm^{-1} at about 10°C.

Nitrobenzene

Nitrobenzene was investigated in two different samples. Sample 1 was a C.P. Baker Company product, sample 2 was obtained by double distillation of Baker's technical nitrobenzene. The experimental values for both samples checked well within the limits of the experimental error which was about 1 percent. Fig. 8 shows the curves for dielectric constants and absorptions at different temperatures. Table V, based on a

TABLE V. *Nitrobenzene.**

$a = 2.4 \times 10^{-8}$ cm; $\lambda = 1.82$ m.

t°C	η (poise)	ϵ_0	ϵ_1	$\epsilon'_{obs.}$	$\epsilon'_{calc.}$	$\epsilon''_{obs.}$	$\epsilon''_{calc.}$
60	0.0109	2.36	28.61	28.58	26.46	0.71	7.2
50	0.0125	2.37	30.03	29.6	26.67	0.82	8.3
40	0.0144	2.38	31.56	30.8	26.37	1.07	11.1
30	0.0168	2.39	33.35	32.3	25.50	1.40	13.5
20	0.0201	2.41	35.46	34.2	23.27	1.96	15.95

* Debye's Eqs. (1) and (2) were used in obtaining $\epsilon'_{calc.}$ and $\epsilon''_{calc.}$. (See Table VI.)

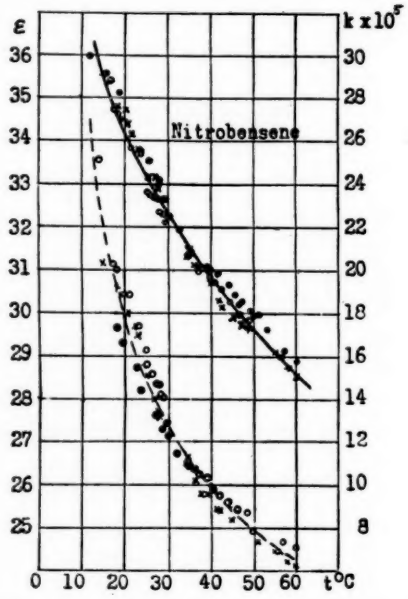

FIG. 8. Variation with temperature of dielectric constant ϵ (——) and absorption k (- - - -) for nitrobenzene at $\lambda = 1.82$ m.

value of $a = 2.4 \times 10^{-8}$ cm for the molecular radius of nitrobenzene according to Johnston and Williams,[3] shows great discrepancies between experimental and theoretical values. For this highly associated fluid, Eqs. (1), (2) and (3) are not sufficient. Taking the experimental values for the dielectric constant of nitrobenzene, we can compute again the molecular radius from Eq. (1). This is found to be $a = 1.53 \times 10^{-8}$ cm at 20°C. The value computed this way is too small, in agreement with what was found above for quinoline and by Mizushima for glycerine.

DISCUSSION OF RESULTS

The foregoing shows that as long as the molar polarizations at normal concentration and at infinite dilution are not very different as in the case of alcohols and chlorobenzene, Eqs. (1), (2) and (3) yield, at least qualitatively, values for the real and the imaginary parts of dielectric constants in agreement with experiment. This conclusion checks not only with the results of Mizushima, but also with the more

recent* results of Goldhammer,[6] Malsch,[7] and Girard and Abadie[8] who investigated alcohols and alcohol solutions. The latter, however, were tested at different wave-lengths from those used in the present investigation. For fluids where molar polarization at infinite dilution P_∞ differs very much from that at normal concentration P_n as in the case of quinoline, where this ratio $P_\infty/P_n \leqq 1.7$ (Rolinski[9]), and nitrobenzene, where $P_\infty/P_n \leqq 3.6$, and possibly glycerine, Eqs. (1) and (2) need a correction. At first, it seemed that such a correction for associations could be easily made in accord with Debye's theory of association,[10] where the molecules are assumed to produce associated molecular groups, having a smaller or a larger electric moment. This theory was developed by Wolfke[11] and the theoretical molar polarization curves as a function of the concentration for different alcohols agreed well with the experimental ones. For chlorobenzene, quinoline, and nitrobenzene the computation of the degree of association was in good accordance with the experimental data. If we want to apply, however, this theory to measurements at a high frequency, we must introduce in the equations for the molar polarization, P, a frequency factor $1/(1+i\omega t)$ Debye[4] (p. 90).

The equation will then be:

$$P_{(\omega)} = \frac{\epsilon-1}{\epsilon+2}\frac{M}{\rho} = \frac{4\pi}{3} N\alpha_0 + \frac{4\pi}{3} N_0 \frac{\mu^2}{3KT}\left(\frac{1}{1+i\omega t}\right) \quad (4)$$

where:

$P_{(\omega)}$ = molar polarization at a given frequency;
M = molecular weight;
ρ = density;
N = total number of molecules per mole;
N_0 = number of unassociated molecules;
α_0 = molecular polarizability taking account of the distortion effect;
μ = electric moment;
$\omega = 2\pi \times$ frequency.

Deducing the expression for ϵ we can find, however, that this substitution does not change the final expressions (1) and (2), as found by Debye. The above theory of association cannot, therefore, explain the discrepancies encountered at a higher frequency.

Malsch[12] recently proposed a correction of the Debye equations, based on the introduction of an additional internal force, as already used by Lorentz.[13] This internal force is due to the interaction of the molecules and, therefore, can be considered the result of association. Such an assumption brings the problem back to a correction of the Clausius Mossotti relation, which can be then deduced from:

$$F = E + (4\pi/3)(1+\nu)P$$

where

F = total force acting on a molecule per unit charge;
E = field strength;
P = polarization = electric moment per unit volume;
ν = factor for the introduction of an additional force.

We have then according to Malsch:[12]

$$\left(\frac{\epsilon-1}{\epsilon+2}\frac{M}{\rho}T\right)_{\text{obs.}} = \frac{(4\pi/3)N\alpha T}{1-\nu(\rho/M)(4\pi/3)N\alpha}$$

where $\alpha = \alpha_0 + \mu^2/3KT$. Having the experimental values for the molar polarization at normal concentration and at infinite dilution, we can find ν as a function of the temperature. The correction factor in Debye's Eqs. (1) and (2) would then be:

$$z = \frac{\epsilon_1 + 2 + (\epsilon-1)\nu}{\epsilon_0 + 2 + (\epsilon_0 - 1)\nu}$$

instead of $(\epsilon_1+2)/(\epsilon_0+2)$. Finally the Debye equations will have the form:

$$\epsilon' = \epsilon_0 + (\epsilon_1 - \epsilon_0)/[1+(z\omega t)^2] \quad (5)$$

$$\epsilon'' = \epsilon_1 - \epsilon_0 z\omega t/[1+(z\omega t)^2]. \quad (6)$$

If we now apply this new equation to nitro-

* The present investigation was made in 1931. Since that time, several papers appeared dealing with a similar subject.

[6] Goldhammer, Phys. Zeits. **33**, 361 (1932).

[7] Malsch, Ann. d. Physik **12**, 865 (1932); Phys. Zeits. **33**, 19 (1932).

[8] Girard and Abadie, Comptes Rendus **195**, 119, 217 (1932).

[9] Rolinski, Phys. Zeits. **29**, 658 (1928).

[10] Debye, Handbuch d. Radiologie, Vol. 6.

[11] Wolfke, Phys. Zeits. **29**, 713 (1928); Comptes Rendus de la Soc. Pol. de Phys.

[12] Malsch, Phys. Zeits. **33**, 383 (1932).

[13] Lorentz, Wied. Ann. **9**, 641 (1880).

TABLE VI. *Nitrobenzene.**

$a=2.4\times10^{-8}$ cm; $\lambda=1.82$ m.

t°C	$\epsilon'_{obs.}$	$\epsilon'_{calc.}$	$\epsilon''_{obs.}$	$\epsilon''_{calc.}$
60	28.58	28.26	0.71	2.9
50	29.60	29.47	0.82	3.96
40	30.8	30.58	1.07	5.0
30	32.3	31.99	1.40	6.3
20	34.2	33.11	1.96	8.4

* Debye-Malsch Eqs. (5) and (6) were used in computing $\epsilon'_{calc.}$ and $\epsilon''_{calc.}$. (See Table V.)

benzene, we see from Table VI that the agreement between experimental and theoretical values is much better for the dielectric constant. For the absorption, the discrepancy is still very great, although it is better than that in Table V. In Tables V and VI, the molecular radius was assumed to be 2.4×10^{-8} cm which is a rather small value, since x-ray studies indicate that it should be about 3.0×10^{-8} cm-4.0×10^{-8} cm in which case the correction used above would still be insufficient. If this correction were applied to the alcohols, then all values would be overcorrected unless we would assume higher radii. For instance, for ethyl alcohol, with a radius of 2.0×10^{-8} cm and the correction of Malsch, we again find a good agreement between theoretical and experimental data. *n*-Propyl alcohol, however, would seem to be overcorrected unless a higher radius were taken. The corrections for isobutyl alcohol, amyl alcohol, and chlorobenzene are negligible. Applying the correction to quinoline, we find a much bigger radius, that of 2.6×10^{-8} cm instead of 2.3×10^{-8} cm as found without correction. The bigger radius certainly seems more reasonable. From the above, however, we can see that without a knowledge of the exact molecular radius, no quantitative comparison as to the validity of the introduced corrections can be made, since even a small change in the radius will change considerably the computed results. As it was pointed out by Oncley and Williams,[14] the radii can be several times larger, at low temperatures, than kinetic theory values because of association effects. This would bring the association phenomena back to the Debye association theory[10] mentioned above. However, only comparatively small parts of the alcohol molecules would have a double moment, as can be seen from the comparison of polarization at infinite dilution and of that at normal concentration. Therefore the correction of the average relaxation time would be small. In a triple molecule with a zero resultant moment there would be no influence on the relaxation time.

Since there are, at present, insufficient data available for molecular radii at different temperatures for associated fluids, we have to use the kinetic theory values as a first approximation, or preferably x-ray data, so far as they are known.

Another way of explaining the discrepancy between the theoretical and experimental data would be that of Oncley and Williams.[14] On the basis of many experiments with solutions of various polar substances in mineral oils of varying viscosities, they found that there was no dispersion even at 1.727×10^{7} cycles. These results are consistent with the experiments of Goldhammer[6] and Weigle and Lüthi.[15]

Oncley and Williams give a probable explanation of the results by the failure of Stokes' law. The reason for such a result may be either because the application of a law in a form of Stokes' law is not justified, or because the use of macroscopic viscosity is not permissible. The experiments of Oncley and Williams on floricin and rosin solutions seem to indicate that Stokes' law is true in its general form. Therefore, we must assume that for the calculation of the relaxation time of an associated fluid, we have to use a corrected macroscopic viscosity.

Such a correction has been used by Goldhammer,[6] who found a much better agreement between experimental and theoretical data for a solution of *n*-butyl alcohol in paraffin oil at $\lambda=0.72$ m if the viscosity were decreased 15 percent.

The same procedure applied to nitrobenzene would, in our case, give a higher value for the molecular radius of nitrobenzene than 2.4×10^{-8} cm which is rather small.

[14] Oncley and Williams, Phys. Rev. **43**, 341 (1933).

[15] Weigle and Lüthi, Comptes Rendus **49**, 130 (1932).